

**DESIGN, SYNTHESIS, AND EVALUATION OF CYSTEINE
PROTEASE INHIBITORS**

A Dissertation
Presented to
The Academic Faculty

by

Amy J. Campbell

In Partial Fulfillment
of the Requirements for the Degree
Doctor of Philosophy in the
School of Chemistry and Biochemistry

Georgia Institute of Technology
December 2005

DESIGN, SYNTHESIS, AND EVALUATION OF CYSTEINE PROTEASE INHIBITORS

Approved by:

Dr. James C. Powers, Advisor
School of Chemistry and Biochemistry
Georgia Institute of Technology

Dr. Donald Doyle
School of Chemistry and Biochemistry
Georgia Institute of Technology

Dr. Sheldon May
School of Chemistry and Biochemistry
Georgia Institute of Technology

Dr. Niren Murthy
School of Bioengineering
Georgia Institute of Technology

Dr. Christoph Fahrni
School of Chemistry and Biochemistry
Georgia Institute of Technology

Date Approved: Nov. 15, 2005

To my nieces, Ashley Lindley and Megan White,
and to my nephews, Austen Lindley and Caleb White.

ACKNOWLEDGEMENTS

First and foremost, I would like to thank my advisor, Dr. James C. Powers. He has earned my respect on both a professional and a personal level, showing intelligence and knowledge to which I aspire, as well as care and concern for the well-being of each group member. Also, I sincerely thank Chris Powers, for all her support, care and encouragement.

I could not have made it without my group members, both present and past: Asli Ovat, Benison Forfeke, Teman Juhar, Sylvia S. Bridges, Drs. Marion Götz, Özlem D. Ekici, Juliana G. Asgian, Karen E. James, Brian Rukamp, and Karrie A. Rukamp. I especially thank Dr. Karen James, for all the time spent training me in my early days at graduate school, and Dr. Marion Götz, for all the time spent encouraging me through difficulties and stressful times. I will also never forget the fun times that Marion, Sylvia, Özlem, and I had during our various ‘movie nights’, lunches together, and the trip to the ACS meeting in New York City.

Also, I especially thank Zhao Zhao Li—for her dedicated and focused work ethic and for her valuable insights. To the undergraduates that I worked with directly or indirectly—especially George Cyriac, Tiffany Stark, Ryan Ianucci, and Brad Bolton—it was a privilege to work with and beside you.

There were many other people that made life at Georgia Tech more interesting and productive: Swapan Jain, Garland Stewart, Russell Seals, Dr. Leslie Gelbaum, David Bostwick, Ty Fife, Cam Tyson, Marsha Moore, and many others. You all have given me your time and effort, and I greatly appreciate it.

To my family-away-from-family, Mission Possible, it has been a precious two years. You have provided me with so much, beyond what can be described in just a few sentences.

I thank my two sisters, Mary and Jill. You both have shown such love, concern, and understanding. I am fortunate to have sisters who are also friends. You both inspire me. To Mary, I am confident that you will make an excellent nurse and am excited that you are pursuing that career. To Jill, it has been so good to have you here in Atlanta. You have provided me with a bit of home that helps me keep a proper perspective.

To my nieces, Ashley and Megan, and my nephews, Austen and Caleb—each of you make me want to achieve great things. I thank my parents, Pastor Tom Campbell and Mrs. Gail Campbell. You have always provided steadfast love that I feel no matter how much physical distance separates us.

Finally, I thank God, Creator and Sustainer of the universe, for giving me this opportunity.

TABLE OF CONTENTS

	Page
ACKNOWLEDGEMENTS	iv
LIST OF TABLES	viii
LIST OF FIGURES	ix
LIST OF SYMBOLS AND ABBREVIATIONS	xii
SUMMARY	xx

CHAPTER

1	Introduction.....	1
	Proteases.....	1
	Cysteine Proteases.....	3
	Clan CA proteases.....	4
	Clan CD proteases.....	5
	General overview of therapeutic potential.....	6
	Substrate mechanism of hydrolysis.....	7
	Irreversible Enzyme Kinetics.....	8
2	Epoxy succinyl Aza-Peptides as Inhibitors of Clan CA Cysteine Proteases.....	12
	Introduction.....	12
	Cathepsin B.....	12
	Calpain I.....	13
	Previous work with epoxy succinyl inhibitors.....	16
	Chemistry.....	23
	Results and Discussion.....	27
	Kinetics.....	27
	Discussion.....	30
	Conclusions.....	34
	Experimental.....	35
3	Aza-Peptide Epoxides as Inhibitors of Caspases: How Epoxide Stereochemistry and Prime Side Interactions Influence Reactivity and Selectivity.....	49
	Introduction.....	49
	Caspases and apoptosis.....	49
	Caspase structure.....	52
	Non-prime sequence specificity between caspases.....	54
	The S1' subsite of caspases.....	56
	Previous work with peptidyl caspase inhibitors.....	57
	Inhibitor Design.....	58

Aza-peptide epoxides.....	58
Relevance of selectivity between caspases.....	60
Aza-peptide epoxide mechanism of inhibition.....	61
Objectives.....	63
Chemistry.....	63
Epoxide synthesis.....	63
Aza-peptide epoxide synthesis.....	65
Stereospecificity of aza-peptide epoxide inhibitors.....	66
Results and Discussion.....	69
Epoxide stereochemistry effects.....	69
Prime side substituent effects.....	73
Combined effect of prime side substituent and epoxide stereochemistry	77
Implications for selectivity between apoptotic caspases.....	79
Stereochemical preference.....	83
Aza-peptide epoxides versus aza-peptide Michael acceptors.....	95
Conclusions.....	100
Perspectives on Aza-peptide Epoxides.....	101
Experimental.....	103
REFERENCES.....	127

LIST OF TABLES

	Page
Table 2.1: Inhibition of clan CA proteases by epoxysuccinyl inhibitors.....	17
Table 2.2: Previous work with aza-peptide epoxides and epoxysuccinyl aza-peptides...	22
Table 2.3: Inhibition of clan CA proteases by aza-E-64d and analogues.....	27
Table 2.4: Inhibition of clan CA proteases by aza-E-64c and analogues.....	28
Table 3.1: A selection of published apoptotic caspase crystal structures.....	53
Table 3.2: Non-prime sequence preferences of caspases.....	55
Table 3.3: Sequence alignment of S1' subsite residues in apoptotic caspases.....	56
Table 3.4: Previous work with aza-peptide epoxides.....	60
Table 3.5: Epoxide stereochemistry effects.....	71
Table 3.6: Prime side substituent effects.....	75
Table 3.7: Combined effect of epoxide stereochemistry and prime side substituent.....	78
Table 3.8: Aza-peptide epoxides vs. aza-peptide Michael acceptors.....	97

LIST OF FIGURES

	Page
Figure 1.1: Protease nomenclature.....	1
Figure 1.2: Evolutionary clans of proteases.....	2
Figure 1.3: Protease catalytic residues.....	3
Figure 1.4: Cysteine protease mechanism of substrate hydrolysis.....	8
Figure 1.5: Irreversible enzyme kinetics.....	9
Figure 1.6: Progress curve for the inhibition of caspase-3.....	10
Figure 2.1: Proposed involvement of calpains in toxicant-induced hepatic necrosis.....	15
Figure 2.2: E-64 and E-64c.....	16
Figure 2.3: Mechanism of cysteine protease inhibition by epoxysuccinyl inhibitors.....	18
Figure 2.4: Binding of E-64c with papain, Form I.....	19
Figure 2.5: Binding of E-64c with papain, Form II.....	19
Figure 2.6: Aza-peptide epoxide and epoxysuccinyl aza-peptide inhibitor designs.....	21
Figure 2.7: Non-aza counterpart of aza-peptide epoxides.....	22
Figure 2.8: Aza-E-64c.....	23
Figure 2.9: Synthesis of hydrazide intermediate.....	24

Figure 2.10: Synthesis of Boc-ALeu-NH-R intermediates.....	24
Figure 2.11: Synthesis of Boc-ALeu-NR intermediates.....	25
Figure 2.12: Synthesis of Boc-ALeu-OBzl intermediate.....	25
Figure 2.13: Synthesis of aza-E-64c and analogues.....	26
Figure 2.14: Proposed conformational change of aza-E-64c.....	30
Figure 2.15: NOESY experiment of HO-(<i>R,R</i>)-Eps-ALeu-NH-butyl in DMSO- d_6	31
Figure 3.1: Apoptotic cascade of caspases.....	51
Figure 3.2: Caspase structure.....	54
Figure 3.3: Commonly used caspase inhibitor warheads.....	58
Figure 3.4: Aza-peptide epoxide inhibitor design for caspases.....	59
Figure 3.5: Proposed mechanism of inhibition based on caspase-1 crystal structures....	62
Figure 3.6: Mechanism of inhibition based on caspase-3 crystal structures.....	62
Figure 3.7: Synthesis of stereospecific (<i>S,S</i>) epoxide moieties.....	64
Figure 3.8: Synthesis of (<i>cis</i>) epoxide moieties.....	65
Figure 3.9: Synthesis of aza-peptide epoxide inhibitors.....	66
Figure 3.10: ^1H NMR of Cbz-DEVaD-EP-CON(Bzl) $_2$ stereoisomers.....	67
Figure 3.11: Conversion of aldehyde inhibitor to aza-peptide epoxide inhibitor.....	85

Figure 3.12: Relative positions of AAsp carbonyl (CO1) to oxyanion hole.....	86
Figure 3.13: Comparison of AAsp and Arg64 interactions.....	87
Figure 3.14: Schematic of Cbz-DEVaD-(<i>S,S</i>)-EP-CON(Bzl) ₂ model.....	88
Figure 3.15: Schematic of Cbz-DEVaD-(<i>R,R</i>)-EP-CON(Bzl) ₂ model.....	89
Figure 3.16: Schematic of caspase-3 – Cbz-DEVaD-(<i>S,S</i>)-EP-CON(Bzl) ₂ complex.....	91
Figure 3.17: Proposed mechanism of inhibition.....	93
Figure 3.18: Michael acceptor moiety synthesis.....	95
Figure 3.19: Aza-peptide Michael acceptor synthesis.....	96
Figure 3.20: Aza-peptide epoxide versus aza-peptide Michael acceptor.....	98

LIST OF SYMBOLS AND ABBREVIATIONS

Å	angstrom
AA	amino acid residue
AAsp (aD)	aza-aspartic acid
Ac	acetyl
AD	Alzheimer's disease
AFC	7-amino-4-trifluoromethylcoumarin
Agm	agmantine (1-amino-4-guanidino-butane)
AHph	aza-homophenylalanine
Ala (A)	alanine
ALeu	aza-leucine
AMC	7-amino-4-methylcoumarin
Apaf-1	apoptosis activating factor-1
Arg (R)	arginine
Asn (N)	asparagine
Asp (D)	aspartic acid

Boc	<i>tert</i> -butoxycarbonyl
Brij	polyoxyethylenelaurylether
Bzl	benzyl, CH ₂ Ph
CARD	caspase-recruitment domain
casp	caspase
Cbz	benzyloxycarbonyl
CDCl ₃	deuterated chloroform
CDI	1,1'-carbonyldiimidazole
CHAPS	3-[(3-cholamidopropyl)dimethylammonio]-1-propanesulfonate
CH ₂ Cl ₂	methylene chloride
CMK	chloromethylketone
Cys (C)	cysteine
D	aspartic acid
DD	death domain
DED	death effector domain
DMF	<i>N,N</i> -dimethylformamide
DMSO	dimethylsulfoxide

DMSO-d ₆	dimethylsulfoxide-d ₆ deuterated
D ₂ O	deuterium oxide
DTT	dithiothreitol
E	glutamic acid
E-S	enzyme-substrate
E-64	<i>trans</i> -epoxysuccinyl-L-leucylamino-(4-guanidino)butane
E-64c	<i>trans</i> -epoxysuccinyl-L-leucylamino(3-methyl)butane
EDC	1-(3-dimethylaminopropyl)-3-ethylcarbodiimide hydrochloride
EDTA	ethylenediaminetetraacetic acid
ee	enantiomeric excess
EP	epoxide
Eps	epoxysuccinyl
ESI-MS	electrospray ionization mass spectrometry
Et ₃ N	triethylamine
Et ₂ O	diethyl ether
EtOAc	ethyl acetate
EtOH	ethanol

F	phenylalanine
FAB	fast atom bombardment
FMK	fluoromethylketone
FT-IR	Fourier transform infrared spectroscopy
Fum	fumarate
Gln (Q)	glutamine
Glu (E)	glutamic acid
Gly (G)	glycine
HEPES	N-2-hydroxyethylpiperazine-N'-2-ethanesulfonic acid
His (H)	histidine
HOBt	<i>N</i> -hydroxybenzotriazole
HRMS	high resolution mass spectrometry
¹ H NMR	proton nuclear magnetic resonance
[I]	inhibitor concentration
IAP	inhibitor of apoptosis protein
ICE	interleukin-1-beta-converting enzyme, caspase-1
IR	infrared spectroscopy

IBCF	isobutyl chloroformate
Ile (I)	isoleucine
isoamyl	3-methyl-butyl
K	lysine
k	rate constant
K_i	inhibition constant
K_M	Michaelis constant (M)
k_{obs}	observed rate constant
J	coupling constant
Leu (L)	leucine
Lys (K)	lysine
MD	muscular dystrophy
MeCN	acetonitrile
MeI	methyl iodide
MeOH	methanol
Met (M)	methionine
MHz	megahertz

min	minutes
ML-IAP	melanoma inhibitor of apoptosis protein
mM	millimolar
min	minutes
mL	milliliter
MS	mass spectrometry
m/z	mass to charge ratio
N	asparagine
NaBH ₃ CN	sodium cyanoborohydride
Napth	naphthyl
NI	no inhibition
NMM	<i>N</i> -methylmorpholine
NOE	nuclear Overhauser effect
NOESY	nuclear Overhauser enhanced spectroscopy
Pd	palladium
PEG	polyethylene glycol
Ph	phenyl

Phe (F)	phenylalanine
PhPr	phenyl propyl carbonyl
PIPES	1,4-piperazinebis(ethanesulfonic acid)
<i>p</i> Na	<i>para</i> -nitroanilide
Pro (P)	proline
<i>p</i> -TsOH	<i>para</i> -toluenesulfonic acid
ppm	parts per million
Q	glutamine
R	arginine
RFU	relative fluorescence unit
s	second
SAR	structure activity relationships
Ser (S)	serine
SMAC	second mitochondrial activator of caspases
S _N 2	secondary nucleophilic substitution
Suc	succinyl
<i>t</i>	time

TBI	traumatic brain injury
<i>t</i> -Bu	<i>tert</i> -butyl
<i>t</i> -BuLi	<i>tert</i> -butyl lithium
<i>t</i> -BuOOH	<i>tert</i> -butylhydroperoxide
TEA	triethylamine
TFA	trifluoroacetic acid
THF	tetrahydrofuran
Thr (T)	threonine
TLC	thin layer chromatography
Trp (W)	tryptophan
Tyr (Y)	tyrosine
UV	ultraviolet
v	velocity
Val (V)	valine
W	tryptophan
Y	tyrosine

SUMMARY

This research involved the design, synthesis, and evaluation of irreversible cysteine protease inhibitors. Specifically, irreversible inhibitors of clan CA and clan CD cysteine proteases were studied. This research offers new and valuable insights into recently developed classes of inhibitors.

Both clan CA and clan CD proteases have a variety of physiological and pathological roles. Several members of these clans are current drug targets. In particular, both clans have members that have been implicated in cell death pathways, including apoptosis, or programmed cell death. In particular, caspases, clan CD proteases, play an important role in the protein degradation that occurs in apoptosis.

However, clan CA proteases, such as calpains and cathepsins, have also been implicated as playing an essential role in apoptosis and other cell death pathways. Many of the caspase inhibitors used in apoptotic studies have shown cross reactivity with clan CA proteases. Thus, in these cases, the anti-apoptotic effect of these inhibitors could be due to the broad-spectrum effects of these inhibitors with a variety of cysteine proteases.

Recently, the Powers laboratory designed a new class of inhibitors highly specific for clan CD proteases, aza-peptide epoxides. Most importantly, the aza-peptide epoxides designed for caspases show no cross-reactivity with clan CA proteases such as cathepsin B and calpain I. Aza-peptide epoxides designed for clan CA proteases also showed little to no inhibition of clan CA proteases. However, the inhibition rate constants of the non-aza counterparts of the aza-peptide epoxides, designed for clan CA proteases, are not known in the literature. Thus, the exact cause of the poor inhibition was unclear.

E-64c, an epoxysuccinyl inhibitor, is known to be a highly potent inhibitor of cathepsin B and calpain I. Thus, to determine if these clan CA proteases could tolerate an aza-residue, aza-E-64c and its analogues were synthesized. These inhibitors, termed epoxysuccinyl aza-peptides, were found to be significantly less potent for cathepsin B, calpain I, and papain than their non-aza counterparts, including E-64c.

Having provided conclusive evidence that aza-peptide epoxides are highly specific for clan CD proteases, we turned our attention to the development of this class of inhibitors for caspases. Some questions about the reactivity of aza-peptide epoxides with caspases remained. In particular, the previous findings showed that the reactivity and selectivity of these inhibitors with caspases were significantly influenced by epoxide stereochemistry and the prime side substituent. Selectivity between caspases is very difficult to achieve. An aza-peptide epoxide inhibitor, highly selective for one individual caspase, would be a valuable biological tool. Its value as a potential therapeutic might be more limited.

Also, the reactivity of the aza-peptide epoxides with the (*cis*) stereochemistry was not yet known. Thus, this second project involved the systematic study of epoxide stereochemistry effects, prime side substituent effects, and the combined effect of these two variables. In all, this second project resulted in the synthesis of 15 new aza-peptide epoxides. All inhibitors were tested with all seven apoptotic caspases, caspases-2, -3, -6, -7, -8, -9, and -10.

We found that epoxide stereochemistry, prime side substituent, and the peptidyl sequence have significant effects on potency and selectivity. Most interestingly, differences between the highly homologous caspase-3 and caspase-7 were observed,

offering insights into selectivity between these two caspases. This research also resulted in the synthesis of the most potent aza-peptide epoxide inhibitor to date, with an inhibition rate constant of $3,120,000 \text{ M}^{-1}\text{s}^{-1}$ with caspase-3. In general, the (*S,S*) stereoisomer is the most potent relative to the (*R,R*) and (*cis*) stereochemistries. Modeling studies were done to determine why this is true.

Aza-peptide epoxides were also briefly compared to aza-peptide Michael acceptors, another class of inhibitors highly specific for clan CD proteases. The discussion will focus on how differences in the two warheads affect reactivity and selectivity. This work resulted in the synthesis of the most potent aza-peptide Michael acceptor inhibitor to date, with an inhibition rate constant of $5,620,000 \text{ M}^{-1}\text{s}^{-1}$ with caspase-3.

CHAPTER 1

INTRODUCTION

PROTEASES

Proteases, also known as peptidases, are designated as such because they hydrolyze, or cleave, peptide bonds. Protease nomenclature, first described by Schechter and Berger, is shown in Figure 1.1.¹ The scissile peptide bond, the bond that is cleaved, is shown in light grey.

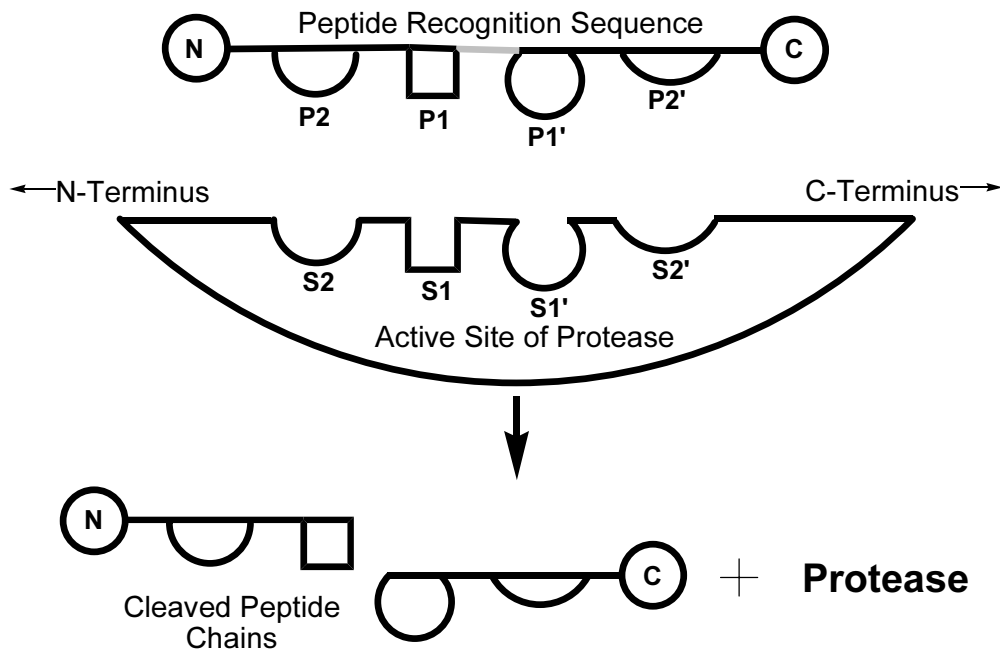


Figure 1.1 Protease nomenclature

Proteases cleave their substrates at specific protease recognition sequences. The length and composition of these recognition sequences varies from protease to protease, although there are some similarities in specificity between different proteases belonging

to the same clan. From the scissile bond, going towards the amino terminus, the residues of the peptide recognition sequence (substrate) are designated P1, P2, P3, etc. Likewise, the residues going towards the carboxy terminus are designated P1', P2', P3', etc. The corresponding subsites in the active site of the protease are designated S1, S2, S3, etc. and S1', S2', S3', etc.

Proteolytic activity is essential for many normal cellular processes. These processes include digestion of proteins, blood clotting, control of blood flow, cell lysis in immune response, and cell protein turnover.² Proteases were first systematically divided into evolutionary related clans and families in 1993 by Rawlings and Barrett.³ The knowledge of proteolytic structure and function has grown dramatically since then, and the original organization of proteases has been modified.⁴ The current classification on the MEROPS database (<http://merops.sanger.ac.uk>) is shown in Figure 1.2.

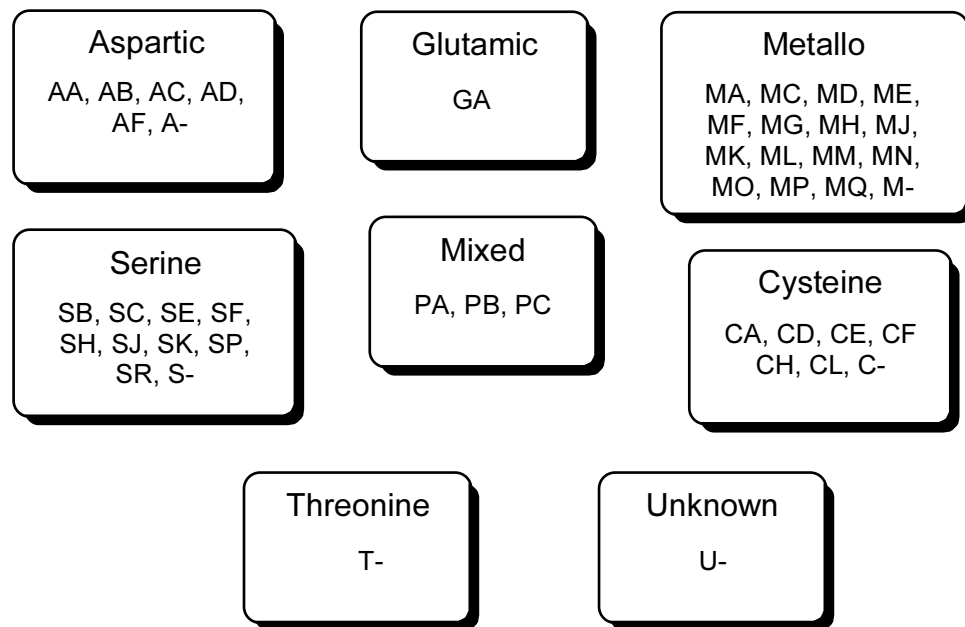


Figure 1.2 Evolutionary clans of proteases

As shown above, proteases are classified in part by their catalytic residue.

Catalytic residues include serine, cysteine, aspartic acid, glutamic acid, threonine (Figure 1.3). Thus, these proteases are designated serine proteases, cysteine proteases, aspartyl proteases, glutamyl proteases, and threonine proteases. Other proteases employ a metal-ion catalyzed mechanism and are termed metalloproteases. There are still several proteases with an unknown catalytic function.

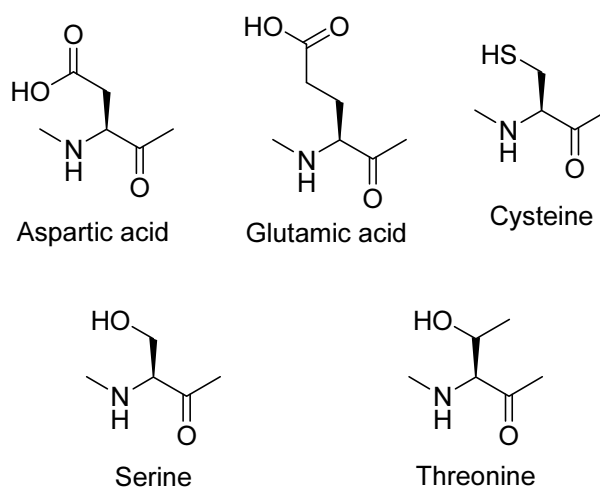


Figure 1.3 Protease catalytic residues

CYSTEINE PROTEASES

Cysteine proteases are widely expressed, with two clans, clan CA and CD, being expressed in all kingdoms of organisms. Clans are evolutionarily related and are classified according to structural similarities, having homologous primary, secondary, tertiary, and quaternary structures. Members of each clan also have the same order of the catalytic residues in the sequence, or primary structure, such as Cys, His, Asn (or Asp) for clan CA and His, Cys for clan CD. Within the same clan, proteases that show a

higher degree of homology to each other are further divided into subgroups known as families. For example, clan CA currently is divided into 24 families on the MEROPS database, with papain and its closest homologues being grouped together in family C1A of clan CA.

Clan CA proteases

Clan CA is the largest clan of cysteine proteases. Several members of this clan are often referred to as ‘papain-like’ proteases. Papain, a plant protease extracted from the papaya plant, has been well-characterized. The active site of papain was described as early as 1957, and high-resolution crystal structures began to appear in the 1980s.^{5,6} Papain has many practical functions. It is the active ingredient in contact lens cleanser and meat tenderizer. Also, papain was likely the active ingredient in the experimental therapy that Harrison Ford underwent, to recover from a back injury sustained while filming *Indiana Jones and the Temple of Doom*.

The cathepsins are important group papain-like proteases. They are highly similar to papain, belonging to the same family, C1A. Some of the most studied cathepsins are cathepsins B, C, F, H, K, L, S, and V. There are several more cathepsins and cathepsin-like proteases. The cathepsin-like proteases are generally found in parasite organisms, while cathepsins are primarily found in mammalian cells, located in the lysosomes, phagosomes, and endosomes. Some cathepsins also participate in trafficking between these organelles and accumulate on other organelles such as the endoplasmic reticulum. These proteases were originally thought to only participate in the non-specific degradation of proteins. Cathepsins have several other physiological roles, such as

proenzyme activation, hormone maturation, bone resorption, epidermal homeostasis, and antigen processing. In recent years, the cathepsins and cathepsin-like proteases have garnered increasing interest as potential drug targets.⁷

Calpains are also interesting clan CA proteases. They are not as similar to papain as the cathepsins, making up the majority of a different family, C2. These proteases are found in the cytosol and require Ca^{2+} for activation. Calpain was first identified in rat brain and skeletal muscle in 1964 by Guroff, and presently more than 13 types of calpain have been identified.⁸ Two types predominate in mammalian cells, μ -calpain (calpain I) and m-calpain (calpain II). The concentration of Ca^{2+} required for activation of calpain I is 50-100 μM , and the concentration required for calpain II activation is 0.2-0.8 mM.⁹ Calpains are essential in a variety of normal physiological processes, such as mitosis, and are required for normal embryonic development.¹⁰⁻¹² The therapeutic potential of calpain inhibition has also been well established, since calpains have been shown to participate in the cytotoxicity present in many disease states.

Clan CD proteases

In the late 1980s, interleukin- 1β , a key hormone in the immune system, was found to be activated by a then-unique protease, now known as caspase-1.^{13,14} Caspase-1 and other proteases were later classified together in clan CD. Interest in caspases and other clan CD proteases has grown dramatically over the last 16 years.

Compared to clan CA, clan CD is a smaller class of cysteine proteases, currently comprised of only five families: clostripain (C11), legumain (C13), caspase (C14), gingipain (C25), and separase (C50). All members of this class show a high specificity

for the P1 residue of a substrate, such as Asp (caspase family), Arg (clostripain family), Asn (legumain family), Arg or Lys (gingipain family), and Arg (separase family). Like clan CA, members of clan CD are also essential for normal physiological functions, such as the involvement of caspases in programmed cell death, or apoptosis. However, members of clan CD have also been identified as drug targets for several disease states, including those diseases involving excessive apoptosis.

General overview of therapeutic potential

While several clan CA and clan CD proteases are essential to many normal physiological functions, in certain disease states their activity becomes excessive. Therefore, much interest has been shown in the therapeutic potential of various cysteine proteases. Of course, inhibition of papain is not therapeutically useful. However, the inhibition of many papain-like enzymes does have therapeutic potential. For example, cathepsins are potential drug targets for treating systemic human diseases such as cancer, osteoporosis, rheumatoid arthritis, atherosclerosis, and asthma.^{7,15-17} Calpains are also involved in a variety of disease states, such as Alzheimer's disease, multiple sclerosis, muscular dystrophy, type 2 diabetes, traumatic brain and spinal cord injury, and cerebral ischemia.^{9,18-23}

Clan CD cysteine proteases are also involved in a variety of disease states, such as gingivitis (gingipains),²⁴ neurodegenerative disorders (caspases), parasitic infections (legumain),²⁵ cancer (separase),²⁶ and bacterial infections (clostripain).^{27,28} The roles of individual members of clan CA and CD overlap in certain disease states. For example, various cathepsins, including cathepsin B, are involved in the same proteolytic

degradation of host hemoglobin done by the clan CD protease legumain in the disease intestinal schistosomias.²⁵ This disease is caused by the parasite *Schistosoma mansoni*. Cathepsin B is also believed to be involved in apoptosis.²⁹ Calpain I, another clan CA protease, regulates neutrophil apoptosis, a process that is also regulated by caspases, members of clan CD.³⁰ Regulation of apoptosis by caspases is discussed extensively in Chapter 3.

Substrate mechanism of hydrolysis

Clan CA and clan CD cysteine proteases differ slightly in their mechanism of substrate hydrolysis. In clan CA cysteine proteases such as papain, the oxyanion hole is composed of the sidechain amide of a glutamine residue and the backbone amide of the catalytic cysteine, while in clan CD cysteine proteases the oxyanion hole consists of only backbone amides.^{31,32} Thus, the oxyanion hole is more flexible in clan CA than in clan CD cysteine proteases.

Also, clan CD cysteine proteases react by what is usually considered a catalytic dyad mechanism. For clan CA cysteine proteases, such as papain, the reaction proceeds by a catalytic triad. This mechanism involves additional stabilization, via hydrogen bonding of the catalytic His to the sidechain carbonyl of an Asn or Asp residue, as shown in the enzyme-substrate complex panel of Figure 1.4.

The thiol of the Cys is polarized by the imidazole of the His, thus allowing for deprotonation.^{33,34} The substrate is non-covalently bound into the active site via hydrogen bonds of the carbonyl of the P1 residue with the oxyanion hole, forming the enzyme-substrate complex. The catalytic cysteine thiol then attacks the P1 carbonyl,

forming a tetrahedral intermediate. The imidazole of the catalytic His then acts as a general acid, protonating the leaving group of the substrate, resulting in the acyl intermediate. Next, the catalytic His abstracts a proton from a water molecule. The activated water molecule then hydrolyzes the thioester of the acyl intermediate bond, resulting in the free enzyme.

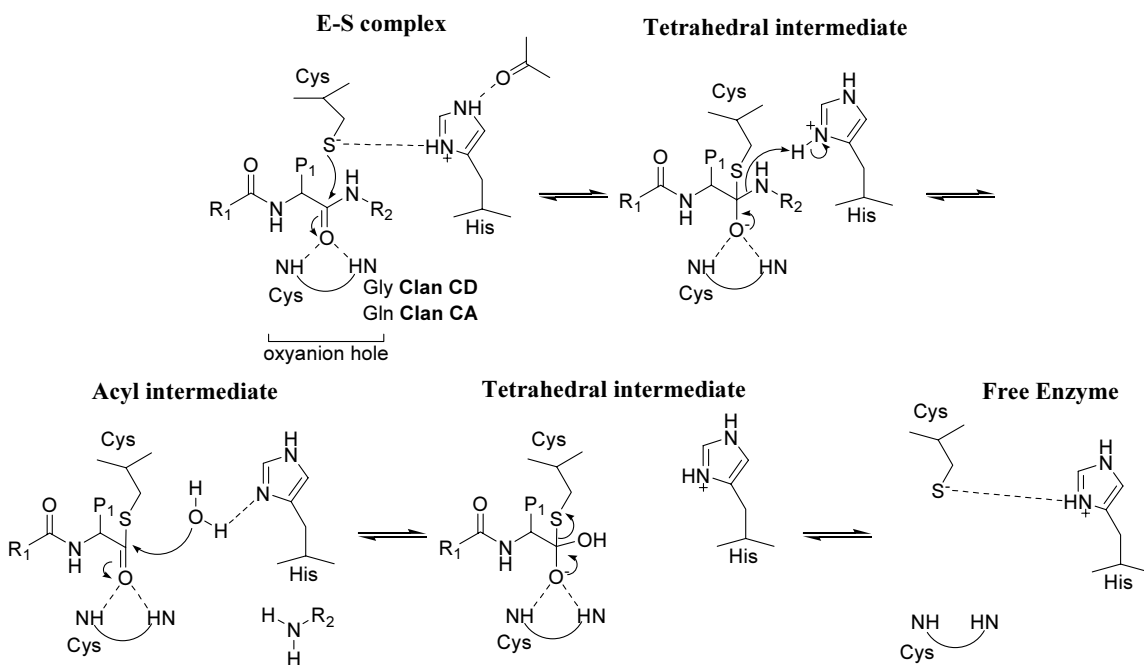


Figure 1.4 Cysteine protease mechanism of substrate hydrolysis, adapted from Ref. 32

IRREVERSIBLE ENZYME KINETICS

Irreversible enzyme kinetics is best described in terms of a second-order rate constant, with the units $\text{M}^{-1}\text{s}^{-1}$. A higher rate constant indicates potent inhibition. While potent inhibition is not the only factor in determining the therapeutic effect of a compound, it is still an important indicator of potential drug viability.

Irreversible kinetics usually proceed through the formation of a reversible enzyme-inhibitor complex (E·I), followed by reaction of the enzyme with the inhibitor in a time-dependent step, forming a covalent enzyme-inhibitor complex.

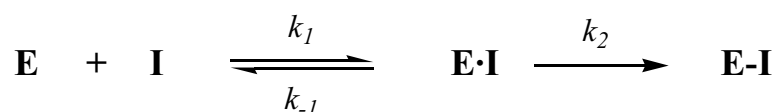


Figure 1.5 Irreversible enzyme kinetics

One method for determining irreversible rate constants is termed the incubation assay method. This method was first described by Kitz and Wilson.³⁵ This method involves incubating the enzyme and inhibitor in buffer, without the presence of the substrate. Aliquots of this solution are taken at various time intervals, and the rate of substrate hydrolysis is measured. The frequency of the time intervals depends on the rate of the inhibition. Higher rates of inhibition result in closer time intervals.

When $[\text{I}] > [\text{E}]$, preferably ten times greater, pseudo-first order kinetics can be assumed. The rate can be calculated from the equation

$$\ln (v_t/v_0) = -k_{\text{obs}} * t$$

where v_t is the rate of hydrolysis at time t , and v_0 is the rate of hydrolysis without the presence of inhibitor. A plot of $\ln (v_t/v_0)$ versus time t gives the negative slope $-k_{\text{obs}}$, as expected with first-order kinetic plots. Thus, the rate is k_{obs} , can then be divided by the inhibitor concentration $[\text{I}]$ to give the second order rate constant $k_{\text{obs}}/[\text{I}]$, with units $\text{M}^{-1}\text{s}^{-1}$.

Pseudo-first-order kinetics are also described by the equation

$$k_{\text{obs}} = k_2/(1 + K_i/[\text{I}]).$$

The linear form of this equation is

$$1/k_{\text{obs}} = K_i/k_2[I] + 1/k_2$$

where $K_i = [E][I]/[E \cdot I] = k_1/k_{-1}$. The rate constant k_2 is a first-order rate constant, and k_2/K_i a second order rate constant.

When $[I] \approx [E]$ second-order kinetics must be used and can be calculated from the equation

$$k_{2\text{nd}}*t = [1/(i - e)]\ln[e(i - x)/i(e - x)]$$

where $e - x$ is the residual enzyme concentration and i is the initial inhibitor concentration. Since inhibitor concentration is included in the calculation, the second order rate constant $k_{2\text{nd}}$ is directly obtained from the equation.

For very fast inhibitors, the progress curve method, first described by Tian and Tsou, must be used.³⁶ First, the inhibitor and substrate are both added to the buffer system, then the enzyme is added. The rate of substrate hydrolysis is then measured continuously for a time appropriate for each enzyme. As the inhibition approaches infinity, product formation becomes constant, thus resulting in a progress curve (Figure 1.6).

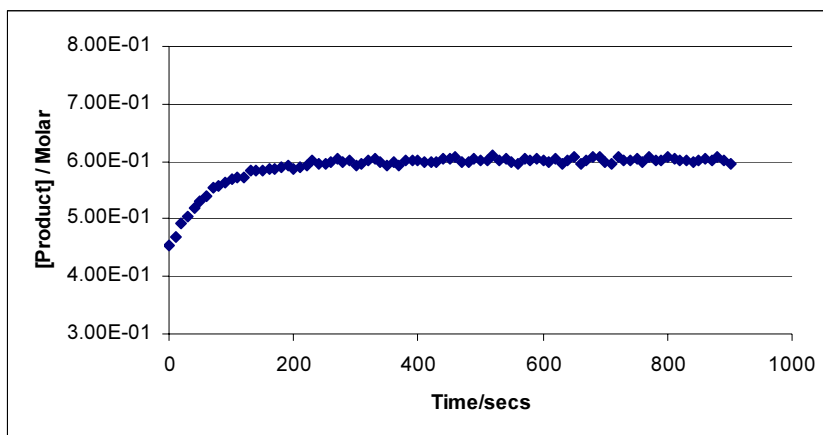


Figure 1.6 Progress curve for the inhibition of caspase-3

The apparent rate constant A can then be calculated from the equation

$$\ln ([P_{\infty}] - [P]) = \ln [P_{\infty}] - A[I]t$$

where $[P]$ and $[P_{\infty}]$ are the product concentrations at t and $t = \infty$ respectively. The rate constant is called an ‘apparent rate constant’ because the reaction is slowed due to the initial presence of the substrate. Unlike the incubation assay method, where the reaction is initiated by the addition of the substrate, the reaction in the progress curve method is initiated by the addition of the enzyme. The apparent rate constants were calculated from the plot of $\ln ([P_{\infty}] - [P])$ versus time t in seconds. The slope of this line equals $A * [I]$, thus the apparent rate constant A can be calculated from the equation

$$A = \text{slope} / [I].$$

For competitive and irreversible inhibition, effect of the substrate concentration on the apparent rate constant is accounted for by the equation

$$k_2 = A * (1 + [S] / K_M).$$

CHAPTER 2

EPOXYSUCCINYL AZA-PEPTIDES AS INHIBITORS OF CLAN CA CYSTEINE PROTEASES

INTRODUCTION

Clan CA cysteine proteases are an important clan of proteases, members of which include papain, calpain I, and cathepsin B. As mentioned in Chapter 1, these proteases have been the subject of much study, and calpain I and cathepsin B are current drug targets for a variety of disease states. Also, papain is a plant protease found in the papaya plant. Thus, papain is not a drug target. However, papain is structurally similar to cathepsin B and calpain I and is highly stable in kinetic assays. Therefore, including papain in the testing of potential clan CA protease inhibitors is logical.

What follows is a brief overview of the biological relevance of cathepsin B and calpain I. This introductory discussion is more specific for these two particular proteases, as opposed to the general overview of them and their close homologues given in Chapter 1. Also, a general overview of epoxysuccinyl inhibitors is given to provide the appropriate background.

Cathepsin B

One of the most studied members of the cathepsins, cathepsin B is primarily found in the lysosome of mammalian cells, being the most widely expressed in the liver, thyroid gland, kidney, and spleen.³⁷ Several x-ray crystal structures of cathepsin B are available.³⁸⁻⁴¹ Cathepsin B participates in physiological functions such as protein

degradation and turnover, proenzyme activation, and hormone maturation. As mentioned, cathepsin B also is involved in apoptosis, although its exact role is not clear.^{17,29}

As a potential drug target, cathepsin B has implications for the diagnosis and/or treatment of disease states such as muscular dystrophy (MD), rheumatoid arthritis, osteoarthritis, and cancer.^{16,17,42,43} The pathology of cathepsin B is related to its ability to degrade components of the extracellular matrix, and cathepsin B is considered to have a causal role in the degradation processes associated with cancer and arthritis.^{16,44} While cathepsin B inhibitors have failed to make it past clinical trials for treating diseases such as MD, and recent interest in cathepsin B as a potential MD drug target has diminished, there is still current interest in the therapeutic potential of cathepsin B inhibition for preventing tumor invasion and metastasis.⁴⁵ Also, recent evidence implicates cathepsin B in the cell death present in Alzheimer's disease.⁴⁶ Thus, while cathepsin B has been extensively studied over several years, there is still ample reason to study this protease and its inhibition.

Calpain I

Often the general term calpain is used throughout the literature, which can be in reference to calpain I, to both calpain I and II, or in reference to all calpains (currently 14 known members). In this discussion, the specific terms calpain I and calpain II will be used when referring to those specific calpains, and the plural term calpains when referring to all calpains.

As mentioned, calpains are clan CA cysteine proteases, found in the cytosol of human cells, requiring Ca^{2+} for activation. Calpain I is widely expressed in mammalian tissues.⁹ Of the two most common calpains, calpain I requires only micro-molar levels of Ca^{2+} for activation, hence its alternate name, μ -calpain. The term calpain 1 (Arabic numeral) is commonly used in the literature; for simplicity, the term calpain I will be used throughout this discussion. Calpain II is also ubiquitously expressed, although higher levels of Ca^{2+} (mM) are required for the activation of calpain II (also referred to as m-calpain or calpain 2).

The exact physiological roles of the calpains are still not completely understood, although they are known to be involved in various physiological functions. For example, calpain I is essential for normal platelet function.⁴⁷ There is strong evidence that calpain I has a pathological role in disease states such as neuronal ischemia (stroke), traumatic brain and spinal cord injury, and Alzheimer's disease.^{18,19,48} Calpains I and II are involved in two cell death pathways, necrosis and apoptosis, and this involvement is linked to their pathological roles.^{30,49,50}

Recently, a mechanism for the involvement of calpains in toxicant-induced liver damage was proposed.⁵¹ In this disease state, which involves extensive hepatic damage due to excessive necrosis, the cell damage continues via necrosis long after the toxicant has been cleared from the system. Previously, the cause of this continued damage had not been clear. Mehendale and Limay discuss evidence that this continued damage is caused by the leakage of calpains from a cell destroyed by necrosis, likely calpain I and II, into the extracellular space. The extracellular space is very Ca^{2+} rich (1.3 mM), thus both calpains I and II would be highly active. These calpains can then attack the

membranes of neighboring cells, thus prolonging the hepatic necrosis (Figure 2.1). Models of chemical-induced liver injury have shown that the calpain inhibitor E-64 decreases the level of liver injury.⁵²

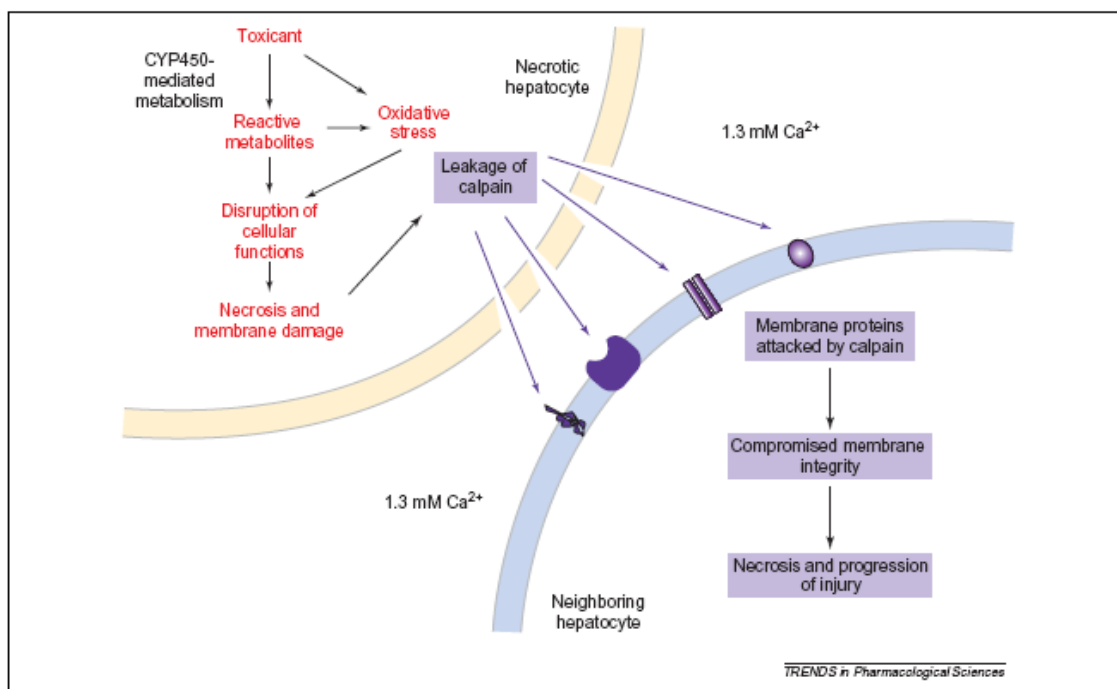


Figure 2.1 Proposed involvement of calpains in toxicant-induced hepatic necrosis⁵¹

Like cathepsin B, the physiological and pathological roles of calpain I are of much interest. The involvement of calpains in diseases continues to be a subject of much interest to the medical community.⁵³ Therefore, like cathepsin B, the study of calpain I inhibition is a worthwhile endeavor.

Previous work with epoxysuccinyl inhibitors

Clan CA cysteine proteases are potently and irreversibly inhibited by epoxysuccinyl inhibitors, and this class of inhibitors has been reviewed several times.⁵⁴⁻⁵⁶ The first epoxysuccinyl inhibitor to be identified was *trans*-epoxysuccinyl-L-leucylamido-4-guanidino-butane, or E-64 (Figure 2.2). E-64 is a natural product, originally isolated in 1978 from *Aspergillus japonicus*.⁵⁷ Following its discovery, E-64 was quickly synthesized and found to be a potent inhibitor of papain, therefore having the potential to inhibit other clan CA proteases, particularly papain-like proteases such as cathepsin B.^{58,59} The same year E-64 was isolated, cathepsin B was implicated to play a pathological role in diseases such as muscular dystrophy, thus generating much interest in the inhibition of cathepsin B.⁶⁰ By 1980, E-64c, one of the most important derivatives of E-64, was synthesized to be a potent and selective inhibitor of cathepsin B (Figure 2.2).⁶¹

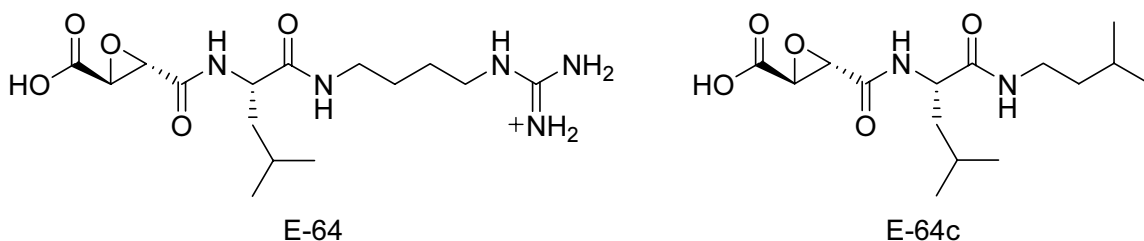


Figure 2.2 E-64 and E-64c

Since then, much interest has been shown in E-64 and its analogues. Various epoxysuccinyl inhibitors have been synthesized and tested with clan CA proteases. One E-64 derivative, EP-460, was designed to be a more potent calpain I and II inhibitor (Table 2.1).⁶² The SAR of E-64c has been studied. The Leu of E-64c has been replaced by other residues, mainly other hydrophobic residues such as Phe, and the isoamyl amide

sidechain has been replaced by other functional groups, such as a benzyl ester and amide.⁶³ These studies have resulted in inhibitors that are equipotent or less potent than E-64c with cathepsin B, although some of these inhibitors have shown increased potency for cathepsins S and L. Some representative inhibitors from these studies are shown in Table 2.1, along with published rate constants for E-64 and E-64c.

Table 2.1 Inhibition of clan CA proteases by epoxysuccinyl inhibitors

Inhibitor	rate ($M^{-1}s^{-1}$)		
	Papain	Cathepsin B	Calpain II
HO-(2 <i>S</i> ,3 <i>S</i>)-Eps-Leu-Agm (E-64) ^{a,b}	638,000	89,400	7,500
HO-(2 <i>R</i> ,3 <i>R</i>)-Eps-Leu-Agm ^{a,b}	60,900	1,900	1,070
HO-(2 <i>S</i> ,3 <i>S</i>)-Eps-Leu-NH-isoamyl (E-64c) ^{a,b}	357,000	298,000	7,450
HO-(2 <i>S</i> ,3 <i>S</i>)-Eps-Leu-NH-(CH ₂) ₄ -NH-Z (EP-460) ^b	n/a	n/a	23,340
HO-(2 <i>S</i> ,3 <i>S</i>)-Eps-Leu-OBzl ^{b,c}	52,500	24,700	n/a
HO-(2 <i>S</i> ,3 <i>S</i>)-Eps-Leu-NHBzl ^{b,c}	90,000	37,600	n/a

^aRef. 64; ^bRef. 62 ; ^cRef. 63

The stereochemistry of the epoxysuccinate greatly influences potent inhibition. In general, the (*S,S*) stereochemistry is preferred over the (*R,R*). Irreversible inhibition is achieved via nucleophilic attack of the cysteine thiolate on the epoxysuccinate moiety of the inhibitors in a S_N2-like reaction. This attack results in the stereochemical inversion of both stereocenters, (*S,S*) → (*R,R*). One stereocenter is inverted as a result of the nucleophilic attack, as expected for a S_N2-like reaction. The other stereocenter is inverted because of a change in priority, using the Cahn-Ingold-Prelog system. Studies have shown that the site of attack is at the carbon next to the carboxylate moiety in E-64c (Figure 2.3).⁶⁵

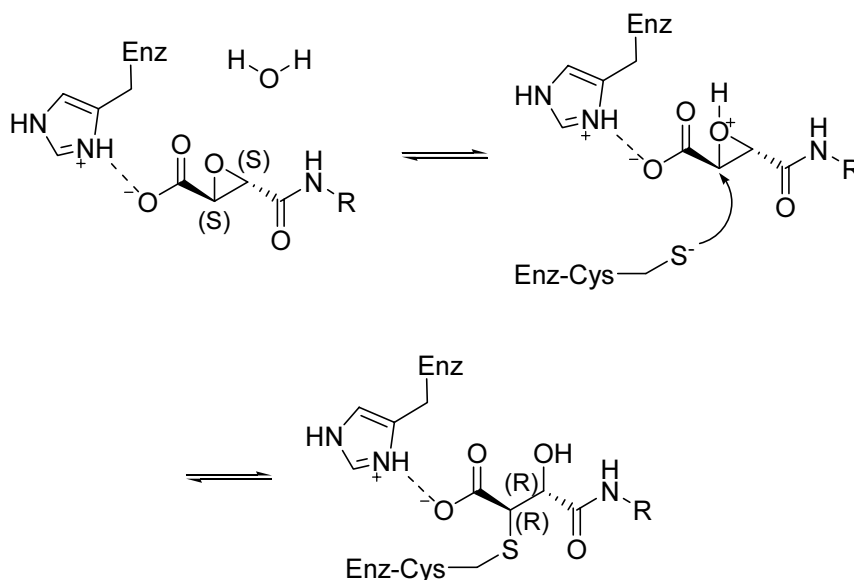


Figure 2.3 Mechanism of cysteine protease inhibition by epoxysuccinyl inhibitors

Crystal structures of the enzyme – inhibitor complexes of E-64c and E-64 to various clan CA cysteine proteases have been published, including papain – E-64,⁶⁶ papain – E-64c (two structures, 1PPP and 1PE6),^{67,68} cathepsin B – E-64c (1ITO),⁶⁹ and calpain I – E-64 (1TLO).⁷⁰ Interestingly, E-64c binds to papain in two different ways. In one binding mode (Form I), the Leu binds in the S2 subsite while the isoamyl sidechain interacts in the S3 subsite (1PE6), while in the other binding mode (Form II), the two interactions are reversed, with the Leu in S3 and the isoamyl sidechain in S2 (1PPP). It is not clear as to which binding mode is preferred, although the E-64c – cathepsin B crystal structure has a binding mode that correlates to form I, as do the E-64 – papain and E-64 – calpain I crystal structures. Also, form II does not allow for parallel- β -sheet interaction with the enzyme. Shown below are the two binding modes of E-64c with papain (Figures 2.4 and 2.5).

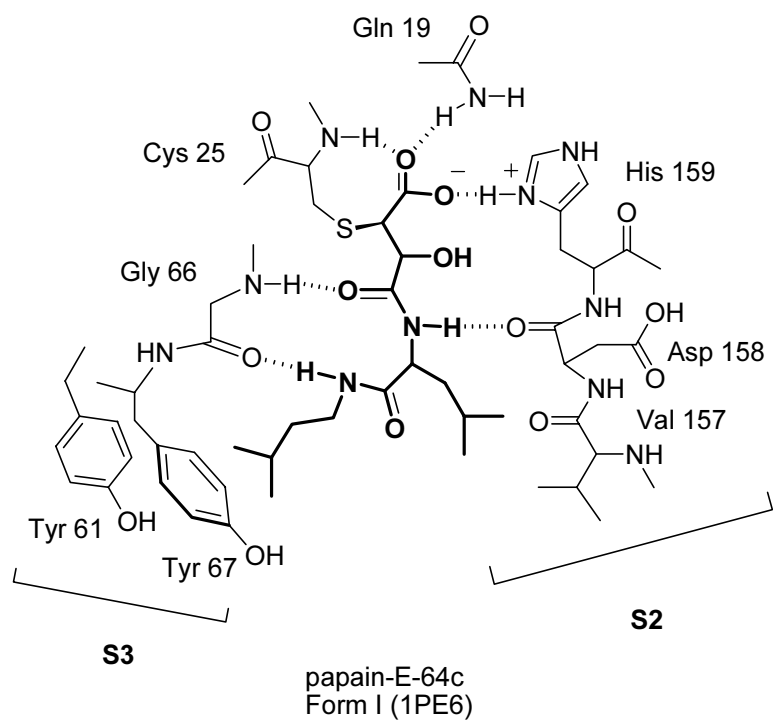


Figure 2.4 Binding of E-64c with papain, Form I⁵⁶

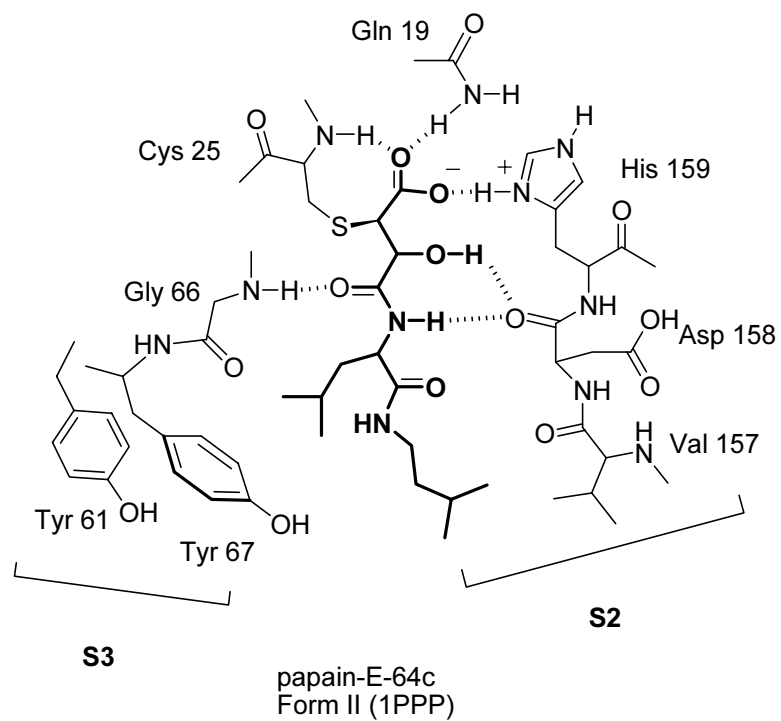


Figure 2.5 Binding of E-64c with papain, Form II⁵⁶

INHIBITOR DESIGN

Several clan CA and clan CD proteases are known to play a role in the apoptotic cell death pathway. The clan CA protease calpain I also has an essential role in necrotic cell death pathway. Much of the study of apoptotic pathways have been done with inhibitors that show cross-reactivity with clan CA proteases (see Chapter 3). Therefore, it is unclear as to whether the inhibition of both clan CA and clan CD proteases is needed to prevent apoptosis. Also, there is increasing evidence that clan CA proteases are involved in a variety of cell death pathways independent of caspases, and these pathways are not completely understood.⁷¹ Thus, there is a great need for inhibitors that are highly specific for one clan of cysteine proteases.

A new class of clan CD cysteine protease inhibitors, aza-peptide epoxides, has recently been developed by the Powers lab (Figure 2.6, top).⁷²⁻⁷⁴ Like E-64, the reactive moiety, or warhead, is an epoxide functional group. The P1 residue is converted to an aza-residue by replacing the alpha-carbon with a nitrogen atom. This conversion allows for the facile coupling of the epoxide to the peptidyl sequence. Using the appropriate peptide sequence, it was initially hypothesized that this design would result in potent clan CD and clan CA proteases inhibitors. Theoretically, the active site cysteine could attack either carbon of the epoxide moiety.

The epoxysuccinyl aza-peptide design is a more direct modification (Figure 2.6, bottom). The backbone for the epoxysuccinyl aza-peptide, which results in a ‘reverse’ binding of the inhibitor, is kept the same as the backbone in E-64. Notice that epoxysuccinyl inhibitors such as E-64 bind in the C → N direction, with respect to the amino acid residue of the inhibitor, instead of the ‘normal’ N → C. Also, an additional

nitrogen atom provides extra spacing between the epoxide moiety and the aza-residue in epoxysuccinyl aza-peptides, compared to aza-peptide epoxides.

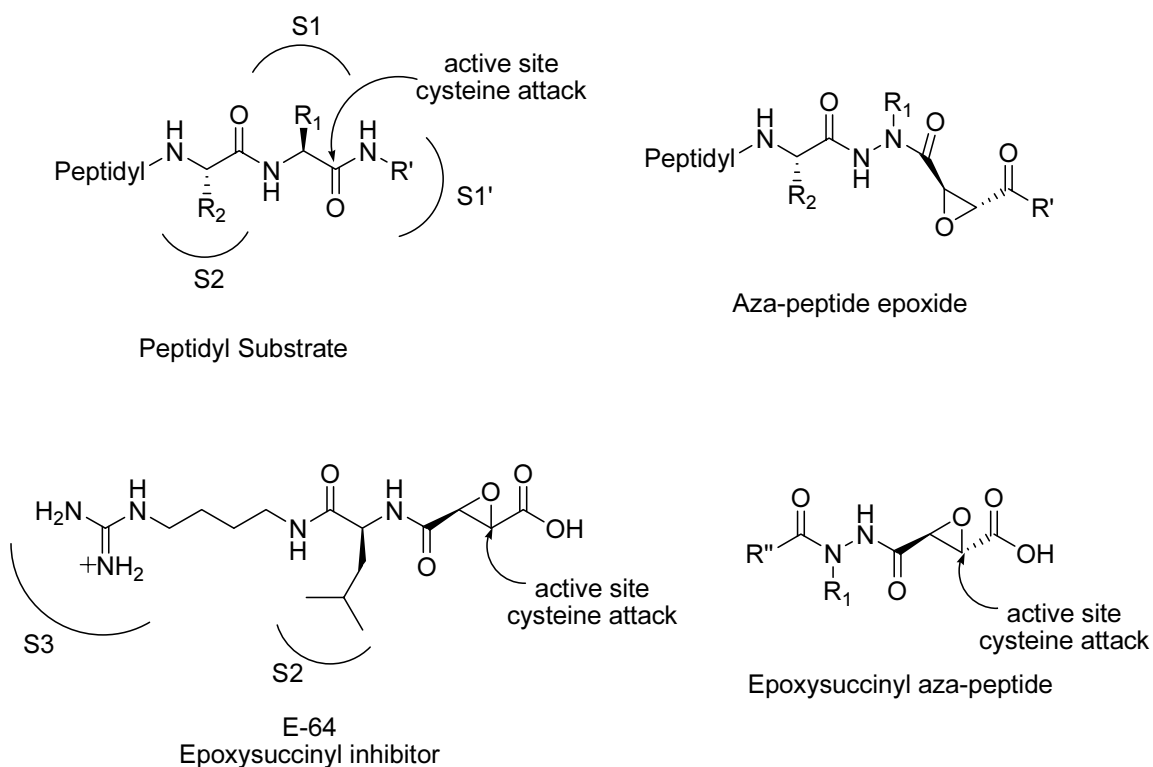


Figure 2.6 Aza-peptide epoxide and epoxysuccinyl aza-peptide inhibitor designs

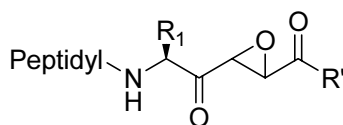
Previous work in the Powers lab showed that aza-peptide epoxide and epoxysuccinyl aza-peptide inhibitors were marginally effective inhibitors of clan CA proteases (Table 2.2).⁷⁵ These inhibitors were mono-, di-, and tripeptides with various hydrophobic residues, corresponding to the substrate specificity of various clan CA proteases.

Table 2.2 Previous work with aza-peptide epoxides and epoxysuccinyl aza-peptides

Inhibitor	$k_{\text{obs}}/[\text{I}] \text{ (M}^{-1}\text{s}^{-1})^a$		
	Papain	Cathepsin B	Calpain I
Cbz-Leu-ALeu-(2 <i>S</i> ,3 <i>S</i>)-EP-CO ₂ Et	10	1.8	8.6
Cbz-Leu-ALeu-(2 <i>R</i> ,3 <i>R</i>)-EP-CO ₂ Et	6.7	NI	1.4
Cbz-Leu-ALeu-(<i>trans</i>)-EP-CO ₂ Et	6.4	23	3.1
Cbz-Leu-ALeu-(<i>cis</i>)-EP-CO ₂ Et	0.4	6.3	1.9
EtO-(2 <i>S</i> ,3 <i>S</i>)-Eps-AHph-OBzl	35	18	3.8
EtO-(2 <i>R</i> ,3 <i>R</i>)-Eps-AHph-OBzl	16	9.1	ND
EtO-(<i>trans</i>)-Eps-AHph-OBzl	27	19	ND

ND = not determined, NI = no inhibition. ^aRate constants were determined by the incubation assay method.⁷³

Both designs were logical. However, the non-aza counterparts of aza-peptide epoxide inhibitors are not known compounds in the literature (Figure 2.7). Also, while the cognate epoxysuccinyl inhibitors of the epoxysuccinyl aza-peptides, EtO-Eps-AHph-OBzl, listed in Table 2.2, are in the literature, the rate constants of these inhibitors with clan CA proteases has not been published.⁷⁶ As discussed, E-64c is one of the most potent inhibitors for clan CA proteases, particularly with cathepsin B and calpains I and II.



'Epoxide inhibitor'
not in literature

Figure 2.7 Non-aza counterpart of aza-peptide epoxides

Therefore, the synthesis of an aza-version of E-64c, aza-E-64c, would allow for a direct comparison of the aza-peptide epoxide inhibitor and its non-aza ‘parent’ compound. Modeling studies done by Dr. Juliana Asgian gave evidence that papain would not tolerate aza-E-64c. Thus, it was hypothesized that clan CA proteases would not tolerate an aza-residue, even within the highly potent E-64c scaffold.

If this were true, then the high specificity of aza-peptide epoxides for clan CD over clan CA proteases is due to the inability of clan CA proteases to tolerate an aza-residue, not merely an artifact of substrate specificities. The expected binding mode of aza-E-64c is shown, along with the expected site of attack, based on the data available for E-64c (Figure 2.8).

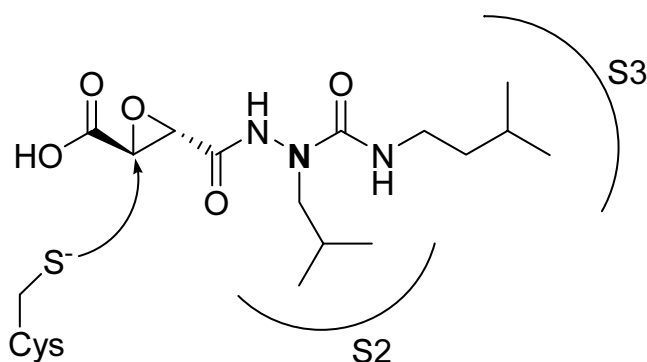


Figure 2.8 Aza-E-64c

CHEMISTRY

The aza-peptide epoxide analogues of E-64c were synthesized by several synthetic routes, with each route requiring the synthesis of the Boc-protected hydrazide **II-3** (Figure 2.9). The coupling of *tert*-butylcarbazate with isobutyraldehyde formed the hydrazone intermediate **II-2**. The subsequent reduction of the hydrazone intermediate using sodium cyanoborohydride resulted in the Boc-protected hydrazide **II-3**.⁷⁷

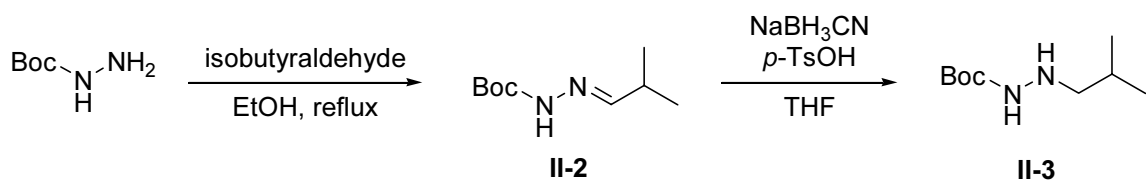


Figure 2.9 Synthesis of hydrazide intermediate

Four different synthetic methods were utilized in the synthesis of the Boc-protected intermediates **II-4** – **II-9**. For the synthesis of aza-E-64c intermediate **II-4**, the commercially available isoamylamine was converted to isoamylisocyanate using triphosgene.⁷⁸ This isocyanate was then coupled to hydrazide **II-3** to give semicarbazide **II-4**. For the synthesis of the aza-E-64c analogues HO(*S,S*)-Eps-ALeu-NH(CH₂)₃CH₃ **II-19a** and HO(*S,S*)-Eps-ALeu-NHCH₂Ph **II-20a**, the commercially available benzyl and butyl isocyanates were directly coupled to the hydrazide **II-3** to give the semicarbazides **II-5** and **II-6** without the use of triphosgene (Figure 2.10).

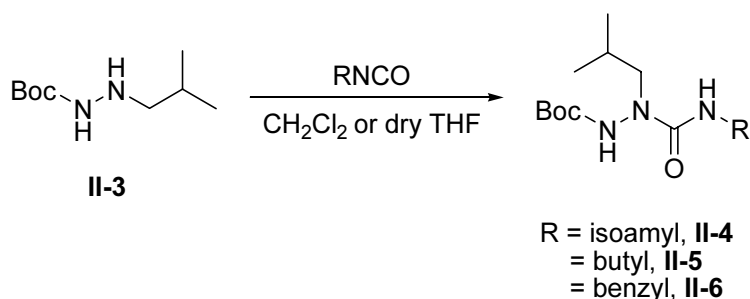


Figure 2.10 Synthesis of Boc-ALeu-NH-R intermediates

The intermediates for the aza-E-64c analogues HO(*S,S*)-Eps-ALeu-*N*-piperidine **II-22** and HO(*S,S*)-Eps-ALeu-*N*-tetrahydroisoquinoline **II-23** were synthesized using a CDI coupling method. This procedure involved reaction with CDI to give the imidazole

ring, then the activation of the imidazole ring via methylation with MeI, followed by reaction with a secondary amine, which gave the semicarbazides **II-8** and **II-9** (Figure 2.11).⁷⁹

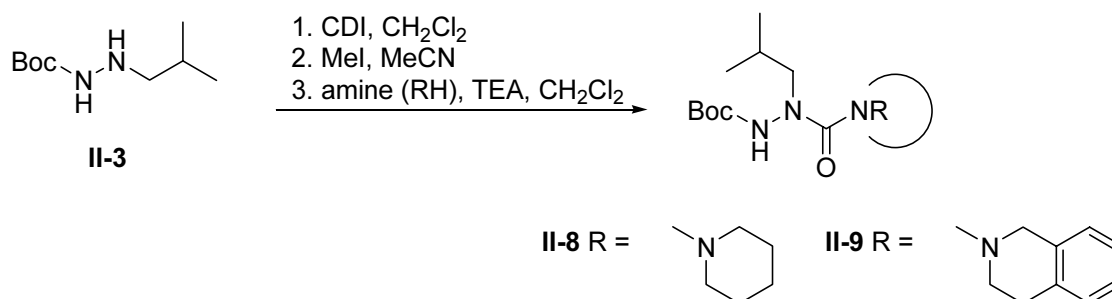


Figure 2.11 Synthesis of Boc-ALeu-NR intermediates

The aza-E-64c analogue HO(*S,S*)-Eps-ALeu-OCH₂Ph **II-21** was also synthesized. Its non-aza counterpart, HO(*S,S*)-Eps-Leu-OCH₂Ph, is a known compound and has been tested with cathepsin B, providing another comparison of an epoxysuccinyl aza-peptide to its non-aza analogue.⁶³ Acylation of Cbz-chloroformate with hydrazide **II-3** gave **II-7** (Figure 2.12).

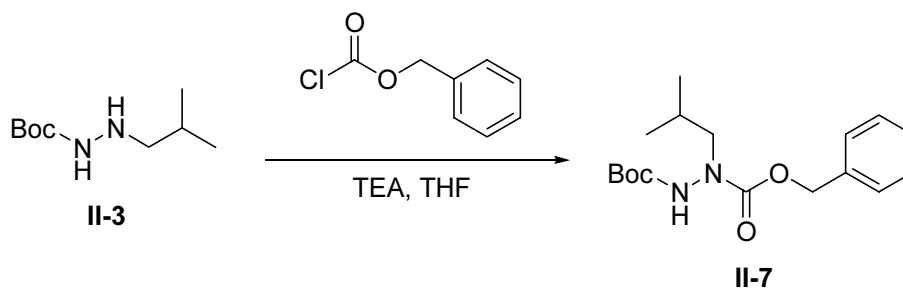


Figure 2.12 Synthesis of Boc-ALeu-OBzl intermediate

To synthesize the final compounds, deprotection of Boc-protected hydrazides **II-4** – **II-9** was accomplished by reaction with 4 N HCl in EtOAc. The mixed anhydride coupling of the resulting HCl salt with monoethyl (2*S*,3*S*)-oxirane-2,3-dicarboxylate gave the aza-peptide epoxysuccinate ethyl esters **II-12a** – **II-17**. The (*R,R*) analogues were similarly prepared by using monoethyl (2*R*,3*R*)-oxirane-2,3-dicarboxylate. Both monoethyl oxirane-2,3-dicarboxylate isomers were synthesized according to previously published procedures.^{73,80,81} The synthesis was completed with the saponification of the ethyl esters **II-12a** – **II-17** to yield the acids **II-18a** – **II-23** (Figure 2.13). All final compounds were characterized by ¹H NMR, high resolution mass spectrometry, and elemental analysis.

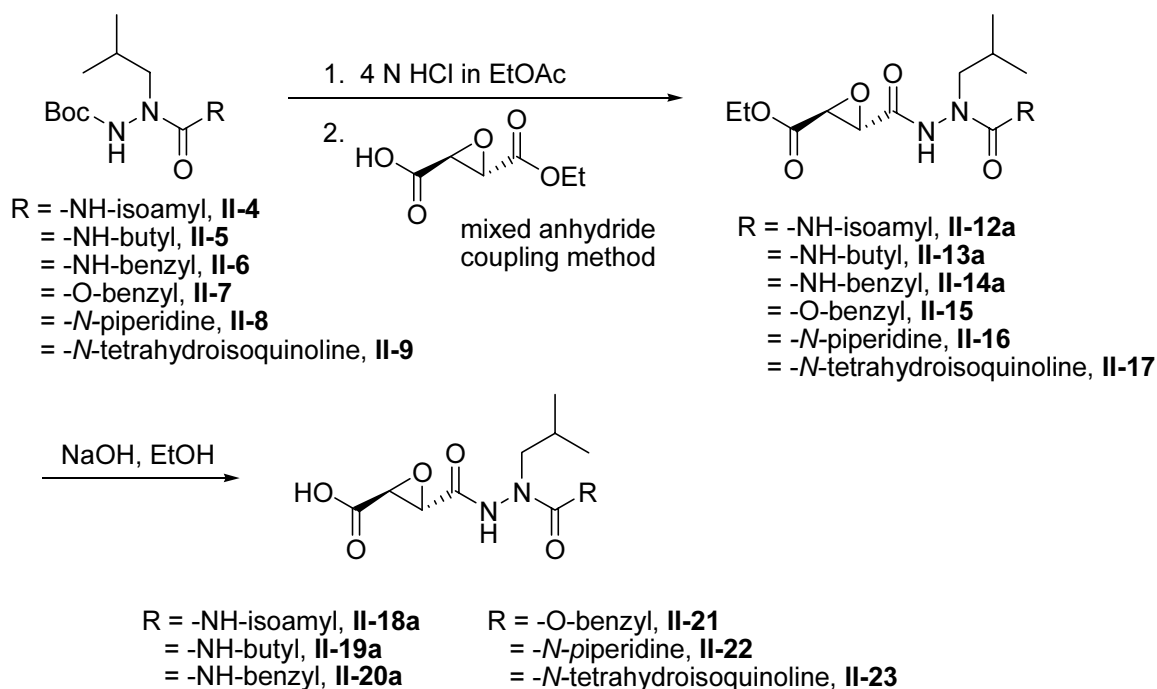


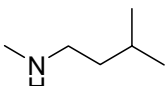
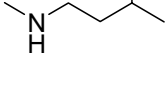
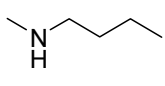
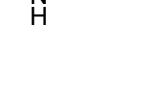
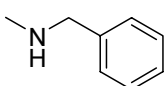
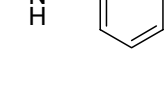
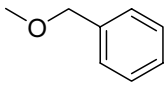
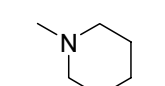
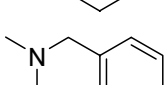
Figure 2.13 Synthesis of aza-E-64c (**II-18a**) and analogues

RESULTS AND DISCUSSION

Kinetics

The synthesis of aza-E-64c also allowed for the facile synthesis of aza-E-64d and its analogues. E-64d was tested as a prodrug for the treatment of MD, although it was eventually dropped from clinical trials due to toxic side effects and poor efficacy.⁸² In E-64d, an ethyl ester group replaces the carboxylate in E-64c, and this ethyl ester is hydrolyzed *in vivo*.⁸³ In comparing previously published data, E-64d ($750 \text{ M}^{-1}\text{s}^{-1}$) is 386-fold less potent for papain than E-64c ($290,000 \text{ M}^{-1}\text{s}^{-1}$), *in vitro*.⁸⁴ The carboxylate group greatly increases potency, since it contributes several strong hydrogen bonding interactions in the S1' subsite.

Table 2.3 Inhibition of clan CA proteases by aza-E-64d and analogues

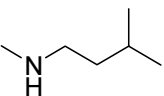
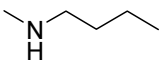
EtO-Eps-ALeu-R		$k_2/(\text{M}^{-1} \text{s}^{-1})$			
	R =	Eps	Papain	Calpain I	Cathepsin B
II-12a		(S,S)	47 ± 1	17 ± 0	< 60
II-12b		(R,R)	< 10	NI	< 60
II-13a		(S,S)	34 ± 10	NI	< 60
II-13b		(R,R)	NI	16 ± 0	< 60
II-14a		(S,S)	64 ± 18	ND	ND
II-14b		(R,R)	NI	16 ± 1	< 60
II-15		(S,S)	81 ± 29	17 ± 3	< 60
II-16		(S,S)	98 ± 11	NI	133 ± 3
II-17		(S,S)	70 ± 17	20 ± 3	83 ± 41

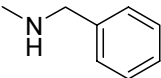
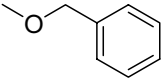
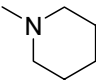
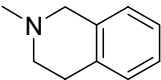
NI = no inhibition, ND = not determined

All aza-E-64d analogues showed little to no potency for papain, cathepsin B, and calpain I, with most showing a 10-fold or greater decrease in the rate constant compared to E-64d (Table 2.3). Also, there is a clear preference for the (*S,S*) stereochemistry over the (*R,R*). Thus, it can be hypothesized that the epoxysuccinyl aza-peptides are binding in the non-prime subsites of clan CA proteases, like E-64c. The (*S,S*) stereoisomers of E-64, E-64c, and their close analogues are more potent inhibitors of clan CA cysteine proteases than the (*R,R*) stereoisomers, when binding in the non-prime subsites.⁶⁴

The kinetics for aza-E-64c and its analogues also showed a decrease in potency compared to E-64c (Table 2.4). Both E-64c and E-64 were tested in this study to make a direct comparison of the inhibitors' potency. In making a direct comparison of E-64c with aza-E-64c **II-18a**, the aza inhibitor is approximately 58.5-fold less potent with papain, 36.6-fold less potent with cathepsin B, and 5.77-fold less potent with calpain I. No significant improvements in potency were observed for any of the aza-E-64c analogues compared to aza-E-64c.

Table 2.4 Inhibition of clan CA proteases by aza-E-64c and analogues

HO-Eps-ALeu- R		rate/(M ⁻¹ s ⁻¹)			
	R =	Eps	Papain	Calpain I	Cathepsin B
II-18a		(<i>S,S</i>)	4,940 ± 1,140	1,370 ± 610	7,190 ± 930
II-18b		(<i>R,R</i>)	165 ± 19	ND	135
II-19a		(<i>S,S</i>)	5,090 ± 340	840	3,660 ± 70
II-19b		(<i>R,R</i>)	279 ± 60	ND	155

II-20a		(<i>S,S</i>)	4,540 ± 250	1,220 ± 260	15,700 ± 1,300
II-20b		(<i>R,R</i>)	189 ± 27	95 ± 1	162 ± 11
II-21		(<i>S,S</i>)	7,100 ± 800	1,110 ± 210	16,300 ± 3,800
II-22		(<i>S,S</i>)	7,450 ± 1,090	541	1,020 ± 220
II-23		(<i>S,S</i>)	4,240 ± 80	506 ± 5	2,040 ± 190
E-64c		(<i>S,S</i>)	289,000 ± 26,000	7,900^a	263,000 ± 22,000^a
E-64		(<i>S,S</i>)	223,000 ± 89,000	ND	42,800 ± 9,200
HO-Eps-Leu-NHBzl		(<i>S,S</i>)	90,000 ± 2,000^b	ND	37,600 ± 800^b
HO-Eps-Leu-OBzl		(<i>S,S</i>)	52,500 ± 800 ^b	ND	24,700 ± 800 ^b

ND = not determined. ^aThese rate constants were obtained using the incubation assay method ($k_{obs}/[I]$) as described.⁷³ All other rate constants were obtained using the progress curve method (k_2). ^bRef. 63

Slight improvements were seen with cathepsin B, as seen with HO-(*S,S*)-Eps-ALeu-NH-Bzl **II-20a** (15,700 M⁻¹s⁻¹) and HO-(*S,S*)-Eps-ALeu-O-Bzl **II-21** (16,300 M⁻¹s⁻¹), but these inhibitors were still less potent than their non-aza analogues, HO-(*S,S*)-Eps-Leu-NH-Bzl (37,600 M⁻¹s⁻¹) and HO-(*S,S*)-Eps-Leu-O-Bzl (24,700 M⁻¹s⁻¹).⁶³ Again, the (*S,S*) stereochemistry is highly preferred, showing that most likely that aza-E-64c and its analogues bind to clan CA proteases in the same manner as E-64c does, in the non-prime subsites.

Discussion

A theoretical study on the conformational properties of aza-peptides has shown that intermolecular hydrogen bonding between N1 and N3 of an aza-peptide can occur, twisting the conformation into a cis-amide bond (N2-CO).⁸⁵ A water molecule, forming the hydrogen bonds shown in Figure 2.13, would logically make this twisted conformation even more likely, since a pseudo six-membered ring has less strain than a pseudo five-membered ring. To potently inhibit the enzymes, the inhibitors must be in the extended, linear conformation (Figure 2.14). So, the decreased potency of the aza-peptide epoxides could be because these inhibitors exist in the twisted conformation and attempt to bind to the enzymes in this conformation.

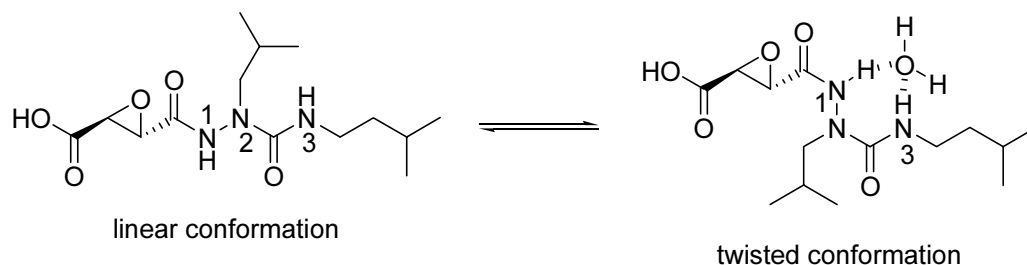


Figure 2.14 Proposed conformational change of aza-E-64c

NMR study. To determine if this twisted, non-extended conformation was possible, the NOESY spectra of HO-(*R,R*)-Eps-ALeu-NH-butyl in DMSO- d_6 and D_2O were acquired. To make a comparison to a non-aza inhibitor, the NOESY spectra of E-64 were also acquired in the same solvents. The NOESY experiment detects through-space interactions of protons up to 5 Å. Dr. Leslie Gelbaum performed these experiments.

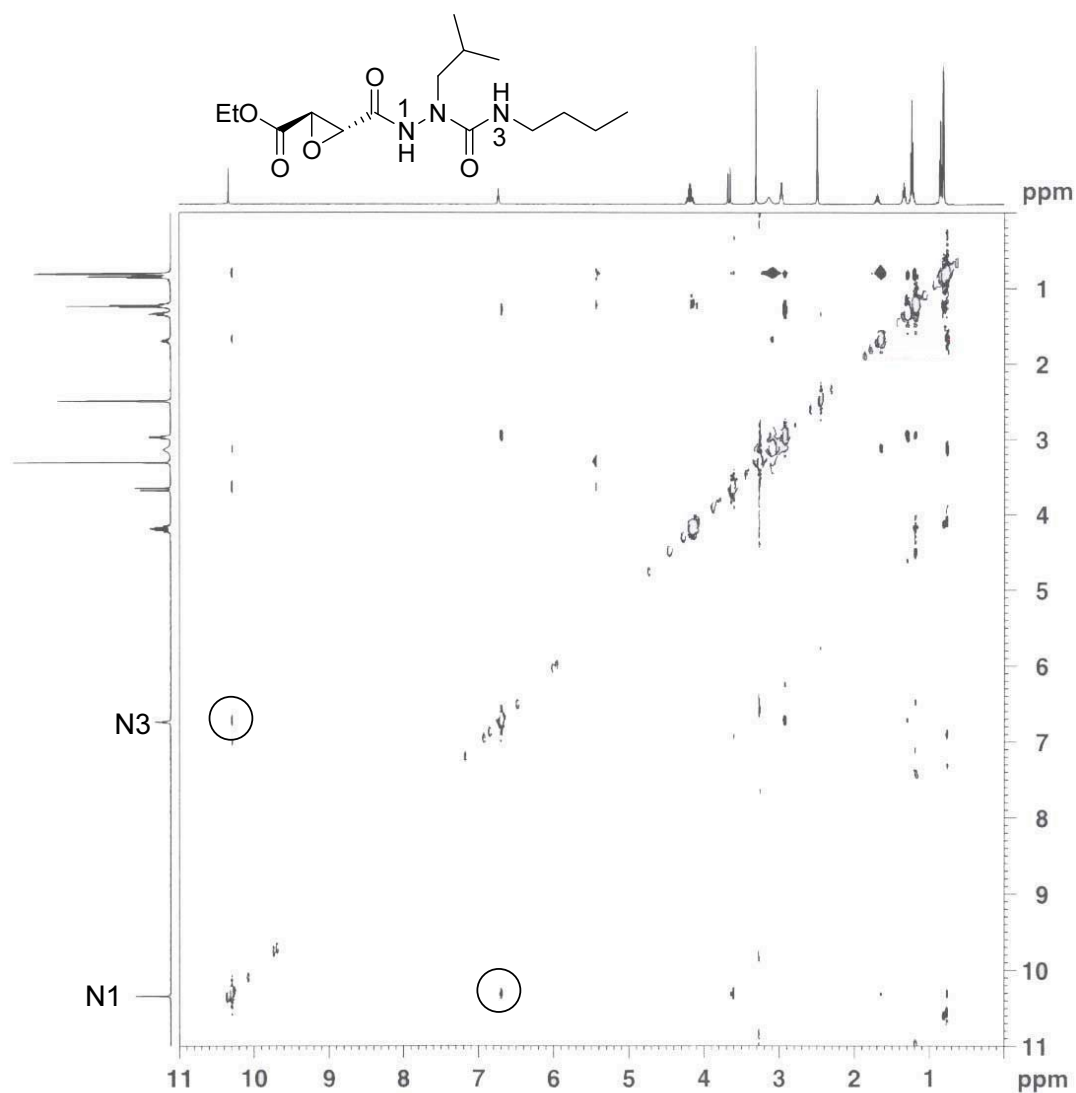


Figure 2.15 NOESY experiment of HO-(*R,R*)-Eps-ALeu-NH-butyl in DMSO- d_6

The NOESY experiment in DMSO- d_6 supports the hypothesis that intramolecular hydrogen bonding can occur in the epoxysuccinyl aza-peptide. There is an NOE between N1 and N3 protons in HO-(*R,R*)-Eps-ALeu-NH-butyl (Figure 2.15). Given that the NOESY experiment detects through-space interactions within 5 Å, it is possible that these two protons would have an NOE even in the non-twisted conformation. However, the NOESY experiment of E-64, which does not contain the aza-residue, did not show an

NOE between these two protons. Thus, the epoxysuccinyl aza-peptides could exist in the twisted conformation, to some extent, in DMSO-d₆.

In D₂O, the nitrogen protons exchange too rapidly to be detected. While there is no evidence that D₂O interacts with the N1 and N3 nitrogens of the epoxysuccinyl aza-peptide, the DMSO-d₆ NOESY experiments indicate that the proposed twisted conformation exists to some extent. This evidence provides an argument for the twisted conformation of the aza-peptide epoxides shown in Figure 2.14.

Active site differences. The twisted conformations of aza-E-64c and its derivatives do provide an elegant explanation as to why these compounds are less potent than their respective non-aza analogues. However, inhibitor HO(*S,S*)-Eps-ALeu-OCH₂Ph **II-21** lacks N3, and therefore cannot form the intramolecular hydrogen bonding shown in Figure 2.15, but still shows decreased potency compared to its non-aza ‘parent’ compound, HO(*S,S*)-Eps-Leu-OCH₂Ph, approximately 1.5-fold with cathepsin B and 7.4-fold with papain, comparing the values shown in Table 2.4 to literature values of HO(*S,S*)-Eps-Leu-OCH₂Ph.⁶³ While this decrease is not as dramatic as the decrease seen in aza-E-64c versus E-64c, the potency of HO(*S,S*)-Eps-ALeu-OCH₂Ph **II-21** is still decreased relative to its non-aza counterpart.

As mentioned, Dr. Juliana Asgian found that aza-E-64c did not allow binding of the isoamyl sidechain in the S3 subsite (unpublished results). She hypothesized that clan CA proteases could not tolerate an aza-residue because of the topology of the active sites of clan CA proteases. The active site of papain and other clan CA proteases has a narrow, canyon like shape. Also, the overall structure of the aza-peptide epoxide is very rigid because the N2-CO bond cannot rotate, as opposed to the CH- α -CO bond which

can rotate. Thus, she proposed that the active sites of clan CA proteases do not have the flexibility to easily accommodate the rigid aza-peptide inhibitor. Therefore, the potency of the epoxysuccinyl aza-peptide inhibitors, compared to their non-aza analogues, is significantly decreased.

In contrast, clan CD proteases tolerate an aza-residue very well. Aza-peptide epoxides are highly potent clan CD inhibitors. The active sites of clan CD proteases are wider and more solvent exposed than those of clan CA proteases. Thus, it is logical to assume that the topology differences explain the high potency of aza-peptide epoxides with clan CD proteases versus the marginal effectiveness that epoxysuccinyl aza-peptides have with clan CA proteases.

Also, the active sites of clan CD proteases contain charged subsites that can make strong hydrogen bonding interactions with the charged residues of clan CD inhibitors. Clan CA proteases in general have mainly hydrophobic subsites. Therefore, the sidechains of the key residues can only make favorable van der Waals contacts. Some hydrogen bonding interactions are present, but not to the extent seen in the clan CD protease-inhibitor complexes.

The hydrogen bonding interactions seen in the clan CA proteases – E-64c complexes could be disrupted by the aza-residue (see Figures 2.4 and 2.5, page 19). One cause of these disruptions, mentioned in the above discussion, is the increased rigidity of the inhibitor. In addition, the geometry of the aza-residue is altered slightly from its cognate non-aza residue. The aza-residue nitrogen has a trigonal planar geometry, rather than the tetrahedral geometry of an alpha-carbon. The hydrogen bonding interactions needed for effective binding could be disrupted, since the altered geometry of the ALeu

sidechain would cause it to have a slightly different trajectory into its binding site. In contrast, aza-peptide epoxides such as Cbz-DEVaD-EP-CO₂Et, can have strong hydrogen bonding interactions of the charged P1 aza-residue with the charged S1 subsite (see Chapter 3). These interactions aid in the binding of the aza-peptide epoxide inhibitors, thus resulting in potent inhibition of clan CD proteases. Aza-peptide epoxides and epoxysuccinyl aza-peptides with hydrophobic aza-residues, such as aza-E-64c, do not have this advantage in the inhibition of clan CA proteases.

Therefore, I propose that even with the conformational restrictions of aza-peptides removed, as seen with HO(*S,S*)-Eps-ALeu-OCH₂Ph **II-21**, the structural changes introduced by the aza-residue prevent the epoxysuccinyl aza-peptide inhibitor from interacting effectively with the S2 and S3 subsites of clan CA proteases.

CONCLUSIONS

The simple change of the alpha-carbon to a nitrogen atom, to form the aza-residue, reduced the potency of aza-E-64c and derivatives for clan CA proteases. This research shows that inhibitors with aza-residues bind preferentially to clan CD proteases such as caspases, legumain, and gingipains. The conformational properties of aza-peptidyl inhibitors were proposed as an explanation for the decreased potency caused by the aza-residue. Evidence was found for a twisted conformation caused by intramolecular hydrogen bonding in inhibitors with aza-peptide residues. However, active sites of clan CA and clan CD cysteine proteases have significant differences, both in topology and in subsite specificity. These differences also explain why aza-peptide

epoxides are potent clan CD inhibitors, while aza-peptide epoxides and epoxysuccinyl aza-peptides are only marginal clan CA inhibitors.

EXPERIMENTAL

Chemical Synthesis

Starting materials for synthesis were purchased from Fischer Scientific, Acros Organics and from Sigma Aldrich. E-64c (*L-trans*-epoxysuccinyl-Leu-3-methylbutylamide), and all substrates used in the kinetic assays were purchased from Bachem Bioscience, Inc. Calpain I was purchased from CalBiochem. Cathepsin B, Papain and E-64 (*L-trans*-epoxysuccinyl-Leu-4-guanidinobutylamide), were purchased from Sigma Aldrich. The ^1H NMR spectra were obtained using a Varian Mercury 300 MHz spectrometer. The NOESY experiments were done using a Bruker DRX 500 MHz spectrometer. Electrospray ionization (ESI), fast-atom-bombardment (FAB), and high-resolution mass spectrometry were done using Micro-mass Quattro LC and VG Analytical 70-SE instruments. Elemental analysis was performed by Atlantic Microlab Inc., Norcross, GA.

***N*¹-(*t*-Butyloxycarbonyl)-*N*²-(2-methylpropyl)hydrazine (II-3).** To a solution of *N*-(*t*-butyloxycarbonyl)-hydrazine (5 g, 37.9 mmol) in 100 mL of absolute ethanol was added isobutyraldehyde (3 g, 41.7 mmol). The mixture was heated to reflux for 3 h. The reaction was concentrated, and the oil residue was crystallized by the addition of 50 mL water. The solid was filtered and dried *in vacuo* to give the hydrazone product (6.74 g, 95% yield) homogeneous by TLC (1:19 MeOH:CH₂Cl₂).

A solution of *p*-TsOH (2.79 g, 16.13 mmol) in 13 mL THF was added dropwise over 1 h to a stirred solution of hydrazone (3 g, 16.13 mmol) and NaBH₃CN (1.01 g, 16.13 mmol) in 50 mL THF. After stirring for 4 h at room temperature, the suspension was concentrated, re-dissolved in EtOAc, and washed successively with NaHCO₃ and brine. The aqueous layers were re-extracted with EtOAc, and the combined organic layers were dried over Na₂SO₄ and concentrated. The resulting white solid was taken up in 50 mL of 1 N NaOH and stirred at room temperature for 90 min. The reaction mixture was neutralized with 3 N HCl and extracted four times with CH₂Cl₂. The combined organic layers were washed with brine, dried over Na₂SO₄, and concentrated. The crude product was purified by column chromatography on silica gel (EtOAc:CH₂Cl₂ = 1:4) yielding pure **II-3** (2.24 g, 74%). ¹H NMR (CDCl₃) 0.91-0.94 (d, 6H), 1.46 (s, 9H), 1.69-1.76 (p, 1H), 2.63-2.67 (d, 2H), 3.90 (s, 1H), 6.15 (s, 1H).

***N*¹-(*t*-Butyloxycarbonyl)-*N*²-(*N*-3-methylbutylcarbamoyl)-*N*²-(2-methylpropyl)-hydrazine (II-4, Boc-ALeu-NH-isoamyl).** A solution of isoamylamine (1.56 g, 18.0 mmol) and TEA (2.4 mL) in CH₂Cl₂ (36 mL) was added dropwise to a solution of triphosgene (4.13 g, 13.9 mmol) in CH₂Cl₂ (60.0 mL) at rt. The reaction mixture was refluxed for 4 hours. After cooling to rt, the solvent was removed under reduced pressure. A solution of **II-3** (1.23 g, 6.54 mmol) in CH₂Cl₂ (75 mL) was added to a solution of the impure isocyanate in CH₂Cl₂ (40 mL) at 0 °C. The reaction was stirred at rt overnight and was washed with H₂O and brine. The organic layer was dried with MgSO₄ and concentrated. Chromatography (EtOAc:hexane = 1:2) on a silica gel column afforded a white solid (0.95g, 49 %). ¹H NMR (CDCl₃) 0.91 (d, *J* = 6.8 Hz, 12H, ALeu CH₃, isoamyl CH₃), 1.37 (q, *J* = 7.2 Hz, 2H, NHCH₂CH₂CH), 1.48 (s, 9H, *t*-Bu), 1.84 (m,

1H, ALeu CH), 3.23 (s, 4H, NHCH₂CH₂CH, ALeu CH₂), 5.24 (s, 1H, NH), 6.10 (s, 1H, NH). MS (ESI): *m/z* 302.2 (M + H⁺).

***N*¹-(*t*-Butyloxycarbonyl)-*N*²-(*N*-3-butylcarbamoyl)-*N*²-(2-methylpropyl)hydrazine (II-5, Boc-ALeu-NH-butyl).** A solution of benzyl isocyanate (0.56 g, 4.24 mmol) in dry THF (30 mL) was added dropwise to a solution of **II-3** (0.81 g, 4.29 mmol) in dry THF (60 mL) dropwise at 0 °C. The reaction was stirred at 0 °C for 15 minutes and was then stirred at rt overnight. The solvent was removed under reduced pressure. Recrystallized from MeOH:CH₂Cl₂ = 1:9/hexane, giving a white solid (1.0 g, 74 %). ¹H NMR (CDCl₃) 0.93 (d, *J* = 6.8 Hz, 6H, ALeu CH₃), 1.44 (s, 9H, *t*-Bu), 1.86 (m, 1H, ALeu CH), 3.23 (s, 2H, ALeu CH₂), 4.43 (s, 2H, CH₂Ph), 5.66 (s, 1H, NH), 6.29 (s, 1H, NH), 7.28 (m, 5H, CH₂Ph). MS (ESI): *m/z* 322.1 (M + H⁺).

***N*¹-(*t*-Butyloxycarbonyl)-*N*²-(*N*-3-benzylcarbamoyl)-*N*²-(2-methylpropyl)hydrazine (II-6, Boc-ALeu-NH-benzyl).** Compound **II-6** was prepared as the same method as **II-5** using CH₂Cl₂ as the solvent instead of dry THF. ¹H NMR (CDCl₃) 0.91 (m, 9H, ALeu CH₃, butyl CH₃), 1.33 (m, 2H, NHCH₂CH₂CH₂CH₃), 1.46 (m, 11H, *t*-Bu, NHCH₂CH₂CH₂CH₃), 1.84 (m, 1H, ALeu CH), 3.21 (s, 4H, ALeu CH₂, NHCH₂CH₂CH₂CH₃), 5.30 (s, 1H, NH), 6.22 (s, 1H, NH). MS (ESI): *m/z* 288.1 (M + H⁺).

***N*¹-(*t*-Butyloxycarbonyl)-*N*²-(*N*-3-benzyloxycarbonyl)-*N*²-(2-methylpropyl)hydrazine (II-7, Boc-ALeu-O-benzyl).** Cbz-chloroformate was added dropwise to a solution of **II-3** (0.50 g, 2.66 mmol) in dry THF (20 mL). TEA (0.31 g, 3.01 mmol) was added and the reaction mixture was heated to reflux for 5 h. The solvent was removed, and the residue was taken up in EtOAc (20 mL). The organic layer was washed with H₂O (10 mL) and

brine (10 mL), was dried with Na₂SO₄, and was concentrated. Chromatography (EtOAc:hexane = 3:7) on a silica gel column afforded a white solid (0.45 g, 52 %). ¹H NMR (CDCl₃) 0.91 (s, 6H, ALeu CH₃), 1.44 (s, 9H, *t*-Bu), 1.93 (m, 1H, ALeu CH), 3.34 (s, 2H, ALeu CH₂), 5.16 (s, 2H, CH₂Ph), 6.36 (s, 1H, NH), 7.31 (m, 5H, CH₂Ph).

***N*¹-(*t*-Butyloxycarbonyl)-*N*²-(*N*-piperidine-1-carbonyl)-*N*²-(2-methylpropyl)-**

hydrazine (II-8, Boc-ALeu-*N*-piperidine). A solution of **II-3** (0.48 g, 2.56 mmol) in

CH₂Cl₂ (5 mL) was added to a solution of CDI (0.49 g, 3.03 mmol) in CH₂Cl₂ (10 mL).

The reaction mixture was refluxed for 24 h. After cooling to rt, the reaction mixture was washed with cold H₂O (20 mL), dried with Na₂SO₄, and concentrated. The light yellow gel was dissolved in MeCN (5 mL), and was followed by the dropwise addition of MeI (1.06 g, 7.48 mmol). The reaction was allowed to stir 24 h at rt. The solvent was

removed, and the dark yellow gel was dissolved in CH₂Cl₂ (20 mL). A solution of piperidine (0.48 g, 5.65 mmol), TEA (0.8 mL) in CH₂Cl₂ (5 mL) was added dropwise.

The reaction mixture was stirred overnight at rt and then concentrated. Chromatography

(EtOAc:hexane = 1:1) on a silica gel column afforded a white solid (0.31 g, 17 %). ¹H NMR (CDCl₃) 0.91 (d, *J* = 6.8 Hz, 6H, ALeu CH₃), 1.46 (s, 9H, *t*-Bu), 1.57 (m, 4H, NCH₂CH₂CH₂), 1.66 (m, 2H, NCH₂CH₂CH₂), 1.95 (m, 1H, ALeu CH), 3.06 (s, 2H, ALeu CH₂), 3.31 (m, 4H, NCH₂CH₂CH₂), 6.59 (s, 1H, NH).

***N*¹-(*t*-Butyloxycarbonyl)-*N*²-(*N*-1,2,3,4-tetrahydroisoquinoline-2-carbonyl)-*N*²-(2-**

methylpropyl)hydrazine (II-9, Boc-ALeu-*N*-tetrahydroisoquinoline). Compound **II-**

9 was prepared by the same method used for **II-8**. ¹H NMR (CDCl₃) 0.93 (d, *J* = 6.8 Hz, 6H, ALeu CH₃), 1.42 (s, 9H, *t*-Bu), 1.97 (m, 1H, ALeu CH), 2.89 (s, 2H, ALeu CH₂),

3.16 (m, 2H, $\text{NCH}_2\text{CH}_2\text{ArH}$), 3.64 (m, 2H, $\text{NCH}_2\text{CH}_2\text{ArH}$), 4.54 (s, 2H, NCH_2ArH), 6.54 (s, 1H, NH), 7.18, (m, 4H, ArH).

(2*S*,3*S*)-3-(*N*²-(*N*-3-methylbutylcarbonyl)-*N*²-2-methylpropylhydrazinyl)-oxirane-2-carboxylic acid ethyl ester (II-12a, EtO(*S,S*)-Eps-ALeu-NH-isoamyl).

Semicarbazide **II-4** (0.214 g, 0.711 mmol) was cooled to 0°C and dissolved in 4N HCl in EtOAc (2.2 mL, 8.8 mmol). The mixture was allowed to stir at 0°C until reaction was complete by TLC. The reaction was concentrated, and the residue was triturated in ether to yield the solid hydrochloride salt (151 mg, 0.502 mmol, 90%).

A solution of ethyl(2*S*,3*S*)-oxirane-2,3-dicarboxylate (0.115 g, 0.719 mmol) in 10 mL EtOAc was cooled to -20°C. To this solution was added NMM (0.085 g, 0.841 mmol) followed by isobutylchloroformate (IBCF) (0.112 g, 0.817 mmol) dropwise. The solution was allowed to stir for 20 min during which a white precipitate formed. A DMF solution of the hydrochloride salt (0.151 g, 0.638 mmol) and NMM (0.087 g, 0.861 mmol) was added to the flask, and the reaction was allowed to stir for 1 h at -20°C, then at room temperature overnight. The solvents were removed, and the residue was dissolved in EtOAc and washed with equal volumes of water, 2% citric acid, saturated NaHCO_3 , and brine. The organic layer was dried over Na_2SO_4 and concentrated. The crude product was purified by column chromatography on silica gel ($\text{EtOAc}:\text{CH}_2\text{Cl}_2 = 1:2$) to yield **II-12a** (58 mg, 26%). ^1H NMR (CDCl_3) 0.91 (m, 12H, ALeu CH_3 , isoamyl CH_3), 1.36 (m, 5H, $\text{CH}_3\text{CH}_2\text{O}$, $\text{NHCH}_2\text{CH}_2\text{CH}$), 1.59 (m, 1H, isoamyl CH), 1.76 (m, 1H, ALeu CH), 3.30 (m, 4H, ALeu CH_2 , $\text{NHCH}_2\text{CH}_2\text{CH}$), 3.59 (d, $J = 1.6$ Hz, 1H, epoxide CH), 3.78 (d, $J = 1.6$ Hz, 1H, epoxide, CH), 4.29 (m, 2H, $\text{CH}_3\text{CH}_2\text{O}$), 7.69 (s, 1H, NH). HRMS (FAB) Calcd. for $\text{C}_{16}\text{H}_{30}\text{N}_3\text{O}_5$: 344.21855. Observed m/z 344.21786. Anal.

Calcd. for C₁₆H₂₉N₃O₅: C, 55.96; H, 8.51; N, 12.24. Found: C, 55.74; H, 8.44; N, 11.94%.

(2*R*,3*R*)-3-(*N*²-(*N*-3-methylbutylcarbamoyl)-*N*²-2-methylpropylhydrazinocarbonyl)-oxirane-2-carboxylic acid ethyl ester (II-12b, EtO(*R,R*)-Eps-ALeu-NH-isoamyl). (59

mg, 23%) ¹H NMR (CDCl₃) 0.90 (m, 12H, ALeu CH₃, isoamyl CH₃), 1.36 (m, 5H, CH₃CH₂O, NHCH₂CH₂CH), 1.59 (m, 1H, isoamyl CH), 1.76 (m, 1H, ALeu CH), 3.30 (m, 4H, ALeu CH₂, NHCH₂CH₂CH), 3.58 (d, *J* = 1.6 Hz, 1H, epoxide CH), 3.79 (d, *J* = 1.6 Hz, 1H, epoxide, CH), 4.29 (m, 2H, CH₃CH₂O), 7.70 (s, 1H, NH). HRMS (FAB)

Calcd. for C₁₆H₃₀N₃O₅: 344.21855. Observed *m/z* 344.21962. Anal. Calcd. for C₁₆H₂₉N₃O₅: C, 55.96; H, 8.51; N, 12.24. Found: C, 55.70; H, 8.65; N, 12.20%.

(2*S*,3*S*)-3-(*N*²-(*N*-benzylcarbamoyl)-*N*²-2-methylpropylhydrazinocarbonyl)oxirane-2-carboxylic acid ethyl ester (II-14a, EtO(*S,S*)-Eps-ALeu-NH-benzyl). (32 mg, 22%)

¹H NMR (CDCl₃) δ 0.92 (d, *J* = 8 Hz, 6H, ALeu CH₃), 1.34 (t, *J* = 6 Hz, 3H, CH₃CH₂), 1.79 (m, 1H, ALeu CH), 3.38 (m, 6H, ALeu CH₂), 3.58 (d, *J* = 1.8 Hz, 1H, epoxide CH), 3.79 (d, *J* = 2 Hz, 1H, epoxide CH), 4.27 (m, 2H, CH₃CH₂), 4.42 (d, *J* = 7.2 Hz, 2H, CH₂Ph), 5.12 (t, *J* = 6 Hz, 1H, NH), 7.28 (m, 5H, ArH), 7.63 (s, 1H, NH). HRMS (FAB)

Calcd. for C₁₈H₂₆N₃O₅: 364.18725. Observed *m/z* 364.18764. Anal. Calcd. for C₁₈H₂₅N₃O₅·0.3H₂O: C, 58.62; H, 7.00; N, 11.40. Found: C, 58.77; H, 7.11; N, 11.11%.

(2*R*,3*R*)-3-(*N*²-(*N*-benzylcarbamoyl)-*N*¹-2-methylpropylhydrazinocarbonyl)oxirane-2-carboxylic acid ethyl ester (II-14b, EtO(*R,R*)-Eps-ALeu-NH-benzyl). (44 mg,

18%) ¹H NMR (CDCl₃) δ 0.94 (d, *J* = 8.4 Hz, 6H, ALeu CH₃), 1.33 (t, *J* = 5.6 Hz, 3H, CH₃CH₂), 1.88 (m, 1H, ALeu CH), 3.32 (m, 6H, ALeu CH₂), 3.56 (d, *J* = 1.8 Hz, 1H,

epoxide *CH*), 3.75 (d, *J* = 2 Hz, 1H, epoxide *CH*), 4.27 (m, 2H, *CH*₃*CH*₂), 4.41 (d, *J* = 5.6 Hz, 2H, *CH*₂Ph), 5.13 (t, *J* = 6 Hz, 1H, *NH*), 7.28 (m, 5H, ArH), 7.76 (s, 1H, *NH*).

HRMS (FAB) Calcd. for C₁₈H₂₆N₃O₅: 364.187725. Observed *m/z* 364.18743. Anal.

Calcd. for C₁₈H₂₅N₃O₅·0.3H₂O: C, 58.62; H, 7.00; N, 11.40. Found: C, 58.66; H, 6.92; N, 11.43%.

(2*S*,3*S*)-3-(*N*²-(*N*-butylcarbamoyl)-*N*¹-2-methylpropylhydrazinocarbonyl)oxirane-2-carboxylic acid ethyl ester (II-13a, EtO(*S,S*)-Eps-ALeu-NH-butyl). (83 mg, 35%) ¹H

NMR (CDCl₃) δ 0.93 (m, 9H, ALeu *CH*₃ and butyl *CH*₃), 1.38 (m, 5H, *CH*₃*CH*₂ and *NHCH*₂*CH*₂*CH*₂*CH*₃), 1.48 (m, 2H, *NHCH*₂*CH*₂*CH*₂*CH*₃), 1.78 (m, 1H, ALeu *CH*), 3.31 (m, 6H, ALeu *CH*₂ and *NHCH*₂*CH*₂*CH*₂*CH*₃), 3.59 (d, *J* = 1.8 Hz, 1H, epoxide *CH*), 3.70 (d, *J* = 2 Hz, 1H, epoxide *CH*), 4.29 (m, 2H, *CH*₃*CH*₂), 4.80 (s, 1H, *NH*), 7.67 (s, 1H, *NH*). HRMS (FAB) Calcd. for C₁₅H₂₈N₃O₅: 330.20290. Observed *m/z* 330.20202.

Anal. Calcd. for C₁₅H₂₇N₃O₅·0.4H₂O: C, 53.52; H, 8.32; N, 12.48. Found: C, 53.68; H, 8.35; N, 12.33%.

(2*R*,3*R*)-3-(*N*²-(*N*-butylcarbamoyl)-*N*²-2-methylpropylhydrazinocarbonyl)oxirane-2-carboxylic acid ethyl ester (II-13b, EtO(*R,R*)-Eps-ALeu-NH-butyl). (135 mg, 33%)

¹H NMR (CDCl₃) δ 0.92 (m, 9H, ALeu *CH*₃ and butyl *CH*₃), 1.35 (m, 5H, *CH*₃*CH*₂ and *NHCH*₂*CH*₂*CH*₂*CH*₃), 1.46 (m, 2H, *NHCH*₂*CH*₂*CH*₂*CH*₃), 1.78 (m, 1H, ALeu *CH*), 3.30 (m, 6H, ALeu *CH*₂ and *NHCH*₂*CH*₂*CH*₂*CH*₃), 3.60 (d, *J* = 1.8 Hz, 1H, epoxide *CH*), 3.71 (d, *J* = 2 Hz, 1H, epoxide *CH*), 4.28 (m, 2H, *CH*₃*CH*₂), 4.79 (s, 1H, *NH*), 7.65 (s, 1H, *NH*). HRMS (FAB) Calcd. for C₁₅H₂₈N₃O₅: 330.20290. Observed *m/z* 330.20321.

Anal. Calcd. for C₁₅H₂₇N₃O₅: C, 54.69; H, 8.26; N, 12.76. Found: C, 54.71; H, 8.09; N, 12.74%.

(2*S*,3*S*)-3-(*N*²-(*N*-benzyloxycarbonyl)-*N*²-2-methylpropylhydrazinocarbonyl)-oxirane-2-carboxylic acid ethyl ester (II-15, EtO(*S,S*)-Eps-ALeu-O-benzyl). (40 mg, 27%) ¹H NMR (CDCl₃) δ 0.91 (m, 6H, ALeu CH₃), 1.32 (t, *J* = 7.2 Hz, 3H, CH₃CH₂), 1.84 (m, 1H, ALeu CH), 3.32 (m, 2H, ALeu CH₂), 3.72 (m, 2H, epoxide CH), 4.25 (d, *J* = 6.4, 2H, CH₃CH₂), 5.10 (s, 2H, CH₂Ar), 7.31 (m, 5H, ArH), 7.65 (s, 1H, NH). HRMS (ESI) Calcd. for C₁₃H₂₅N₂O₆: 365.171262. Observed *m/z* 365.1706.

(2*S*,3*S*)-3-(*N*²-(*N*-piperidine-1-carbonyl)-*N*²-2-methylpropylhydrazinocarbonyl)-oxirane-2-carboxylic acid ethyl ester (II-16, EtO(*S,S*)-Eps-ALeu-*N*-piperidine). (67 mg, 43%) ¹H NMR (CDCl₃) δ 0.91 (dd, *J* = 4.8 Hz and 2Hz, 6H, ALeu CH₃), 1.31 (t, *J* = 7.6 Hz, 3H, CH₃CH₂), 1.88 (m, 1H, ALeu CH), 3.04 (m, 6H, NCH₂CH₂CH₂CH₂), 3.34 (m, 6H, ALeu CH₂ and NCH₂CH₂), 3.59 (d, *J* = 1.6 Hz, 1H, epoxide CH), 3.70 (d, *J* = 2 Hz, 1H, epoxide CH), 4.24 (m, 2H, CH₃CH₂), 7.96 (s, 1H, NH). HRMS (FAB) Calcd. for C₁₆H₂₈N₃O₅: 342.20290. Observed *m/z* 342.20849. Anal. Calcd. for C₁₆H₂₇N₃O₅: C, 56.29; H, 7.97; N, 12.31. Found: C, 56.45; H, 8.15; N, 12.30%.

(2*S*,3*S*)-3-(*N*²-(*N*-1,2,3,4-tetrahydroisoquinoline-2-carbonyl)-*N*²-2-methylpropylhydrazinocarbonyl)-oxirane-2-carboxylic acid ethyl ester (II-17, EtO(*S,S*)-Eps-ALeu-*N*-tetrahydroisoquinoline). (69 mg, 50%) ¹H NMR (CDCl₃) δ 0.95 (dd, *J* = 6.4 Hz and 2.8 Hz, 6H, ALeu CH₃), 1.31 (t, *J* = 7.2 Hz, 3H, CH₃CH₂), 1.89 (m, 1H, ALeu CH), 2.91 (t, *J* = 6 Hz, 2H, CH₂Ar), 3.16 (m, 2H, ALeu CH₂), 3.55 (d, *J* = 1.6 Hz, 1H, epoxide CH), 3.66 (t, *J* = 5.6 Hz, 2H, CH₂N), 3.70 (d, *J* = 2Hz, 1H, epoxide CH), 4.26 (m, 2H, CH₃CH₂), 4.55 (s, 2H, NCH₂Ar), 7.18 (m, 4H, ArH), 7.94 (s, 1H, NH). HRMS (ESI) Calcd. for C₂₀H₂₈N₃O₅: 390.202896. Observed *m/z* 390.2034.

(2*S*,3*S*)-3-(*N*²-(*N*-3-methylbutylcarbamoyl)-*N*²-2-methylpropylhydrazinocarbonyl)-oxirane-2-carboxylic acid (II-18a, HO(*S,S*)-Eps-ALeu-NH-isoamyl). A solution of **II-12a** (0.045 g, 0.131 mmol) in 1.5 mL EtOH was cooled to 0°C. To the solution was added 1M NaOH (143 µL), and the reaction was allowed to stir for 1 h at 0°C, then at room temperature until reaction was shown to be complete by TLC. The solvent was removed, and the white solid residue was taken up in water (15 mL) and washed once with EtOAc (5mL). The aqueous layer was cooled to 0°C and the pH was adjusted to 3 with 3N HCl. The aqueous layer was extracted four times with EtOAc (50 mL), and the combined EtOAc layers were dried over Na₂SO₄ and concentrated. The crude product was recrystallized from ether/hexanes to yield the white solid **II-18a** (9 mg, 23%). ¹H NMR ((CD₃)₂SO) 0.81 (d, *J* = 6.8 Hz, 6H, isoamyl CH₃), 0.85 (d, *J* = 6.4 Hz, 6H, ALeu CH₃), 1.26 (q, *J* = 7.2 Hz, 1H, NHCH₂CH₂CH), 1.52 (m, 1H, isoamyl CH), 1.69 (m, 1H, ALeu CH), 2.98 (m, 2H, NHCH₂CH₂CH), 3.13 (s, 2H, ALeu CH₂), 3.53 (d, *J* = 1.6 Hz, 1H, epoxide CH), 3.58 (d, *J* = 1.6 Hz, 1H, epoxide CH), 6.73 (t, *J* = 5.2 and *J* = 6.4, 1H, NH), 10.30 (s, 1H, NH). HRMS (FAB) Calcd. for C₁₄H₂₆N₃O₅: 316.18725. Observed *m/z* 316.18838. Anal. Calcd. for (C₁₄H₂₅N₃O₅·0.25Na·0.03H₂O) C, 52.26; H, 8.02; N, 13.06. Found: C, 52.42; H, 7.98; N, 12.67%.

(2*R*,3*R*)-3-(*N*²-(*N*-3-methylbutylcarbamoyl)-*N*²-2-methylpropylhydrazinocarbonyl)-oxirane-2-carboxylic acid (II-18b, HO(*R,R*)-Eps-ALeu-NH-isoamyl). (9 mg, 20%) ¹H NMR ((CD₃)₂SO) 0.83 (d, *J* = 6.8 Hz, 6H, isoamyl CH₃), 0.86 (d, *J* = 6.4 Hz, 6H, ALeu CH₃), 1.27 (q, *J* = 7.2 Hz, 1H, NHCH₂CH₂CH), 1.51 (m, 1H, isoamyl CH), 1.68 (m, 1H, ALeu CH), 2.97 (m, 2H, NHCH₂CH₂CH), 3.34 (s, 2H, ALeu CH₂), 3.55 (d, *J* = 1.6 Hz, 1H, epoxide CH), 3.59 (d, *J* = 1.6 Hz, 1H, epoxide CH), 6.72 (t, *J* = 5.2 and *J* =

6.4, 1H, NH), 10.31 (s, 1H, NH). HRMS (FAB) Calcd. for C₁₄H₂₆N₃O₅: 316.18725.

Observed *m/z* 316.18745. Anal. Calcd. for (C₁₄H₂₅N₃O₅·0.1Na·0.5H₂O) C, 51.47; H, 8.02; N, 12.86. Found: C, 51.70; H, 7.94; N, 12.62%.

(2*S*,3*S*)-3-(*N*²-(*N*-benzylcarbamoyl)-*N*²-2-methylpropylhydrazinocarbonyl)oxirane-2-carboxylic acid (II-20a, HO(*S,S*)-Eps-ALeu-NH-benzyl). (32 mg, 68%) ¹H NMR ((CD₃)₂SO) δ 0.81 (d, *J* = 8 Hz, 6H, ALeu CH₃), 1.74 (m, 1H, ALeu CH), 3.21 (m, 6H, ALeu CH₂), 3.55 (d, *J* = 1.8 Hz, 1H, epoxide CH), 3.60 (d, *J* = 2 Hz, 1H, epoxide CH), 4.19 (m, 2H, CH₂Ph), 7.24 (m, 5H, ArH), 7.40 (t, *J* = 4 Hz, 1H, NH), 10.26 (s, 1H, COOH). HRMS (FAB) Calcd. for C₁₆H₂₂N₃O₅: 336.155595. Observed *m/z* 336.15721. Anal. Calcd. for C₁₆H₂₁N₃O₅·0.025Na·0.05H₂O: C, 57.02; H, 6.43; N, 12.47. Found: C, 57.07; H, 6.41; N, 12.17%.

(2*R*,3*R*)-3-(*N*²-(*N*-benzylcarbamoyl)-*N*²-2-methylpropylhydrazinocarbonyl)oxirane-2-carboxylic acid (II-20b, HO(*R,R*)-Eps-ALeu-NH-benzyl). (37 mg, 65%) ¹H NMR ((CD₃)₂SO) δ 0.82 (d, *J* = 8 Hz, 6H, ALeu CH₃), 1.75 (m, 1H, ALeu CH), 3.25 (m, 6H, ALeu CH₂), 3.56 (d, *J* = 1.8 Hz, 1H, epoxide CH), 3.59 (d, *J* = 2 Hz, 1H, epoxide CH), 4.18 (m, 2H, CH₂Ph), 7.28 (m, 5H, ArH), 7.45 (t, *J* = 4 Hz, 1H, NH), 10.31 (s, 1H, COOH). HRMS (FAB) Calcd. for C₁₆H₂₂N₃O₅: 336.155595. Observed *m/z* 336.15648. Anal. Calcd. for C₁₆H₂₁N₃O₅: C, 57.30; H, 6.31; N, 12.53. Found: C, 57.12; H, 6.35; N, 12.31%.

(2*S*,3*S*)-3-(*N*²-(*N*-butylcarbamoyl)-*N*²-2-methylpropylhydrazinocarbonyl)oxirane-2-carboxylic acid (II-19a, HO(*S,S*)-Eps-ALeu-NH-butyl). (31 mg, 51%) ¹H NMR ((CD₃)₂SO) 0.92 (m, 9H, ALeu CH₃, butyl CH₃), 1.23 (m, 2H, NHCH₂CH₂CH₂CH₃), 1.34 (m, 2H, NHCH₂CH₂CH₂CH₃), 1.66 (m, 1H, ALeu CH), 2.95 (m, 2H,

NHCH₂CH₂CH₂CH₃), 3.13 (m, 2H, ALeu CH₂), 3.57 (d, *J* = 2.0 Hz, 1H, epoxide CH), 3.60 (d, *J* = 1.8 Hz, 1H, epoxide CH), 6.73 (t, 1H, NH), 10.31 (s, 1H, NH). HRMS (FAB) Calcd. for C₁₃H₂₄N₃O₅: 302.17160. Observed *m/z* 302.16944. Anal. Calcd. for C₁₃H₂₃N₃O₅·0.03H₂O·0.15Na·0.025C₆H₁₄: C, 51.35; H, 7.85; N, 13.67. Found: C, 51.44; H, 7.77; N, 13.55%.

(2*R*,3*R*)-3-(*N*²-(*N*-butylcarbamyol)-*N*²-2-methylpropylhydrazinocarbonyl)oxirane-2-carboxylic acid (II-19b, HO(*R,R*)-Eps-ALeu-NH-butyl). (54 mg, 64%) ¹H NMR ((CD₃)₂SO) 0.93 (m, 9H, ALeu CH₃, butyl CH₃), 1.24 (m, 2H, NHCH₂CH₂CH₂CH₃), 1.32 (m, 2H, NHCH₂CH₂CH₂CH₃), 1.69 (m, 1H, ALeu CH), 2.99 (m, 2H, NHCH₂CH₂CH₂CH₃), 3.17 (m, 2H, ALeu CH₂), 3.56 (d, *J* = 2.0 Hz, 1H, epoxide CH), 3.59 (d, *J* = 1.8 Hz, 1H, epoxide CH), 6.79 (t, 1H, NH), 10.35 (s, 1H, NH). HRMS (FAB) Calcd. for C₁₃H₂₄N₃O₅: 302.17160. Observed *m/z* 302.17331. Anal. Calcd. for C₁₃H₂₃N₃O₅·0.025H₂O·0.2Na·0.25C₄H₈O: C, 51.82; H, 7.92; N, 12.95. Found: C, 51.88; H, 7.87; N, 12.88%.

(2*S*,3*S*)-3-(*N*²-(*N*-benzyloxycarbonyl)-*N*²-2-methylpropylhydrazinocarbonyl)-oxirane-2-carboxylic acid (II-21, HO(*S,S*)-Eps-ALeu-O-benzyl). (28 mg, 86%) ¹H NMR ((CD₃)₂SO) δ 0.83 (m, 6H, ALeu CH₃), 1.78 (m, 1H, ALeu CH), 3.19 (d, *J* = 6 Hz, 2H, ALeu CH₂), 3.58 (m, 2H, epoxide CH), 5.05 (s, 2H, CH₂Ar), 7.30 (m, 5H, ArH), 10.72 (s, 1H, COOH). HRMS (TOF): 337.1. Observed *m/z* 337.139962. Calcd. for C₁₆H₂₁N₂O₆·0.05H₂O·0.15Na: C, 56.39; H, 6.21; N, 8.22. Found: C, 56.49, H, 6.19, N, 8.18%.

(2*S*,3*S*)-3-(*N*²-(*N*-piperidine-1-carbonyl)-*N*²-2-methylpropylhydrazinocarbonyl)-oxirane-2-carboxylic acid (II-22, HO(*S,S*)-Eps-ALeu-*N*-piperidine). (40 mg, 78%)

¹H NMR ((CD₃)₂SO) δ 0.81 (d, *J* = 8 Hz, 6H, ALeu CH₃), 1.38 (m, 4H, NCH₂CH₂CH₂), 1.50 (d, *J* = 4 Hz, 2H, CH₂CH₂CH₂), 1.78 (m, 1H, ALeu CH), 3.00 (d, *J* = 3.2 Hz, 2H, ALeu CH₂), 3.14 (t, *J* = 6 Hz, 4H, NCH₂CH₂CH₂), 3.47 (d, *J* = 2 Hz, 1H, epoxide CH), 3.57 (d, *J* = 1.8 Hz, 1H, epoxide CH), 10.37 (s, 1H, COOH). HRMS (TOF) Calcd. for C₁₄H₂₄N₃O₅: 314.3596. Observed *m/z* 314.171596. Anal. Calcd. for C₁₄H₂₃N₃O₅: C, 53.66; H, 7.40; N, 13.41. Found: C, 53.69; H, 7.44; N, 13.23%.

(2*S*,3*S*)-3-(*N*²-(*N*-1,2,3,4-tetrahydroisoquinoline-2-carbonyl)-*N*²-2-methylpropyl-hydrazinocarbonyl)-oxirane-2-carboxylic acid (II-23, HO(*S,S*)-Eps-ALeu-*N*-tetrahydroisoquinoline). (45 mg, 77%) ¹H NMR (400 MHz, (CD₃)₂SO) δ 0.85 (dd, *J* = 3.6 Hz and 2.8 Hz, 6H, ALeu CH₃), 1.78 (m, 1H, ALeu CH), 2.74 (t, 2H, CH₂Ar), 3.07 (m, 2H, ALeu CH₂), 3.43 (d, *J* = 1.8 Hz, 1H, epoxide CH), 3.56 (d, *J* = 2.0 Hz, 1H, epoxide CH), 4.34 (s, 2H, NCH₂Ar), 7.12 (m, 4H, ArH), 10.31 (s, 1H, NH), 10.67 (s, 1H, COOH). HRMS (TOF) Calcd. for C₁₈H₂₄N₃O₅: 362.4036. Observed *m/z* 362.171596. Anal. Calcd. for C₁₈H₂₃N₃O₅·0.05Na·0.05H₂O·0.3C₄H₈O₂: C, 59.15; H, 6.59; N, 10.78. Found: C, 59.40; H, 6.80; N, 10.70%.

Enzymatic Assays

The progress curve method, as described by Tian and Tsou, was used for all kinetic assays unless otherwise indicated, with [I]/[E] ratio greater than or equal to 10:1.³⁶ All assays were done using a Tecan Spectra Fluor microplate reader.

Papain. The papain kinetic buffer (55 mM HEPES, 2.5 mM EDTA, pH 7.5) was supplemented with DTT (0.1 mM) to a DTT concentration of 0.85 μM. To of papain kinetic buffer with DTT (222 μL), Cbz-Phe-Arg-*p*Na in DMSO (20 μL) was added. A

4.2 μL aliquot of DMSO (control) or inhibitor was then added. The reaction was initiated by the addition of the activated enzyme (4.2 μL). Papain was activated by the addition of 0.1 mM DTT (35 μL) and papain kinetic buffer (955 μL) to papain enzyme stock in DMSO (10 μL , approximate concentration 1.18 mg/mL). The final volume in the reaction well was 250.4 μL . Absorbance was measured at $\lambda = 405 \text{ nm}$. Final concentrations of DTT (0.81 μM), Cbz-Phe-Arg-*p*NA ($5.59 \times 10^{-4} \text{ M}$), inhibitor ($2.10 \times 10^{-7} \text{ M}$ to $1.68 \times 10^{-4} \text{ M}$), and papain (approximately $8.61 \times 10^{-6} \mu\text{M}$) were calculated. For papain, the k_2 values are 1.70 higher than the apparent rate constant because of the final substrate concentration of $5.59 \times 10^{-4} \text{ M}$ and the $K_M = 0.798 \mu\text{M}$.

Cathepsin B. To a well with 237 μL cathepsin B kinetic buffer (0.1 M sodium phosphate, 1.25 mM EDTA, 0.01% Brij 35, pH 6.0) was added 5 mL of Cbz-Arg-Arg-AMC (20 mM) and 4.2 mL of DMSO (control) or inhibitor in DMSO. The reaction was initiated by the addition of a 4.2 μL aliquot of activated enzyme. The final volume in the reaction well was 250.4 μL . The enzyme was activated by the addition of cathepsin B kinetic buffer (267 μL) and 0.1 M DTT (3 μL) to the enzyme stock solution (30 μL). Activation was complete after approximately 30 minutes. The reaction was monitored by the release of 7-amino-4-methylcoumarin ($\lambda_{\text{ex}} = 360 \text{ nm}$, $\lambda_{\text{em}} = 465 \text{ nm}$). Final concentrations of Cbz-Arg-Arg-AMC (0.40 mM), inhibitor ($9.06 \times 10^{-7} \text{ M}$ to $1.68 \times 10^{-4} \text{ M}$), and cathepsin B (approximately $3.02 \times 10^{-9} \text{ M}$) were calculated. For cathepsin B, the k_2 values are 2.74 higher than the apparent rate constant because of the final substrate concentration of $4.0 \times 10^{-4} \text{ M}$ and the $K_M = 2.3 \mu\text{M}$.

Calpain I. Calpain kinetic buffer (50 mM HEPES, pH 7.5) was supplemented with cysteine (6.5 μM) and CaCl_2 (13 μM). To this buffer (235 mL) was added a 6.5 μL

aliquot of Suc-Leu-Tyr-AMC in DMSO and a 4.2 μL aliquot of DMSO (control) or inhibitor solution in DMSO. The reaction was initiated by the addition of a 4.2 μL aliquot of enzyme (0.8 mg/mL) to the well. The reaction was monitored by the release of 7-amino-4-methylcoumarin ($\lambda_{\text{ex}} = 360 \text{ nm}$, $\lambda_{\text{em}} = 465 \text{ nm}$). Total volume in the reaction well was 249.9 μL . Final concentrations of Suc-Leu-Tyr-AMC (1.30 mM), inhibitor ($2.63 \times 10^{-6} \text{ M}$ to $1.68 \times 10^{-4} \text{ M}$), and calpain I ($1.20 \times 10^{-7} \text{ M}$) were calculated. For calpain I, the k_2 values are 1.274 higher than the apparent rate constant because of the final substrate concentration of $1.3 \times 10^{-3} \text{ M}$ and the $K_M = 4.74 \mu\text{M}$.

CHAPTER 3

AZA-PEPTIDE EPOXIDES AS INHIBITORS OF CASPASES: HOW EPOXIDE STEREOCHEMISRY AND PRIME SIDE SUBSTITUENT EFFECT POTENCY AND SELECTIVITY

INTRODUCTION

Caspases and apoptosis

Apoptosis, or programmed cell death, is necessary for normal organism development. However, in certain disease states, such as neurodegenerative disorders and traumatic brain and spinal cord injury, apoptosis becomes excessive. Since apoptotic caspases perform the protein degradation that is an essential part of the apoptotic cascade, they have been identified as potential drug targets for disease states with excessive apoptosis.⁸⁶⁻⁸⁹ Caspase-independent apoptosis pathways have been proposed.⁹⁰⁻⁹² Nevertheless, caspase involvement in apoptosis has been and continues to be an area of extensive study.^{32,93-101}

As mentioned, caspases are members of clan CD. These proteases have a strict preference for an aspartic acid at the P1 residue, hence their name, *cysteiny*l *aspartate* specific *proteases*. To date, at least 12 human caspases have been identified: caspases-1, -2, -3, -4, -5, -6, -7, -8, -9, -10, -13, and -14.^{87,93} The first caspase to be identified was caspase-1. Caspase-1, or interleukin-1 β converting enzyme (ICE), was originally thought to be involved in apoptosis.¹⁰² Later, apoptosis was found to involve other 'ICE-like' proteases.¹⁰³

Since then, seven caspases have been found to be essential to the apoptotic signaling cascade: caspases-2, -3, -6, -7, -8, -9, and -10.^{93,100,104} There are two groups of apoptotic caspases: initiator caspases (caspase-2, -8, -9, and -10) and executioner caspases (caspase-3, -6, and -7).⁹³ Over 280 different proteins are the natural substrates for caspases. Some of these proteins are cleaved to complete the cell death cycle, while others are cleaved simply because they contain the correct recognition sequence.^{104,105}

Two separate but interconnected activation pathways for apoptotic caspases have been identified (Figure 3.1). In the extrinsic pathway, death receptors such as FAS, located on the cellular membrane, are ligated with death receptor ligands such as Trail (TNF-related apoptosis-inducing ligand). Inside the cell, the zymogens of caspases-2, -8, and -10 are recruited by forming protein complexes with the death domains (DD) of the receptor. These complexes are formed via the caspase-recruitment domain (CARD) of caspase-2 or the death effector domain (DED) of caspases-8 and 10. Initiator caspases possess some activity as zymogens, but much more activity is observed upon cleavage of the CARD and DED domains. Initiator caspases-8 and -10 activate the executioner caspases-3 and -7. In addition to cleaving various substrates, caspase-3 activates caspase-6. Caspase-6 provides an amplification loop via activation of caspases-8 and -10. Caspase-3 also activates caspases-8 and -10, providing an additional amplification loop. All three executioner caspases cleave various substrates, completing the apoptotic cell death cycle.

The intrinsic pathway is initially activated via chemical stress, particularly DNA damaging agents, which results in the release of cytochrome *c* from the mitochondria. Cytochrome *c* then forms a protein complex with Apaf-1 and caspase-9; this complex is

known as the apoptosome. Like caspase-2, caspase-9 has a CARD domain that aids in the formation of the apoptosome. The apoptosome is important because it enables the dimerization of caspase-9, and dimerization is needed for activity. Once active, caspase-9 can then go on to cleave caspases-3 and -7. Again, caspase-3 can amplify the apoptotic cascade by aiding the activation of caspase-9.

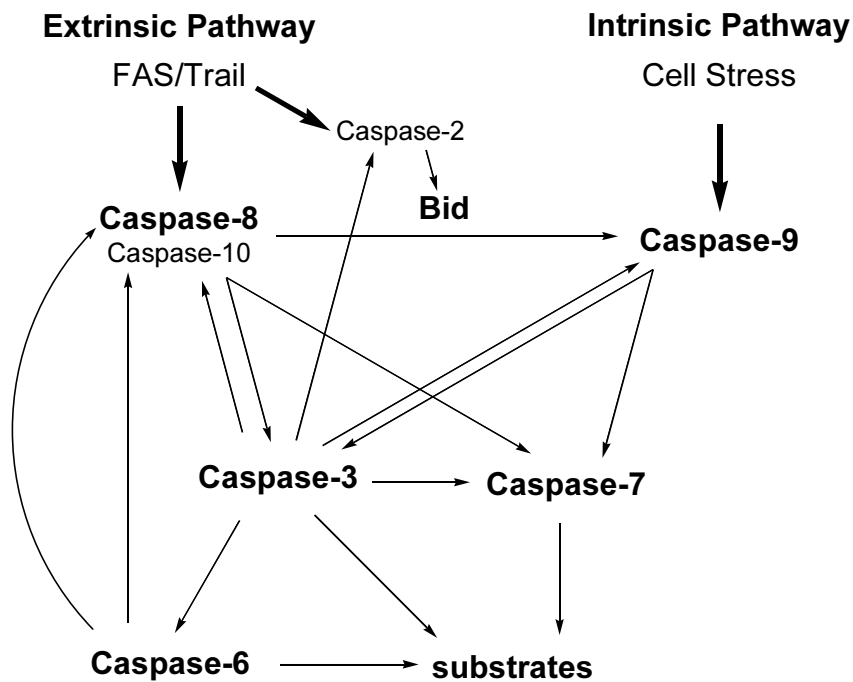


Figure 3.1 Apoptotic cascade of caspases, adapted from Ref. 87

The two apoptotic pathways are linked in several ways, and the activation of one pathway often results in the activation of the other pathway. A caspase-8 and -10 substrate is the protein Bid, a member of the Bcl-2 family of proteins. The cleaved Bid protein plays a role in the activation of caspase-9 via cytochrome *c* release from the mitochondria.¹⁰⁶⁻¹⁰⁸ Caspase-2 also performs a similar function through the proteolytic

processing of the protein Bid.¹⁰⁹⁻¹¹¹ Caspase-6 is known to be essential for the activation of the extrinsic pathway initiator caspases when the intrinsic pathway is activated first.¹¹²

Caspase activity is regulated by endogenous caspase inhibitors, referred to as inhibitor of apoptosis protein (IAPs). In most cells, XIAP can interact with caspases-3, -7, and -9. The interaction of XIAP with caspases is down-regulated by the second mitochondrial activator of caspases (SMAC), which acts as an antagonist on the XIAP protein. Additional IAPs, such as ML-IAP, down-regulate the pro-apoptotic activity of SMAC.³²

Caspase structure

As mentioned, procaspases have regulatory domains that are removed upon activation, although initiator caspases do not require removal of these domains to show some activity.^{32,113-118} For procaspases-2 and -9, the intrinsic pathway initiator caspases, there is one regulatory domain referred to as the caspase-recruitment domain (CARD). For procaspases-8 and -10, the extrinsic pathway initiator caspases, there are two regulatory domains, each referred to as a death effector domain (DED). For procaspases-3, -6, and -7, the executioner caspases, an N-terminus peptide is cleaved to give the active caspases.⁹³

Caspase structure has been studied extensively and several structures have been deposited in the Protein Data Bank.¹¹⁹ An extensive table is available in the recent review by Fuentes-Prior and Salvesen.³² Shown below is a brief selection of available apoptotic caspase crystal structures (Table 3.1).

Table 3.1 A selection of published apoptotic caspase crystal structures

Caspase	PDB	Description	Ref.
Caspase-2	1PYO	Ac-LDESD-CHO	120
Caspase-3	n/a	7 inhibitors, 1 peptidyl and 6 peptidomimetic, bound in the active site (2.20 – 3.11 Å)	121
	1PAU	Ac-DEVD-CHO (2.5 Å)	122
	1CP3	Ac-DVAD-FMK (2.3 Å)	123
	1QX3	Unoccupied substrate binding site (1.9 Å)	124
	1I3O	Complex with natural inhibitor XIAP (2.7 Å)	125
	1QA8	isatin sulfonamide inhibitor (2.8 Å)	126
Caspase-7	1F1J	Ac-DEVD-CHO (2.35 Å)	127
Caspase-8	1QTN	Ac-IETD-CHO (1.2 Å)	128
	1F9E	Cbz-DEVD-CHO (2.9 Å)	129
	1QDU	Cbz-EVD-CMK (2.8 Å)	130
	1I4E	Complex with natural inhibitor p35 (3.0 Å)	131
Caspase-9	1JXQ	Cbz-EVD-CMK (2.8 Å)	116
	1NW9	Complex with natural inhibitor XIAP (2.4 Å)	132

In addition to the crystal structure work, homology modeling studies have been done with human caspases-2, -4, -5, -6, -9, and -10.^{133,134} The sequence homology between the human caspases ranges from 24 – 57%. Three pairs have >40% sequence homology: caspases-3 and -6 (42%), caspases-3 and -7 (57%) and caspases -8 and -10 (48%).⁹³

In general, the tertiary structure of caspase monomers consists of a twisted beta-sheet sandwiched between two layers of alpha-helices. There are two catalytic domains connected by a linker loop region. Each monomer has two catalytic domains, a large subunit and a small subunit. Active caspases and active initiator procaspases generally exist as dimers.³² Shown is the x-ray crystal structure (1F1J) of caspase-7 (Figure 3.2).¹²⁷ The aldehyde inhibitor Ac-DEVD-CHO, shown in blue, is bound in the active site. The

approximate positions of the large and small subunits, dimer interface, and active site are indicated. Beta-sheets are indicated in yellow, alpha-helices in red, and loop regions in green.

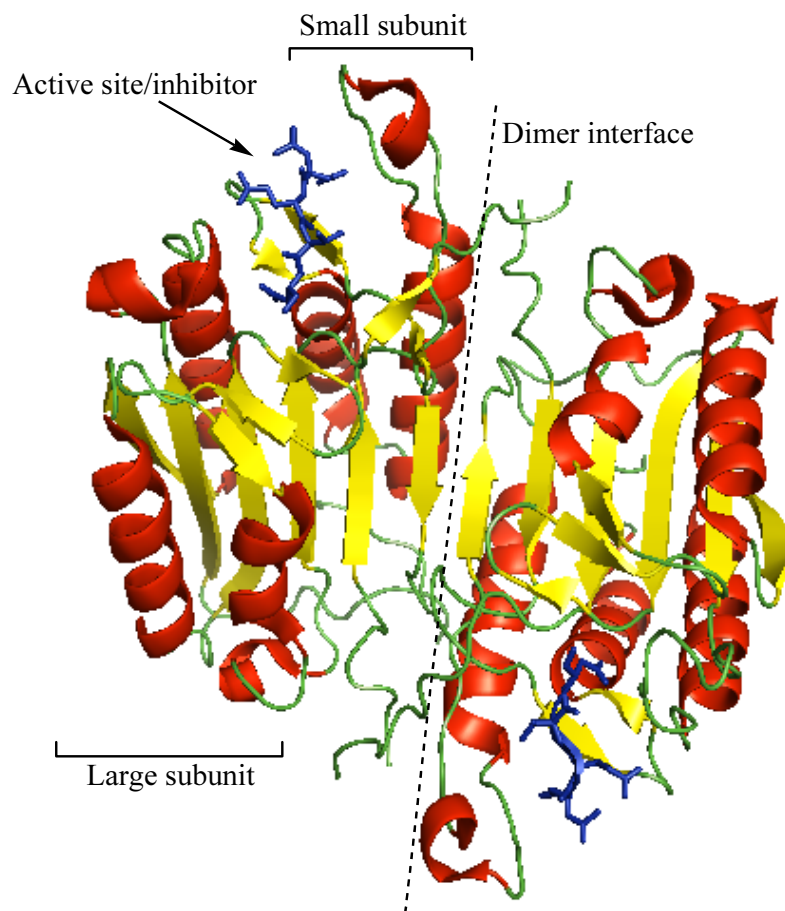


Figure 3.2 Caspase structure

Non-prime side sequence specificity between caspases

Several substrate specificity studies for caspases have been done.¹³⁵⁻¹⁴⁰ These studies focus primarily on the non-prime subsites of caspases: S2, S3, and S4, although some include a scan of the S1' subsite. Most caspases require a tetrapeptide recognition

sequence.¹³⁸ Caspase-2 is the only known exception, requiring a pentapeptide recognition sequence.¹³⁹ The non-prime sequence preferences of the human apoptotic caspases are listed below in Table 3.2. Other sequences that are well tolerated by these caspases are also shown in parentheses. The sequences shown are based on both substrate specificity studies and peptidyl inhibitor potency. Many of these sequences are commercially available as N-terminus protected (Cbz or Ac) substrates and inhibitors.

Table 3.2 Non-prime sequence preferences of caspases

Caspase	Sequences [P5]-P4-P3-P2-P1	Ref.
Caspase-2	[V]-D-V-A-D	139
Caspase-3	D-E-V-D	139,140
Caspase-6	V-E-H-D (VEID, IETD, DEVD)	73,139,140
Caspase-7	D-E-V-D	139,140
Caspase-8	L-E-T-D (AEVD, DEVD, IETD)	73,135,140,141
Caspase-9	L-E-H-D	140
Caspase-10	L-E-X-D (VEHD, DEVD)	135,142

X = several amino acids tolerated

All caspases have a strict requirement for an Asp in the S1 subsite. The S2 subsite is slightly more variable between different caspases, although most apoptotic caspases show some tolerance for a Val in that position. Caspase-9 seems to be the only exception, preferring a His in the S2 subsite. Also, most apoptotic caspases tolerate a Glu in the S3 subsite. The S4 subsite has the most promise for differentiating between caspases. In general, caspases-6, -8, -9, and -10 show a preference for a hydrophobic residue in this position. Caspases-2, -3, and -7 prefer an Asp in the S4 subsite. However, all apoptotic caspases, with the exception of caspase-9, show good reactivity with an Asp

in the S4 subsite. Clearly, there are definite limitations to obtaining significant selectivity between individual caspases using only the non-prime binding subsites.

The S1' subsite of caspases

Several caspases, including all the apoptotic caspases, were sequence-aligned in a homology modeling study.¹³⁴ This study contrasted and compared the binding of aldehyde inhibitors in the S1, S2, S3, and S4 subsites. Thus, the S1' subsite was not studied. However, the sequence alignment showed that there are differences in the key S1' subsite residues (Table 3.3). The numbering shown is for caspase-3, except for residue 253. This residue is only found in caspase-8, which contains a loop that is not found in other caspases.

Table 3.3 Sequence alignment of S1' subsite residues in apoptotic caspases¹³⁴

Caspases	253*	61	123	128	166	204
<i>Executioner caspases</i>						
Caspase-3	-	M	E	F	T	Y
Caspase-6	-	L	E	Y	N	Y
Caspase-7	-	M	E	Y	T	Y
<i>Initiator caspases</i>						
Caspase-2	-	L	V	Y	D	Y
Caspase-8	K*	I	D	Y	D	M
Caspase-9	-	L	C	Y	E	Y
Caspase-10	-	L	R	Y	E	L

Positional substrate scanning studies of the S1' subsites of caspases-1, -3, -6, and -8 revealed that caspases generally prefer relatively small amino acids, such as Ala, Ser,

Gly, in that subsite, but aromatic amino acids such as Phe and Tyr are also well tolerated. Charged amino acids were not tolerated.¹¹⁸

While the S1' subsite does not seem to show variation in substrate specificity between caspases, the size of the S1' subsites does vary slightly from caspase to caspase. Of the available crystal structures, caspase-2 has the most closed S1' subsite, with a canyon-like shape. Other caspases, particularly caspase-3, have relatively larger, bowl-shaped S1' subsites. The differences between caspases in the S1' subsites are subtle, and there has been little work done thus far to discern what effect these inhibitors have on selectivity between caspases, although it was recently shown that binding interactions in the S1' subsite of caspase-3 does increase potency.¹²¹

Previous work with peptidyl caspase inhibitors

Several mono-, di-, tri-, and tetrapeptidyl inhibitors of caspases have been synthesized.^{141,143-151} Much of the work has focused on using an aldehyde, a halomethylketone, or an acyloxymethylketone as the warhead (Figure 3.3). The warheads most frequently used in biological studies, aldehydes and halomethylketones, have been shown to effectively inhibit clan CA proteases (cathepsins and calpains).¹⁵²⁻¹⁵⁴ Clan CA proteases, such as cathepsin B and calpain I, are involved in apoptosis and other cell death processes.

Cross reactivity of caspase inhibitors with clan CA proteases makes it difficult to determine what target is contributing to a potentially therapeutic effect. For example, a commonly used halomethylketone caspase-3 inhibitor, Cbz-DEVD-FMK, was recently found to reduce calpain activity, thus implying that the neuroprotective effects of this

inhibitor could be due in part to calpain inhibition.¹⁵⁵ Also, since calpain is also involved in necrotic cell death, the neuroprotective effects of Cbz-DEVD-FMK are likely due to its anti-necrotic effect in addition to its anti-apoptotic effect.

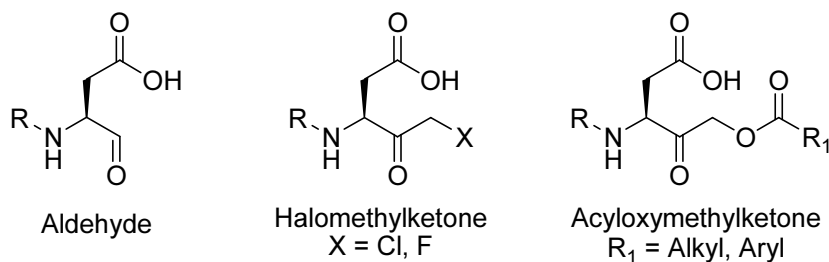


Figure 3.3 Commonly used caspase inhibitor warheads,
R = peptidyl or peptidomimetic chain

INHIBITOR DESIGN

Aza-peptide epoxides

The Powers lab designed the aza-peptide epoxide as a warhead for cysteine proteases (Figure 3.4). As mentioned in Chapter 2, the design was based on the epoxysuccinyl natural product, E-64, and its analogues. E-64, which contains an epoxysuccinyl as the warhead, is a potent clan CA cysteine protease inhibitor. Shown below is the design of caspase aza-peptide epoxide inhibitor. An appropriate peptide sequence, based on the sequence specificity of caspases, is synthesized, with an AAsp as the P1 residue. No other amino acid in the peptidyl chain is an aza-residue. The scissile peptide bond of the substrate is replaced by the epoxide moiety. Theoretically, either the C2 or C3 carbon of the epoxide moiety could be attacked by the catalytic cysteine thiolate, forming a covalent bond and irreversibly inhibiting the enzyme.

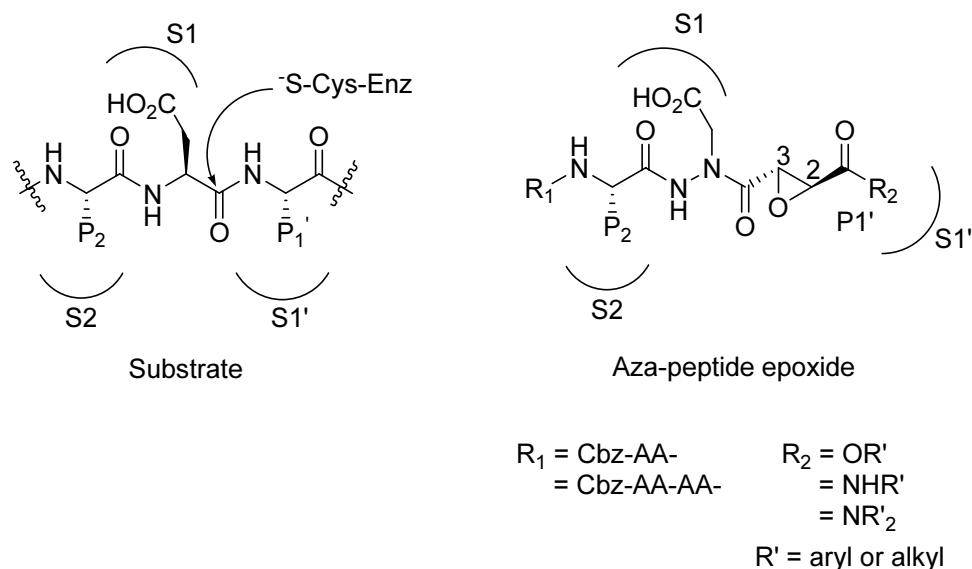


Figure 3.4 Aza-peptide epoxide inhibitor design for caspases

Initially, it was hypothesized that aza-peptide epoxides would be potent clan CA and clan CD cysteine protease inhibitors, with the appropriate sequence. However, aza-peptide epoxides did not potently inhibit clan CA proteases. In addition, epoxysuccinyl aza-peptides, the direct aza-analogues of the potent clan CA protease inhibitor E-64c, were synthesized and tested with clan CA. Like aza-peptide epoxides, aza-E-64c and its analogues were also found to be poor clan CA protease inhibitors (see Chapter 2). Thus, clan CA proteases do not tolerate an aza-residue. However, aza-peptide epoxides are potent inhibitors of clan CD proteases.⁷²⁻⁷⁴ The primary advantage of aza-peptide epoxides is that, unlike aldehydes and halomethylketones, this design shows no cross-reactivity with clan CA cysteine proteases.⁷³

Previous work with aza-peptide epoxide inhibitors has shown that both epoxide stereochemistry and the prime side substituent have effects on reactivity and selectivity between caspases (Table 3.4). For Cbz-DEVaD-EP-CO₂Et, the (*S,S*) stereoisomer is

more potent than the (*R,R*), while the (*R,R*) stereoisomer is more selective for caspase-3 over caspase-8 than the (*S,S*). Also, Cbz-IETaD-(*R,R*)-EP-CO₂Et is more selective for caspase-6 over caspase-8, whereas the (*S,S*) stereoisomer is not. Replacing the ethyl ester with larger, more hydrophobic groups on the prime side increases the reactivity of the inhibitors, as seen by comparing Cbz-DEVaD-EP-CO₂Bzl (1,910,000 M⁻¹s⁻¹) to Cbz-DEVaD-EP-CO₂Et (1,070,000 M⁻¹s⁻¹).

Table 3.4 Previous work with aza-peptide epoxides⁷³

Inhibitor	EP	k_2 (M ⁻¹ s ⁻¹)		
		Caspase-3	Caspase-6	Caspase-8
Cbz-DEVaD-EP-CO ₂ Et	(<i>S,S</i>)	1,070,000 ± 155,000	5,440 ± 140	95,500 ± 13,000
	(<i>R,R</i>)	464,000 ± 186,000	475	785 ± 120
Cbz-DEVaD-EP-CO ₂ Bzl	(<i>S,S</i>)	1,910,000 ± 209,000	12,700 ± 2,070	188,000 ± 52,000
Cbz-IETaD-EP-CO ₂ Et	(<i>S,S</i>)	4,080 ± 360	45,800 ± 4,200	52,800 ± 11,000
	(<i>R,R</i>)	2,630 ± 360	34,000 ± 1,100	8,800 ± 2,700

Relevance of selectivity between caspases

Certainly, a general, or pan-caspase inhibitor could be a more effective therapeutic than a selective caspase inhibitor.^{87,156} Several peptidomimetic inhibitors and some peptidyl inhibitors have been synthesized with this goal in mind.^{87,147,149,151,157-161} Pan-caspase inhibitors have made it to phase 2 clinical trials, and there are several pan-caspase inhibitors in phase 1 clinical trials and preclinical studies.¹⁰¹

However, caspase-3 specific inhibitors are also being studied in preclinical trials.¹⁰¹ Also, several non-peptide inhibitors of caspases have been identified. The most significant class of non-peptide inhibitors of caspases are the isatin sulfonamides.¹⁶² These compounds are potent inhibitors selective for caspases-3 and -7. Several caspase-3 specific peptidomimetic caspase inhibitors are reported in the literature.¹⁶³⁻¹⁶⁵ Clearly, there is interest in selectivity between caspases, and specific inhibitors could have therapeutic potential.

Selective, irreversible inhibition between caspases is also important for determining additional information about the individual roles of caspases in the apoptotic cascade. Irreversible caspase inhibitors have long been identified as tools for studying apoptosis.¹⁶⁶ Other strategies for determining the roles of caspases exist, and these techniques have provided much of the information shown in Figure 3.1 (see page 51). However, the roles of individual caspases may vary, depending on how apoptosis is induced.¹⁶⁷ Selective caspase inhibition is needed for correctly elucidating these roles. The selectivity of some commercially available ‘caspase-specific’ inhibitors are not sufficient for this task.

Aza-peptide epoxide mechanism of inhibition

The first two aza-peptide epoxides, synthesized by Zhao Zhao Li, were co-crystallized with caspase-1. The crystal structures of PhPr-VAaD-(*trans*)-EP-CO₂CH₂Ph and PhPr-VAaD-(*trans*)-EP-COCH₂CH₂Ph bound to caspase-1 were determined by Ron Rubin (unpublished results). These crystal structures showed the site of attack to be at the epoxide carbon furthest away from the AAsp (Figure 3.5).

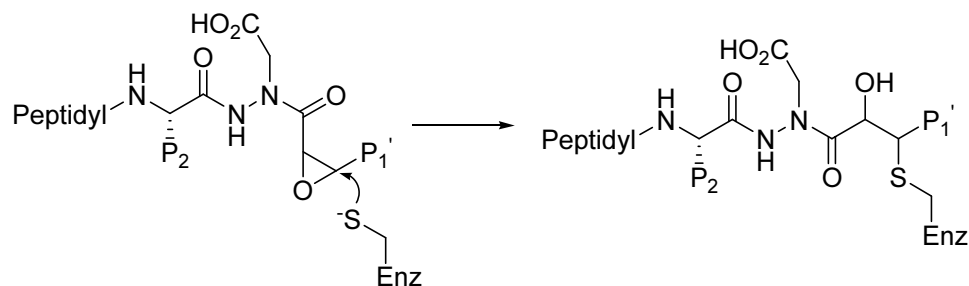


Figure 3.5 Proposed mechanism of inhibition based on caspase-1 crystal structures

However, recent crystal structures of aza-peptide epoxides bound to caspase-3 have shown that the site of attack is at the epoxide carbon near the AAsp. These structures were determined by Ganesen Rajkumar (University of Zurich; Dr. Markus Grütter's lab). Structurally, there are no obvious reasons for the difference in the site of attack between caspases-1 and -3. Perhaps there are minor variations between the active sites of caspase-1 and -3 that cause this switch, but thus far these variations have not been determined. The site of attack should be the same for all caspases. Based on the recent high-resolution caspase-3 crystal structures (1.67 – 2.05 Å), the cysteine thiolate clearly attacks the carbon near the AAsp (Figure 3.6). Additional details about the aza-peptide epoxide mechanism, with respect to epoxide stereochemistry, determined by the new crystal structures and modeling data, are discussed in the Results and Discussion section.

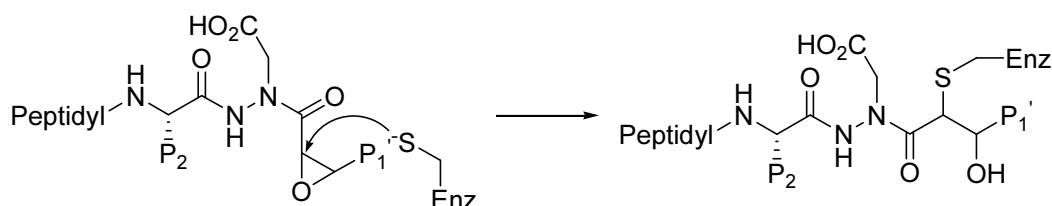


Figure 3.6 Mechanism of inhibition based on caspase-3 crystal structures

Objectives

One of the original goals was to obtain higher selectivity between caspases, utilizing the effects of both epoxide stereochemistry and the prime side substituent. Another goal was to determine why the (*S,S*) stereoisomer is more potent than the (*R,R*) stereoisomer. Also, aza-peptide epoxide inhibitor with the (*cis*) stereochemistry had yet to be synthesized and tested. Thus, the reactivity of this stereoisomer was unknown.

A systematic study of the effects of stereochemistry on reactivity and selectivity was done by completing and synthesizing a series of inhibitors with the Cbz-DEVaD, Cbz-EVaD, and Cbz-AEVaD sequences, with an ethyl ester group as the prime side substituent. Each sequence was coupled with an epoxide of the (*S,S*), (*R,R*) and (*cis*) stereochemistry. The effects of the prime side substituent were studied by synthesizing a series of Cbz-DEVaD aza-peptide epoxide inhibitors with the (*S,S*) stereochemistry, varying only the P1' substituent. The combined effects of epoxide stereochemistry and prime side substituent effects were studied by synthesizing a series inhibitors with the Cbz-DEVaD and Cbz-EVaD sequences with a dibenzyl amide group as the prime side substituent, coupling each sequence with an epoxide containing the (*S,S*), (*R,R*) and (*cis*) stereochemistry. The potency with respect to stereochemistry was expected to be (*S,S*) > (*R,R*) > (*cis*).

CHEMISTRY

Epoxide synthesis

The diethyl epoxysuccinate (*S,S*) and (*R,R*) enantiomers were synthesized by the procedure published by Mori and Iwasawa.^{80,81} To synthesize the diethyl (*S,S*)

epoxysuccinate, diethyl D-(-)-tartrate was treated with 33 % HBr in acetic acid; this reaction proceeded by stereoselective acetylation and bromination. The stereoselectivity was ensured by an anchimeric assistance mechanism. The acetyl group was then hydrolyzed to give the halohydrin intermediate. The diethyl epoxide moiety **III-1** was formed via treatment of the halohydrin with sodium ethoxide. To synthesize the monoethyl epoxide moiety **III-2**, one ethyl ester was selectively hydrolyzed with 1 M KOH, using a previously described procedure.⁸⁴ The monoethyl epoxysuccinate could then be used to synthesize the various amide epoxide moieties by coupling the carboxylate to the appropriate amine, followed by hydrolysis of the remaining ethyl ester with sodium hydroxide to give the amide epoxides (Figure 3.7). The (*R,R*) stereoisomers were synthesized by the same procedure, using diethyl L-(+)-tartrate as the starting material.

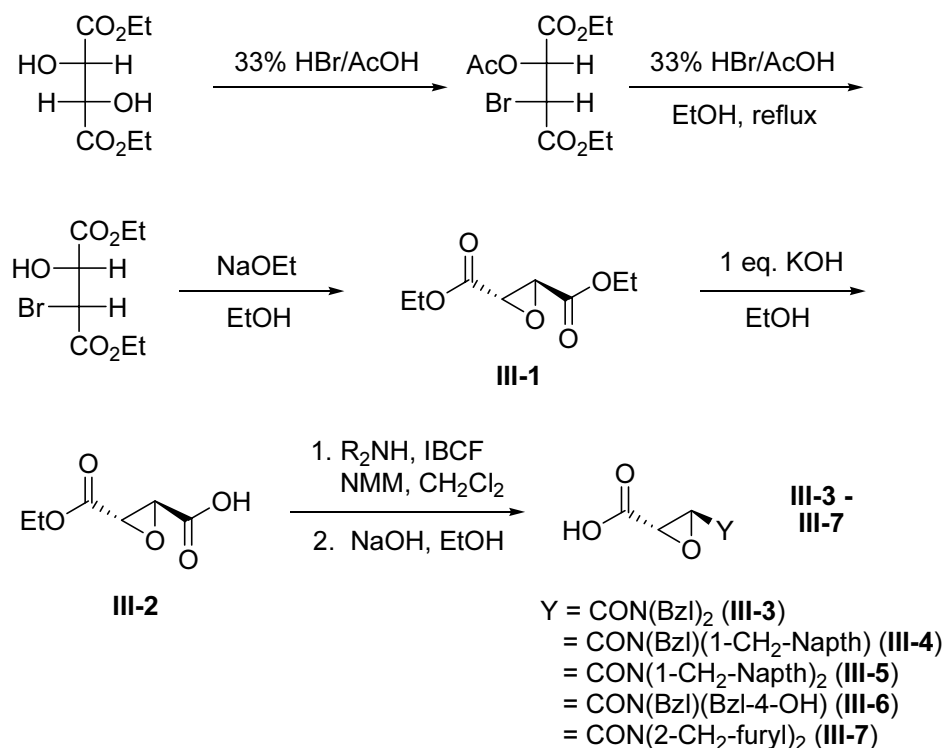


Figure 3.7 Synthesis of the stereospecific (*S,S*) epoxide moieties

The (*cis*) epoxide moiety was synthesized following a previously described procedure.¹⁶⁸ Diethyl maleate was epoxidized with *tert*-butyl lithium peroxide, formed *in situ* with *tert*-butyl hydroperoxide/THF and *tert*-butyl lithium/hexanes. Stereospecificity was ensured by a chelate-locking mechanism. Selective hydrolysis of one ethyl ester to gave the monoethyl epoxysuccinate **III-8**.⁸⁴ This compound was then either directly coupled to the appropriate sequence or used to synthesize the dibenzyl amide epoxide moiety **III-9** using the mixed anhydride coupling method. The (*cis*) epoxide moieties are expected to be a racemic mixture of the (*R,S*) and (*S,R*) stereoisomers (Figure 3.8).

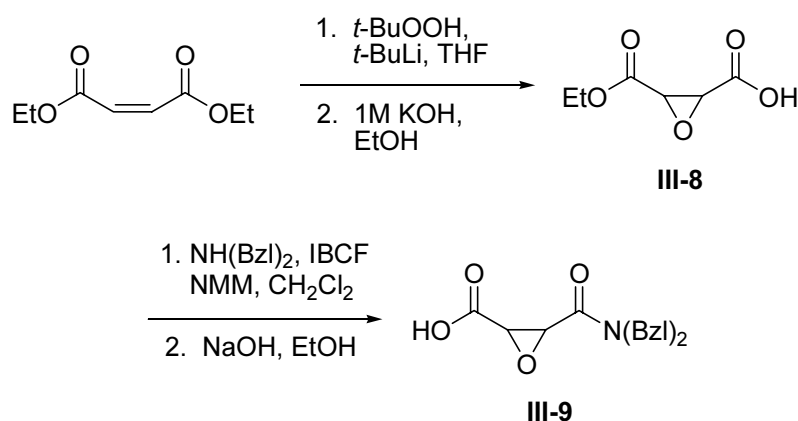


Figure 3.8 Synthesis of the (*cis*) epoxide moieties

Aza-peptide epoxide synthesis

The N-protected methyl ester peptide chains **III-10a – c** were synthesized using standard amino acid coupling methods. Reaction with hydrazine gave the hydrazides **III-11a – c**, which were then reacted with *t*-butylbromoacetate to give the hydrazides **III-12a – c**. All final compounds were synthesized by coupling the appropriate epoxide precursors to the peptidyl sequences using the EDC/HOBt coupling method, as described

previously.⁷³ Removal of the *t*-butyl protecting groups from the acidic sidechains gave the inhibitors **III-13a – c**, **III-14a – b**, and **III-15a – III-18a** (Figure 3.9). All final compounds were characterized by ¹H NMR, exact mass spectrometry, and elemental analysis.

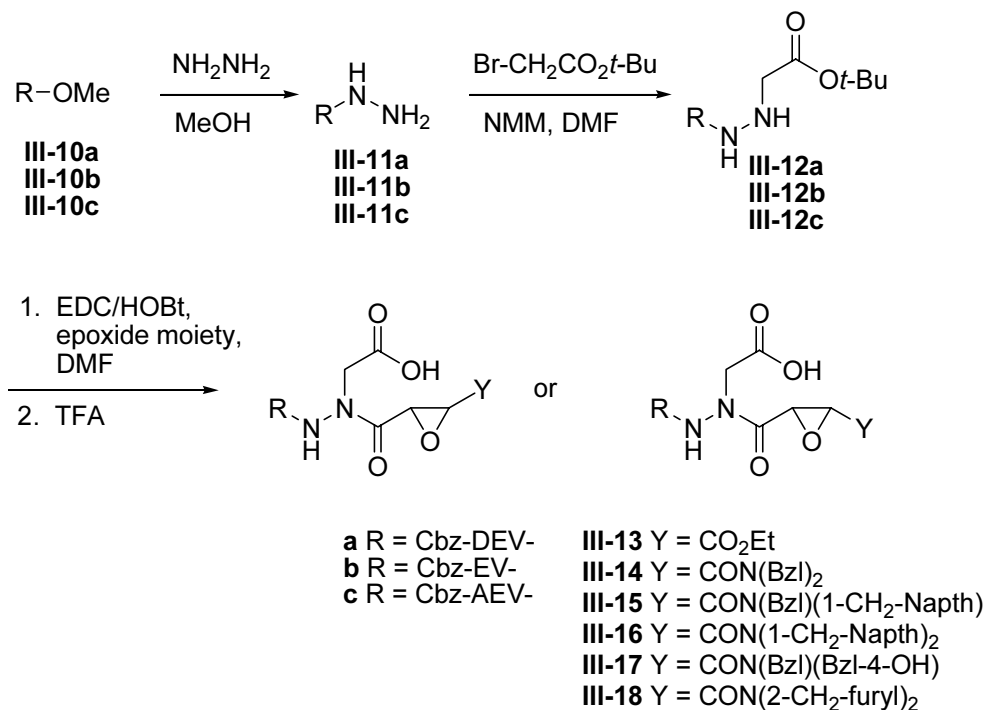


Figure 3.9 Synthesis of the aza-peptide epoxide inhibitors

Stereospecificity of the aza-peptide epoxide inhibitors

As mentioned, the diethyl (*S,S*) epoxysuccinate **III-1** (see Figure 3.7, page 64), and its (*R,R*) enantiomer were synthesized according to the procedure published by Mori and Iwasawa.⁸⁰ The diethyl tartrate starting materials were commercially obtained and are >99 % pure. The syntheses of the epoxysuccinates are highly stereoselective, and the enantiomeric purity of these compounds has been well characterized in the literature.⁸⁴

Also, the synthesis of the diethyl (*cis*) epoxysuccinate was driven by a chelate-locking mechanism and has been shown to proceed under complete stereochemical control.¹⁶⁸ In the synthesis of **III-2** – **III-9** epoxide moieties (see Figures 3.7 and 3.8, pages 64 and 65), there is a chance that the epoxide opens, due to the addition of strong acid and bases at various points in the synthesis. However, if the epoxide opens, it would not be capable of re-cyclisation. Therefore, the enantiomeric purity of the epoxide moieties is expected to be very high.

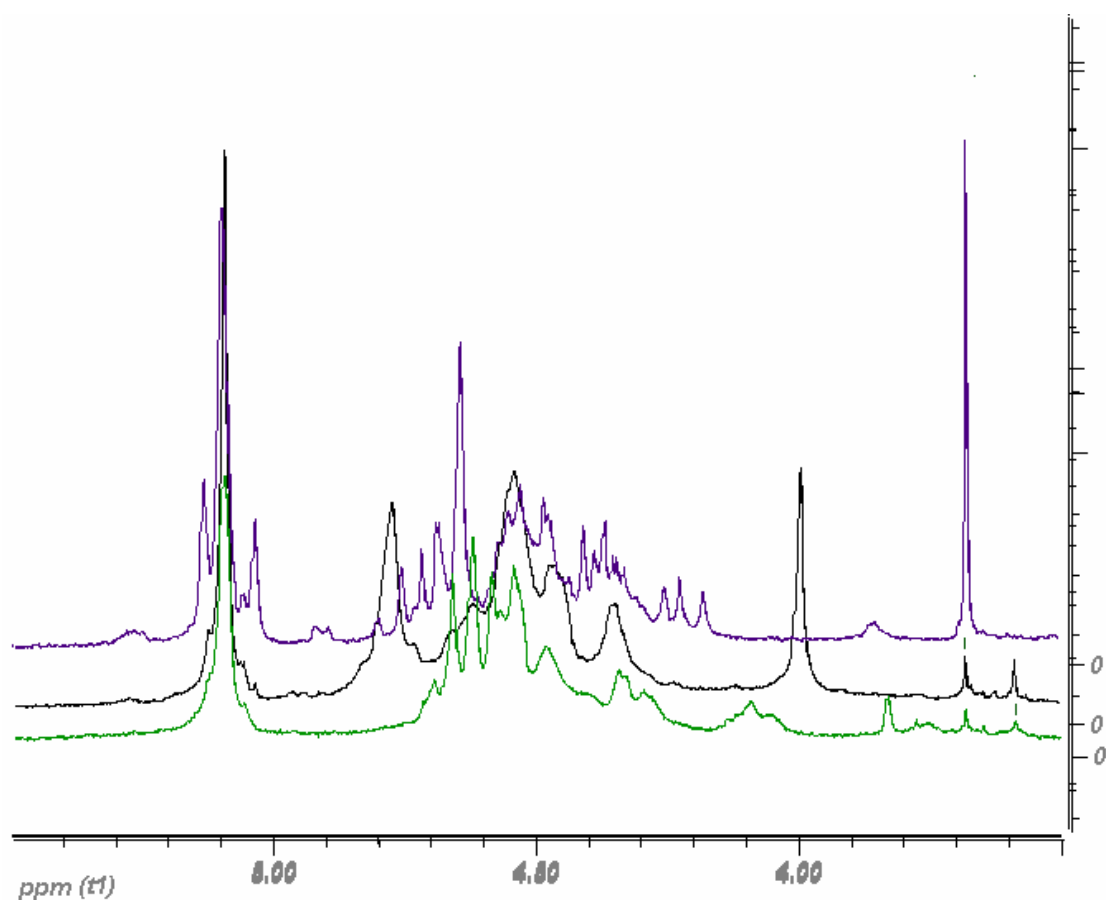


Figure 3.10 ^1H NMR of Cbz-DEVaD-EP-CON(Bzl)₂ stereoisomers; (*S,S*) = black, (*R,R*) = purple, and (*cis*) = green

To confirm, the ^1H NMR spectra of the newly synthesized compounds were analyzed to see if the different stereoisomers gave distinct resonances corresponding the epoxide hydrogens. Shown are the ^1H NMR spectra of (*S,S*), (*R,R*), and (*cis*) Cbz-DEVaD-EP-CON(Bzl)₂ (Figure 3.10). The region from 3.50 to 5.50 ppm is shown. This region contains the methylene group of the Cbz group (~5.1 ppm), all three alpha-hydrogens of the Asp, Glu, and Val residues (~4.4 – 4.7 ppm), and the two epoxide hydrogens (various ppm).

The three stereoisomers are distinct. Interestingly, the (*R,R*) and (*S,S*) HO-CO-EP-CON(Bzl)₂ stereoisomers have identical ^1H NMR spectra, but the final compounds have significantly different spectra. For all three stereoisomers, one epoxide peak is in the multiplet from 4.4 – 4.7 ppm. The other peak appears at 4.0 ppm for the (*S,S*) stereoisomer, 3.7 ppm for the (*R,R*) stereoisomer, and as a multiplet from 4.04-4.14 for the *cis* stereoisomer. The peaks seen from 3.59 – 3.83 are considered to be minor extraneous peaks and are explained in the following discussion.

The ^1H NMR spectra of the Cbz-EVaD-(*S,S*)-EP-CON(Bzl)₂ and Cbz-EVaD-(*R,R*)-EP-CON(Bzl)₂ stereochemical pairs were also found to be distinct. However, the epoxide peaks of Cbz-AEVaD-(*S,S*)-EP-CO₂Et and Cbz-AEVaD-(*R,R*)-EP-CO₂Et stereochemical pairs (3.51 and 3.47 ppm, respectively) did not have large chemical shift differences. In both of these stereochemical series, the (*cis*) stereoisomer has spectrum that is distinct from each the (*S,S*) and the (*R,R*) stereoisomers. Therefore, no cross-contamination of stereoisomers was found in these two stereochemical series.

However, there is a small indication of a possible stereochemical mixture in the spectrum of Cbz-DEVaD-(*S,S*)-EP-CON(Bzl)₂. This stereoisomer has a peak overlap

with the (*R,R*) and/or (*cis*) stereoisomers at 3.68 ppm (Figure 3.10). There is no such cross-overlap of the (*S,S*) stereoisomer in the spectrum of either the (*cis*) or (*R,R*) stereoisomers. Still, based on peak integration, Cbz-DEVaD-(*S,S*)-EP-CON(Bzl)₂ has an approximate enantiomeric excess of greater than 90% ee, thus the (*S,S*) stereoisomer is the predominate stereoisomer. However, given that this racemization did not occur in either the Cbz-EVaD-EP-CON(Bzl)₂ **III-14b** and Cbz-AEVaD-EP-CO₂Et **III-13c** series, some questions remain.

The extraneous peaks in the ¹H NMR spectra at 3.5 – 3.9 ppm can be explained by several alternate explanations. The best alternate explanation is that the *tert*-butyl protecting groups were not completely removed from the acidic sidechains. Based on the ¹H NMR spectra, there is a small amount of *t*-butyl protons, with the amount of the *t*-butyl precursor ranging from approximately 0 – 3.4%. Also, minor peaks from 3.5 – 3.9 ppm, at various ppm appear almost all the ¹H NMR spectra of the three stereochemical series discussed. Thus, we propose that the overlap seen in the spectrum of Cbz-DEVaD-(*S,S*)-EP-CON(Bzl)₂ could be the result of incomplete *t*-butyl group removal and not indicative of an (*R,R*) or (*cis*) contaminant in the (*S,S*) material.

RESULTS AND DISCUSSION

Epoxide stereochemistry effects

The ethyl ester series of inhibitors were synthesized to observe the effects of epoxide stereochemistry alone. The P1' ethyl ester substituent has very little interaction with the S1' subsite. Dr. Juliana Asgian had previously synthesized Cbz-DEVaD-(*S,S*)-

EP-CO₂Et, Cbz-DEVaD-(*R,R*)-EP-CO₂Et, and Cbz-EVaD-(*S,S*)-EP-CO₂Et; the remaining stereoisomers in these series are newly synthesized inhibitors.

With the inhibition of caspase-3 by Cbz-DEVaD-EP-CO₂Et **III-13a**, potency is decreased by about two-fold from the (*S,S*) stereoisomer to the (*R,R*), and about ten-fold from the (*R,R*) to the (*cis*). Thus, the order of reactivity is (*S,S*) > (*R,R*) > (*cis*). For Cbz-EVaD-EP-CO₂Et **III-13b**, the order of reactivity is (*S,S*) > (*R,R*) \approx (*cis*). For Cbz-AEVaD-EP-CO₂Et **III-13c**, the order of reactivity is (*S,S*) > (*cis*) > (*R,R*). These trends are true for all caspases with the exception of caspase-2, which shows little to no reactivity with the (*R,R*) and (*cis*) stereoisomers (Table 3.5).

The order of preference for the Cbz-AEVaD-EP-CO₂Et **III-13c** inhibitors, (*S,S*) > (*cis*) > (*R,R*), was not expected. The AEVD sequence has previously shown to preference for caspase-8 with an aldehyde warhead.¹⁴¹ With caspase-8, the (*cis*) inhibitor (37,100 M⁻¹s⁻¹) is only about 4-fold less potent than the (*S,S*) inhibitor (148,000 M⁻¹s⁻¹), while the (*R,R*) inhibitor (242 M⁻¹s⁻¹) is over 150-fold less potent than the (*cis*).

The order of reactivity differs because there is a S4 directing effect. The inhibitor initially binds in non-prime subsites; the active site Cys then attacks the warhead. While the S4 subsite does not vary enough between caspases to obtain sufficient selectivity using non-prime residues alone, of the four non-prime subsites it has the most influence on potency. Thus, it is not surprising that the binding properties of the S4 subsite influence the reactivity order with respect to epoxide stereochemistry.

Table 3.5 Epoxide stereochemistry effects

	Inhibitor	EP	k_2 (M ⁻¹ s ⁻¹)						
			Casp-2	Casp-3	Casp-6	Casp-7	Casp-8	Casp-9	Casp-10
III-13a	Cbz-DEVaD-EP-CO ₂ Et	(<i>S,S</i>) ^a	11,600 ± 4,200	1,070,000 ± 155,000	5,440 ± 140	271,000 ± 5,000	95,500 ± 13,000	675 ± 20	16,500 ± 1,000
		(<i>R,R</i>) ^a	NI	464,000 ± 186,000	475	179,000 ± 30,000	785 ± 120	ND	1,940 ± 290
		(<i>cis</i>)	NI	47,500 ± 1,700	205 ± 21	10,300 ± 1,100	205 ± 37	NI	583 ± 67
III-13b	Cbz-EVaD-EP-CO ₂ Et	(<i>S,S</i>) ^a	26 ± 2	50,500 ± 2,100	4,180	168,000 ± 600	195,000 ± 24,000	1,810 ± 150	4,000 ± 150
		(<i>R,R</i>)	NI	820 ± 50	21 ± 0	727 ± 61	199 ± 72	48 ± 8	76 ± 19
		(<i>cis</i>)	NI	450 ± 50	20 ± 2	608 ± 35	424 ± 42	35 ± 5	79 ± 18
III-13c	Cbz-AEVaD-EP-CO ₂ Et	(<i>S,S</i>)	18 ± 1	37,400 ± 3,800	9,040 ± 830	19,000 ± 4,000	148,000 ± 6,000	700 ± 94	2,260 ± 150
		(<i>R,R</i>)	NI	980 ± 160	631 ± 9	351 ± 20	242 ± 0	27 ± 5	123 ± 11
		(<i>cis</i>)	NI	7,130 ± 330	1,680 ± 60	3,950 ± 400	37,100 ± 2,100	175 ± 31	887 ± 212

^aThese inhibitors were synthesized by Dr. Juliana Asgian. The testing of these inhibitors with caspases-3, -6, and -8 was done by Dr. Karen E. James.⁷³

With the Cbz-DEVaD sequence, both of these subsites are occupied by an Asp residue. There are extensive hydrogen-bonding interactions in both the S1 and S4 subsites. Therefore, the inhibitor is held in a more rigid conformation and reactivity with respect to epoxide stereochemistry decreases as expected, $(S,S) > (R,R) > (cis)$.

However, with the Cbz-AEVaD sequence, the S1 subsite is occupied by an Asp residue, and the S4 subsite is occupied by an Ala residue. The P4 Ala residue, with its methyl sidechain, can only make relatively weak van der Waals contacts with the S4 subsite. Therefore the inhibitor has far more flexibility in its interactions at other subsites and the *(cis)* stereoisomer can be better tolerated relative to the (R,R) .

The Cbz-EVaD-EP-CO₂Et **III-13b** series confirms that the S4 subsite has a significant influence on potency and reactivity with respect to epoxide stereochemistry. This series shows that occupancy of the S4 subsite is needed to obtain potency with either the (R,R) or *(cis)* stereochemistry, since the inhibitors with this stereochemistry show little to no reaction with all of the apoptotic caspases. Interestingly, when comparing the (S,S) inhibitors of the three series shown, caspases-7, -8, and -9 tolerate non-occupancy of S4 more than caspase-3 (Table 3.5). With both caspases-8 and -9, potency is increased. This difference could have implications towards obtaining selective caspase inhibitors.

These results show that that reactivity with respect to epoxide stereochemistry is sequence-dependent. In general, the (S,S) stereoisomer is the most potent with all apoptotic caspases, but the identity of the P4 residue has a significant influence on the (R,R) versus *(cis)* preference. Also, in general, the presence of a P4 residue is needed to obtain potency with either the (R,R) or *(cis)* stereoisomer.

Prime side substituent effects

Since the (*S,S*) stereoisomer is, in general, the most potent stereoisomer, several Cbz-DEVaD inhibitors were synthesized with the (*S,S*) stereochemistry. The prime side substituent was varied to observe its effects on potency and selectivity. The Cbz-DEVaD sequence reacts potently with caspase-3 (up to $\sim 3,000,000 \text{ M}^{-1}\text{s}^{-1}$), thus all inhibitors in this series are selective for caspase-3.

Previously, Dr. Özlem Ekici had found Cbz-DEVaD-CH=CH-CON(Bzl)₂ to be highly potent and selective for caspase-3 ($3,000,000 \text{ M}^{-1}\text{s}^{-1}$).¹⁴² This inhibitor is an aza-peptide Michael acceptor, another class of inhibitors developed by the Powers lab. It was hypothesized that the P1' dibenzyl amide substituent was the key factor in this inhibitor's potency and selectivity for caspase-3. Thus, its cognate aza-peptide epoxide, Cbz-DEVaD-(*S,S*)-EP-CON(Bzl)₂ **III-14a**, was synthesized. This inhibitor was found to be equipotent to the aza-peptide Michael acceptor, but not as selective for caspase-3 over caspase-8. This selectivity difference is discussed in the subsection titled 'Aza-peptide epoxides versus aza-peptide Michael acceptors.'

Since the S1' subsite of caspase-3 is large and bowl-shaped, it was hypothesized that caspase-3 could tolerate very large, bulky functional groups. Also, it was hypothesized that these large, hydrophobic functional groups would increase selectivity for caspase-3 over caspase-8, because the S1' subsite of caspase-8 is less hydrophobic than that of caspase-3. Thus, the S1' subsite was probed with various bulky hydrophobic functional groups (Table 3.6). Previously, the S1' subsite of caspase-3 had not been probed with such large functional groups. Inhibitors Cbz-DEVaD-(*S,S*)-EP-CONHBzl

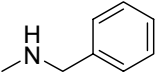
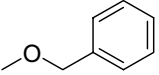
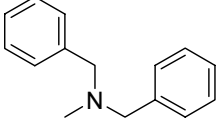
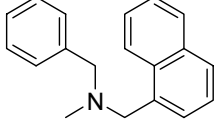
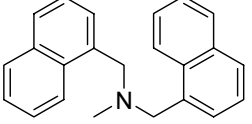
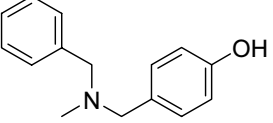
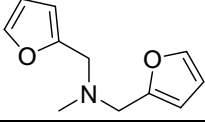
and Cbz-DEVaD-(*S,S*)-EP-CO₂Bzl, included to make appropriate comparisons, were synthesized by Dr. Juliana Asgian.

Cbz-DEVaD-(*S,S*)-EP-CON(Bzl)₂ **III-14a** is the most potent inhibitor of this series (3,120,000 M⁻¹s⁻¹, caspase-3). As mentioned, x-ray crystal structures of caspase-3 and Cbz-DEVaD-(*S,S*)-EP-CONHBzl **JG-1**, Cbz-DEVaD-(*S,S*)-EP-CO₂Bzl **JG-2**, and Cbz-DEVaD-(*S,S*)-EP-CON(Bzl)₂ **III-14a** were done by Ganesen Rajkumar. The crystal structure shows that the dibenzyl amide moiety of Cbz-DEVaD-(*S,S*)-EP-CON(Bzl)₂ **III-14a** makes favorable hydrophobic interactions with the S1' subsite (see Figure 3.16, page 91).

The mono-benzyl amide inhibitor Cbz-DEVaD-(*S,S*)-EP-CONHBzl **JG-1**, displays potency equivalent to Cbz-DEVaD-(*S,S*)-EP-CO₂Et **III-13a** (~1,000,000 M⁻¹s⁻¹, caspase-3). The crystal structure shows that the nitrogen of the monobenzyl amide group hydrogen bonds with the main-chain carbonyl of a Gly, and this interaction prevents the benzyl group from making the hydrophobic contacts seen in the dibenzyl amide inhibitor **III-14a**. Thus, the monobenzyl amide P1' substituent does not increase potency because it does not make any contributions to binding.

The benzyl ester inhibitor Cbz-DEVaD-(*S,S*)-EP-CO₂Bzl **JG-2** does not have this hydrogen bond interaction. Therefore, potency is increased (1,910,000 M⁻¹s⁻¹, caspase-3), because the benzyl group can make some hydrophobic contacts with in the S1' subsite. The additional benzyl group of the dibenzyl amide inhibitor **III-14a** (Cbz-DEVaD-(*S,S*)-EP-CON(Bzl)₂) provides additional favorable interactions and therefore increases potency with respect to the monobenzyl ester inhibitor **JG-2**.

Table 3.6 Prime side substituent effects

Cbz-DEVaD-(<i>S,S</i>)-EP-COR		k_2 (M ⁻¹ s ⁻¹)						
	R	Casp-2	Casp-3	Casp-6	Casp-7	Casp-8	Casp-9	Casp-10
JG-1 ^a		13,000 ± 2,000	1,090,000 ± 95,000	6,000 ± 390	302,000 ± 24,000	84,400 ± 21,600	1,090 ± 150	18,000 ± 3,300
JG-2 ^a		30,300 ± 4,700	1,910,000 ± 210,000	12,700 ± 2,100	306,000 ± 21,000	188,000 ± 52,000	1,600 ± 100	22,000 ± 600
III-14a		786 ± 181	3,120,000 ± 240,000	16,800 ± 7,600	292,000 ± 28,300	235,000 ± 37,000	542 ± 198	3,550 ± 880
III-15a		680 ± 170	567,000 ± 44,000	3,300 ± 200	50,300 ± 3,400	18,100 ± 2,700	50 ± 3	1,040 ± 120
III-16a		359 ± 74	457,000 ± 32,000	5,210 ± 80	63,400 ± 25,400	13,300	66 ± 26	1,370 ± 80
III-17a		1,160 ± 410	1,550,000 ± 290,000	12,100 ± 50	144,000 ± 200	71,200 ± 9,300	283 ± 13	3,140 ± 80
III-18a		1,630 ± 10	1,190,000 ± 50,000	10,400 ± 500	133,000 ± 15,000	133,000 ± 11,000	328 ± 36	12,700 ± 1,200

^aThese inhibitors were synthesized by Dr. Juliana Asgian. The testing of these inhibitors with caspases-3, -6, and -8 was done by Dr. Karen E. James.⁷³

Interestingly, the Cbz-DEVaD-(*S,S*)-EP-CONHBzl **JG-1**, Cbz-DEVaD-(*S,S*)-EP-CO₂Bzl **JG-2**, and Cbz-DEVaD-(*S,S*)-EP-CON(Bzl)₂ **III-14a** did not show any variation in potency with caspase-7 (300,000 M⁻¹s⁻¹). Thus, there is a subtle difference in the S1' subsites of caspases-3 and -7, which are highly homologous (57 % sequence identity).

Larger and more functionalized hydrophobic groups generally reduced the potency of the inhibitors but increased selectivity. For example, Cbz-DEVaD-(*S,S*)-EP-CON-(Bzl)(1-CH₂-Naph) **III-15a** (567,000 M⁻¹s⁻¹, caspase-3) is 5.5-fold less potent with caspase-3 than Cbz-DEVaD-(*S,S*)-EP-CON-(Bzl)₂ **III-14a** (3,120,000 M⁻¹s⁻¹, caspase-3). However, **III-15a** prefers caspase-3 to caspase-8 by 31-fold, an increase of the 13-fold preference for caspase-3 by **III-14a** over caspase-8.

Cbz-DEVaD-(*S,S*)-EP-CON-(Bzl)(CH₂-Ph-OH) **III-17a** was synthesized because initial modeling calculations showed a potential hydrogen bond of the hydroxyl group with the Tyr in the S1' subsite of caspase-3. The crystal structures that later became available showed that this interaction was likely not present, and may prevent effective interaction in the S1' subsite. Thus, **III-17a** (1,550,000 M⁻¹s⁻¹) has a two-fold reduced potency for caspase-3 with respect to Cbz-DEVaD-(*S,S*)-EP-CON-(Bzl)₂ **III-14a**; the selectivity of caspase-3 over caspase-8 is 22-fold.

The smaller P1' substituent of Cbz-DEVaD-(*S,S*)-EP-CON-(2-CH₂-furyl)₂ **III-18a** shows a more broad-spectrum potency, showing that, like the ethyl ester, small disubstituted amides in the P1' position are well tolerated by all the apoptotic caspases. This inhibitor's reduced potency with caspase-3 (1,190,000 M⁻¹s⁻¹) shows that the relatively smaller furyl groups cannot make the favorable hydrophobic interactions that the benzyl groups of **III-14a** make with the enzyme.

In summary, this series of inhibitors showed a potential difference in the S1' subsites of caspases-3 and -7, as shown by **JG-1**, **JG-2**, and **III-14a** (see above discussion). This difference could have implications for caspase-3 versus caspase-7 selectivity, which is difficult to obtain. Also, selectivity for caspase-3 over caspase-8 was increased slightly with large P1' substituents. Selectivity of caspase-3 versus other caspases remained relatively unchanged.

Combined effect of prime side substituent and epoxide stereochemistry

The order of reactivity for the Cbz-DEVaD inhibitors is $(S,S) > (R,R) > (cis)$, while the order of reactivity for the Cbz-EVaD inhibitors is $(S,S) > (R,R) \approx (cis)$ (Table 3.7). Adding steric bulk and varying the epoxide stereochemistry confirms that the (S,S) stereochemistry is strongly preferred, as seen with the Cbz-DEVaD-EP-CON(Bzl)₂ **III-14a** series and the Cbz-EVaD-EP-CON(Bzl)₂ **III-14b** series. The dibenzyl amide group, when compared to an ethyl ester group, accentuates the difference between the stereoisomers.

The (R,R) and (cis) stereoisomers of the Cbz-EVaD-EP-CON(Bzl)₂ **III-14b** series do not inhibit any of the apoptotic caspases, again emphasizing the overall preference of caspases for an (S,S) stereochemistry to obtain high potency. In addition, this series also emphasizes the importance of the S4 subsite. In comparing Cbz-DEVaD- (S,S) -EP-CON(Bzl)₂ **III-14a** to Cbz-EVaD- (S,S) -EP-CON(Bzl)₂ **III-14b**, potency is decreased for each caspase except for caspases-9 and -10 (Table 3.7).

Table 3.7 Combined effect of epoxide stereochemistry and prime side substituent

	Inhibitor	EP	k_2 (M ⁻¹ s ⁻¹)						
			Casp-2	Casp-3	Casp-6	Casp-7	Casp-8	Casp-9	Casp-10
III-14a	Cbz-DEVaD-EP- CON(Bzl) ₂	(<i>S,S</i>)	786 ± 181	3,120,000 ± 240,000	16,800 ± 7,600	292,000 ± 28,000	235,000 ± 37,000	542 ± 198	3,550 ± 880
		(<i>R,R</i>)	NI	23,100 ± 900	120 ± 4	6,750 ± 1,030	NI	ND	41 ± 21
		(<i>cis</i>)	14 ± 3	1,890 ± 70	41 ± 1	428 ± 39	221 ± 29	NI	46 ± 11
III-14b	Cbz-EVaD-EP- CON(Bzl) ₂	(<i>S,S</i>)	12 ± 0	23,200 ± 2,600	6,740 ± 950	58,900 ± 6,300	98,800 ± 4,400	1,320 ± 290	9,310 ± 1,770
		(<i>R,R</i>)	NI	NI	NI	NI	NI	NI	NI
		(<i>cis</i>)	NI	NI	NI	NI	NI	NI	NI

Implications for selectivity between apoptotic caspases

In this discussion, a highly selective and potent inhibitor for caspase-3 is defined as an inhibitor that shows a $>1,000,000 \text{ M}^{-1}\text{s}^{-1}$ rate constant and >100 -fold selectivity for caspase-3 over all other apoptotic caspases. For all other caspases, a highly selective and potent inhibitor is defined as one showing a rate constant $>10,000 \text{ M}^{-1}\text{s}^{-1}$ and >10 -fold selectivity for one caspase over all other apoptotic caspases. The fulfillment of these criteria would provide significant improvements over previously published work with aza-peptide epoxides.⁷³ No aza-peptide epoxide inhibitor discussed above met these criteria. However, this research does present implications towards more selective caspase inhibitors.

Selective caspase-7 aza-peptide epoxide inhibitor. As mentioned, caspases-3 and -7 are highly homologous, showing 57% sequence homology.⁹³ The S1' subsites of the enzymes are very similar, and the only key residue difference is the replacement of Phe in caspase-3 for a Tyr in caspase-7 (see Table 3.3, page 56). Thus, obtaining selectivity for caspase-7 over caspase-3 is very difficult. Both caspase-7 and caspase-3 are highly reactive with the Cbz-DEVaD sequence, with caspase-3 generally being 10-fold more reactive. Interestingly, caspase-7 has a higher affinity than caspase-3 for certain natural substrates, suggesting that small-molecule inhibitors selective for caspase-7 are possible and could have biological applications.¹⁶⁹

Caspase-3 shows a high preference for the P1' dibenzyl amide substituent over the monobenzyl amide and benzyl ester (see Table 3.6, page 75). However, caspase-7 does not show such a distinction. Reactivity of caspase-7 with each of these compounds is virtually the same ($\sim 300,000 \text{ M}^{-1}\text{s}^{-1}$). Comparison of the unoccupied S1' subsites of

caspase-3 (1PAU) and caspase-7 (1F1J) does show that the caspase-7 subsite is about 0.7 Å smaller than the caspase-3 subsite (Met – Thr distance). This evidence, combined with the kinetic data in Table 3.6, suggests that, unlike caspase-3, only one benzyl group is binding in the S1' subsite of caspase-7. Thus, mono-amide groups coupled with the (*S,S*) stereochemistry are the most effective P1' substituent for a selective caspase-7 inhibitor.

Also, caspase-7 tolerates the loss of a P4 residue to a greater extent than caspase-3. For example, simply removing the P4 Asp of Cbz-DEVaD-(*S,S*)-EP-CO₂Et **III-13a** gives the inhibitor Cbz-EVaD-(*S,S*)-EP-CO₂Et **III-13b** that is 3.3-fold selective for caspase-7 (168,000 M⁻¹s⁻¹) over caspase-3 (50,500 M⁻¹s⁻¹). Unfortunately, caspase-8 also tolerates removal of the P4 Asp quite well (195,000 M⁻¹s⁻¹), and the addition of bulky P1' substituents does not increase selectivity for caspase-7 over -8. So, while selectivity can be obtained between caspase-3 and -7, how to obtain selectivity between caspases-7 and -8 with the Cbz-EVaD sequence is currently not clear. However, inhibitors with the Cbz-EVaD sequence, mono-amide P1' substituent groups, and the (*S,S*) stereochemistry would have for selectivity for caspase-7 over caspase-3.

Selective caspase-3 aza-peptide epoxide inhibitor. High potency with caspase-3 can easily be obtained with the Cbz-DEVaD sequence. However, high selectivity (>100-fold) is not seen in the aza-peptide epoxide inhibitors with the (*S,S*) stereochemistry. In particular, it is difficult to obtain high selectivity for caspase-3 over caspases-7 and -8. Caspases-7 and -8 are tolerant of the same P1' substituents that work well with caspase-3, such as the dibenzyl amide of Cbz-DEVaD-(*S,S*)-EP-CON(Bzl)₂ (see Table 3.6, page 75).

However, caspase-8 is less tolerant of the (*R,R*) stereochemistry than caspase-3. Cbz-DEVaD-(*R,R*)-EP-CO₂Et (464,000 M⁻¹s⁻¹, caspase-3), synthesized by Dr. Juliana

Asgian, is the most selective caspase-3 aza-peptide epoxide inhibitor, with 591-fold selectivity over caspase-8, but it is not highly potent ($>1,000,000 \text{ M}^{-1}\text{s}^{-1}$). Also, caspase-3 cannot tolerate both large P1' substituents and the (*R,R*) stereochemistry (Cbz-DEVaD-(*R,R*)-EP-CON(Bzl)₂ **III-14a**, $23,200 \text{ M}^{-1}\text{s}^{-1}$, caspase-3). However, the potency of smaller P1' substituents with the (*R,R*) stereochemistry is not known. Thus, an aza-peptide epoxide inhibitor with the Cbz-DEVaD sequence, (*R,R*) epoxide stereochemistry, smaller P1' could be a highly selective and potent for caspase-3 over caspase-8.

Alternatively, Cbz-DEVaD-(*S,S*)-EP-CON(Bzl)₂ **III-14a** shows good selectivity for caspase-3 versus caspase-7, with 10.7-fold selectivity. As mentioned, there is a difference in the S1' subsites of caspases-3 and -7, with caspase-7 showing no clear preference for the dibenzyl amide in the P1' position, while caspase-3 show a clear preference for the dibenzyl group in the P1' position. Also, there is a 13.3-fold selectivity for caspase-3 versus caspase-8. Further refinements of this structure could lead to an increase in potency and selectivity for caspase-3 versus caspases-7 and -8.

Selective caspase-8 aza-peptide epoxide inhibitor. The caspase-8 specific sequence Cbz-AEVaD was synthesized. Interestingly, the (*cis*) stereoisomer showed greater potency than the (*R,R*) stereoisomer. However, no increase in selectivity for caspase-8 versus any other caspase was observed. Also, the (*cis*) stereochemistry is still less potent than the (*S,S*). The Cbz-AEVaD sequence, coupled with the (*cis*) stereochemistry and a bulkier P1' substituent would likely decrease potency, but that has not yet been proven.

Also, caspase-8 does contain an insertion sequence in the S1' subsite that is not present in any other caspase.¹²⁸ This insertion loop contained a lysine (see Table 3.3,

page 56). Hydrogen bonding interactions with this lysine could allow for favorable interactions of a P1' substituent with either the (*S,S*) or (*cis*) stereochemistry. A P1' substituent capable of such interactions, combined with either the (*S,S*) or (*cis*) stereochemistry of the epoxide and the Cbz-AEVD sequence, could result in an inhibitor that is highly selective and potent for caspase-8.

Selectivity for caspases-2, -6, -9, and -10. Caspase-2 has a smaller S1' subsite than other caspases, thus this caspase tolerates relatively small P1' functional groups.¹²⁰ Caspase-2 seems to highly prefer the (*S,S*) stereochemistry as well. However, since epoxide stereochemistry and sequence identity have a cooperative effect on potency, and caspase-2 is known to prefer a pentapeptide sequence, it cannot be assumed from the present data that caspase-2 only reacts potently with the (*S,S*) stereoisomers.

Selective and potent caspase-6 inhibitors have been synthesized by Dr. Karen James.⁷³ These inhibitors have the Cbz-IETaD sequence and (*R,R*) stereochemistry. This selectivity is very significant, since selectivity for caspase-6 over caspase-8 is very difficult to obtain. However, the present data did not reveal any additional insights about selective caspase-6 inhibitors.

Caspase-9 showed little to no reactivity with the inhibitors tested, with rate constants up to $1,810 \text{ M}^{-1}\text{s}^{-1}$). The most potent inhibitors ($>1,000 \text{ M}^{-1}\text{s}^{-1}$) have the Cbz-EVD sequence. Since this sequence reacts much more potently with caspase-7 and -8 ($>100,000 \text{ M}^{-1}\text{s}^{-1}$), this is not a good route towards selective caspase-9 inhibitors. Based on substrate specificity, and given that caspase-9 tolerates a tri-peptide sequence, the Cbz-EHaD sequence could be a more selective caspase-9 inhibitor (see Table 3.2, page 55). However, such an inhibitor might not show high selectivity over caspase-10.

Caspase-10 also did not show any selectivity for the inhibitors tested. The highest potency was with Cbz-DEVaD-(*S,S*)-EP-CO₂Bzl (22,000 M⁻¹s⁻¹), originally synthesized by Dr. Juliana Asgian. The inhibitor Cbz-AEVD-FMK is commercially available, and is marketed as a caspase-10 specific inhibitor.¹⁶⁷ However, with the aza-peptide epoxide warhead, this sequence is clearly selective for caspase-8 over caspase-10 by 65-fold (see Cbz-AEVaD-(*S,S*)-EP-CO₂Et **III-13c**, Table 3.5, page 71). Also, the aldehyde inhibitor Cbz-AEVD-CHO has been reported to be 200-fold more potent for caspase-8 than for caspase-10.¹⁴¹ Clearly, the Cbz-AEVaD sequence is not a good candidate for a caspase-10 specific inhibitor.

Interestingly, caspase-10 showed a clear preference for a bulky P1' substituent with the Cbz-EVaD sequence. Cbz-EVaD-(*S,S*)-EP-CON(Bzl)₂ (9,310 M⁻¹s⁻¹) is two-fold more potent than Cbz-EVaD-(*S,S*)-EP-CO₂Et (4,000 M⁻¹s⁻¹). Again, this shows that influence that the S4 subsite has on prime side substituent. As with caspase-9, however, the Cbz-EVaD sequence shows a much higher preference for caspases-7 and -8, thus its use as a caspase-10 specific inhibitor is limited. However, the S1' subsite of caspase-10 has an Arg residue (see Table 3.3, page 56). Specific interactions with this residue, combined with the appropriate sequence, could result in a selective caspase-10 inhibitor. The appropriate aza-peptide epoxide sequence for a selective caspase-10 is not known at this time.

Stereochemical preference

In general, (*S,S*) aza-peptide epoxide inhibitors are more potent than (*R,R*) and (*cis*) aza-peptide epoxide inhibitors. This preference has been shown to be true for

several sequences, such as PhPr-VAaD, Cbz-DEVaD, Cbz-LETaD, Cbz-IETaD, Cbz-AEVaD, and Cbz-EVaD.⁷³ However, there had not yet been any studies done to show why the (*S,S*) stereochemistry is more potent. Modeling studies were done to determine why the (*S,S*) stereoisomer is, in general, more potent than the (*R,R*) stereoisomer.

Limitations of modeling. The most significant limitation of the modeling studies is that only the atoms of ligand (inhibitor) and the hydrogen atoms of the enzyme are flexible. The heavy atoms of the enzyme are fixed throughout all the calculations, therefore eliminating any possible lock-and-key fit that is expected to occur with an enzyme – inhibitor complex. Also, to save computational time, only the enzyme residues that are within a 7.5 – 10.0 Å proximity of the inhibitor were included in the docking calculations.

Another limitation was that the inhibitor could not be docked with a covalent bond between the catalytic cysteine and the site of nucleophilic attack. The C – S distance was restrained to 1.81 Å, but repulsive van der Waals forces shift the inhibitor. Thus, certain hydrogen bond distances would be significantly different in the model than in the actual enzyme – inhibitor complex.

Finally, all the models were done with enzyme – inhibitor complexes that contained aldehyde inhibitors (1PAU and 1F1J).^{122,127} The aza-peptide epoxide warhead and P1' substituent were drawn using the MOE builder tool. Again, because the heavy atoms of the enzyme were fixed, the position of the dibenzyl groups in the S1' subsite could not be accurately predicted. Crystal structures of caspase-3 – aza-peptide epoxide complexes later became available, including Cbz-DEVaD-(*S,S*)-EP-CON(Bzl)₂, and there are several similarities between the model and the crystal structure of Cbz-DEVaD-(*S,S*)-

EP-CON(Bzl)₂ with caspase-3. The model and crystal structure correlate enough that conclusions drawn from the models are valid; a more detailed comparison are made in the following discussion.

Modeling studies with the (*S,S*) and (*R,R*) stereoisomers. Modeling studies were done using the Molecular Operating Environment (MOE) software package. The inhibitors Cbz-DEVaD-(*S,S*)-EP-CON(Bzl)₂ and Cbz-DEVaD-(*R,R*)-EP-CON(Bzl)₂ were docked in the active site of caspase-3. The coordinates (PDB 1PAU) contained the peptidyl aldehyde inhibitor, Ac-DEVD-CHO (Figure 3.11). The acetyl amino terminus protecting group was converted to a benzyloxycarbonyl (Cbz) protecting group, and the P1 Asp was converted to an AAsp (aD) using the builder tool in MOE. Likewise, the aza-peptide epoxide warhead and the P1' dibenzyl amide substituent were drawn using the MOE builder tool. The epoxide was drawn closed. The site of attack was restrained to the sulfur atom of the catalytic cysteine to a distance of 1.81 Å.

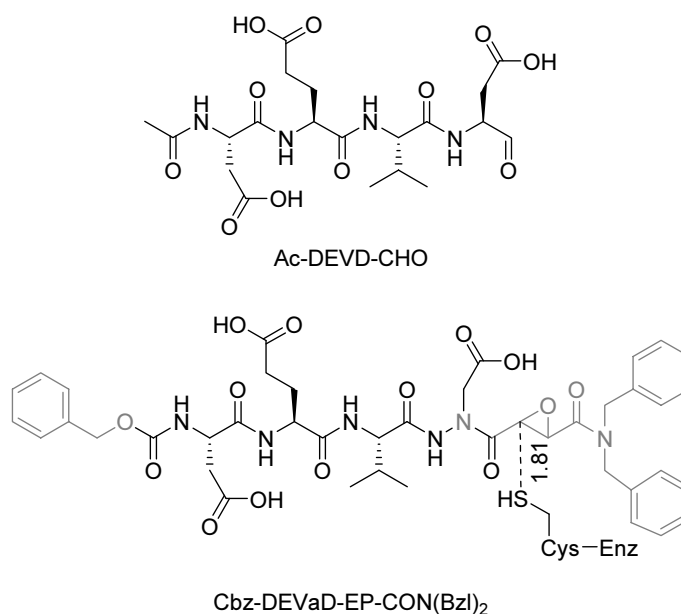


Figure 3.11 Conversion of aldehyde inhibitor to aza-peptide epoxide inhibitor

Epoxysuccinate orientation. In the figures below, the catalytic Cys-His dyad is shown, with the Gly residue in the foreground and the catalytic Cys in the background. The key differences are the orientation the epoxide oxygen and the carbonyl oxygen adjacent to the AAsp. Ideally, this carbonyl (CO1) can form hydrogen bonding interactions with the oxyanion hole formed by the backbone nitrogens of the catalytic Cys and the Gly residue. This same carbonyl will form these interactions in a substrate, and this interaction is key to substrate hydrolysis.³² In the models shown, the CO1 carbonyl is further away from the oxyanion hole in the (*R,R*) stereoisomer than in the (*S,S*) stereoisomer. Also, the AAsp is rotated in a completely different orientation in the (*R,R*) stereoisomer than in the (*S,S*) stereoisomer (Figure 3.12).

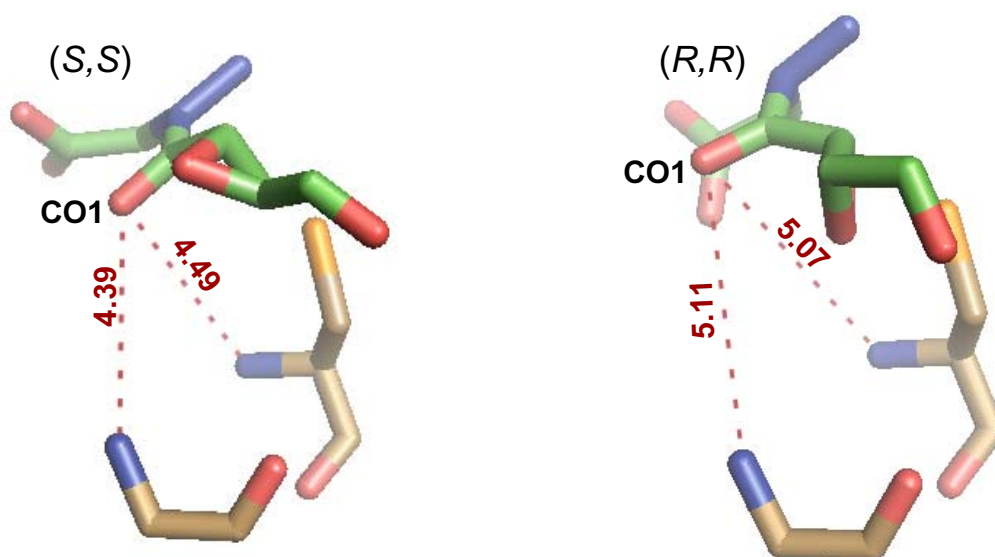


Figure 3.12 Relative positions of AAsp carbonyl (CO1) to oxyanion hole

AAsp orientation. The difference in the AAsp orientation is shown more clearly in the figures below (Figure 3.13). The carboxylate group of the AAsp is ‘parallel’ to the

guanidino group of Arg64 in (*S,S*) inhibitor model, while the same interaction is almost ‘perpendicular’ in the (*R,R*) inhibitor model. The orientation that is seen in the (*S,S*) inhibitor model is also seen in crystal structures of aza-peptide epoxides bound with caspase-3.

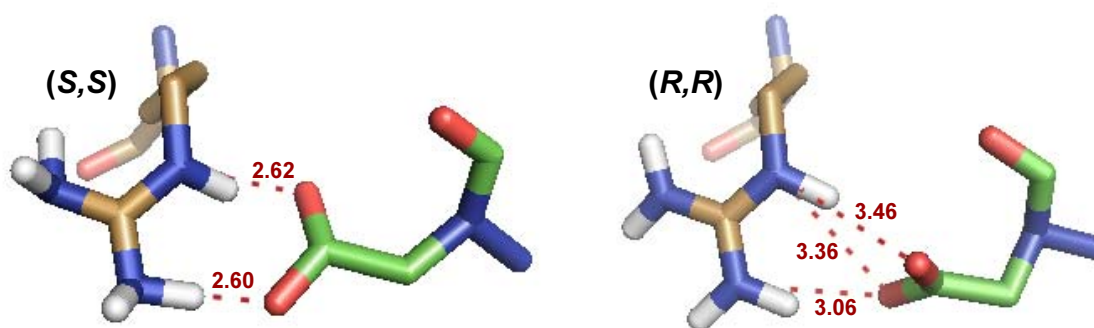


Figure 3.13 Comparison of the AAsp and Arg64 interactions

This reorientation significantly alters the hydrogen bonding system of the AAsp for the (*R,R*) inhibitor relative to the (*S,S*) inhibitor. The hydrogen atoms were added and included in the modeling calculations, thus allowing for examination of the hydrogen bonds’ collinearity. While the bond distances of the potential hydrogen bonds in the (*R,R*) inhibitor are reasonable distances, there is a smaller degree of collinearity in these hydrogen bonds (3.46 Å, 145.61°; 3.36 Å, 144.80°; 3.06 Å, 145.90°) than for the potential hydrogen bonds present in the (*S,S*) inhibitor (2.60 Å, 169.69°; 2.62 Å, 158.08°). This difference indicates that the hydrogen bonding system of the (*S,S*) inhibitor is stronger than that of the (*R,R*) inhibitor.

Additional observations and comments. In the following schematics of the models, potential hydrogen bonds are shown in black and red. Distances that are slightly above or below a reasonable hydrogen bond heavy atom distance (2.50 – 3.70 Å) are shown in black, those within that range are shown in red. The C – S distance is shown in blue. The distances from the CO1 carbonyl to the oxyanion hole are shown in green.

The (*S,S*) inhibitor hydrogen bonding interactions of the model were confirmed by comparing the model to the crystal structure of the same inhibitor bound to caspase-3 (Figures 3.14 and 3.16). Most potential hydrogen bonds shown are present in the crystal structure, the only exception is the potential hydrogen bond between the CO1 carbonyl and the His sidechain present in the model. Also, while the CO1 carbonyl is not within hydrogen bonding distance of the oxyanion hole in the model, it easily is in the crystal structure.

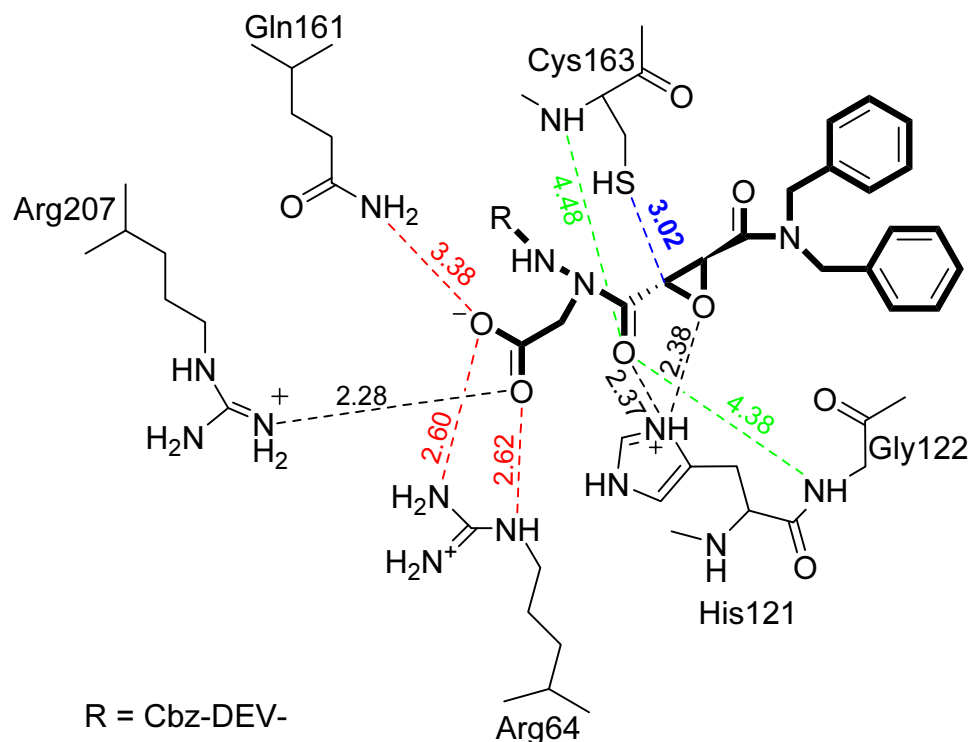


Figure 3.14 Schematic of Cbz-DEVaD-(*S,S*)-EP-CON(Bzl)₂ model

One reason for these differences is the starting position of the CO1 carbonyl in the modeling calculations. A caspase-3– aldehyde inhibitor complex (1PAU) was used for the model, and this carbonyl typically hydrogen-bonds to the His sidechain in these complexes. Also, these differences occur because the distance from the nucleophilic sulfur atom to the site of attack is 3.02 Å, well above the normal C – S bond distance of 1.81 Å. Besides these differences, the (*S,S*) inhibitor model is highly similar to the (*S,S*) inhibitor crystal structure.

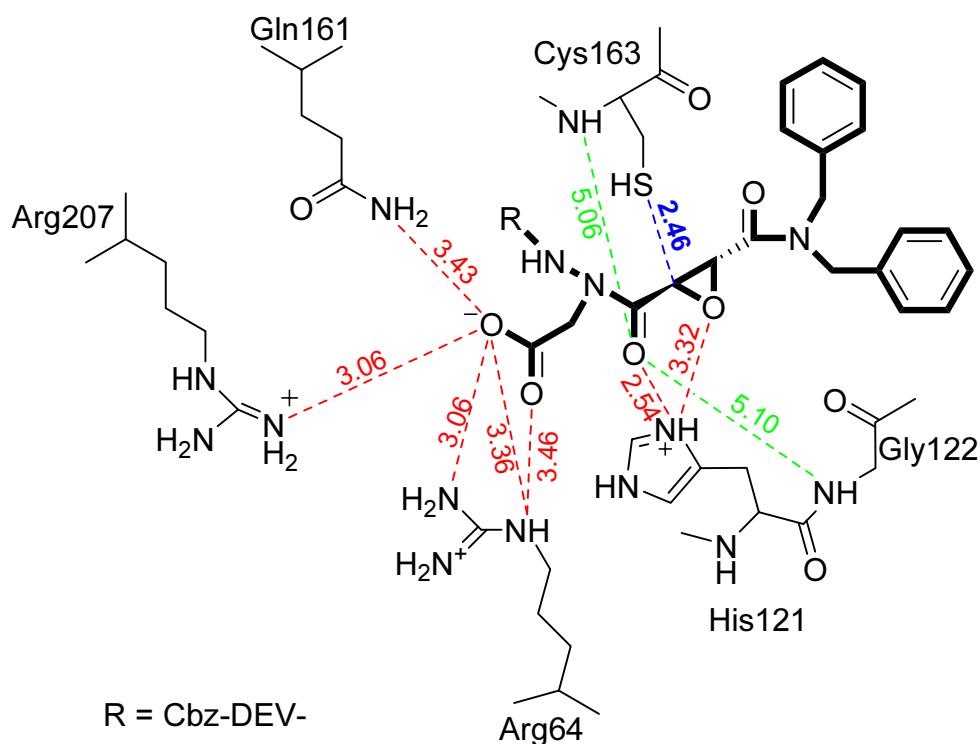


Figure 3.15 Schematic of Cbz-DEVaD-(*R,R*)-EP-CON(Bzl)₂ model

In contrast, the (*R,R*) inhibitor model has significantly different interactions compared to both the (*S,S*) inhibitor model (Figure 3.15). As discussed earlier, the AAsp is rotated differently and the CO1 carbonyl has an orientation that is further away from

the oxyanion hole. Also, the C – S distance is not as great in the (*R,R*) inhibitor model (2.46 Å) as in the (*S,S*) inhibitor model (3.02 Å). Thus, even with an approximate correction for this distance, the CO1 carbonyl still would not be within hydrogen bonding distance of the oxyanion hole.

Thus, for the (*R,R*) inhibitor to have the CO1 carbonyl interacting with the oxyanion hole and effective binding of the AAsp in the S1 subsite, the system must be highly strained. This strain could cause the (*R,R*) inhibitors to be less potent than the (*S,S*) inhibitors, even when there is no steric bulk in the P1' position, such as with Cbz-DEVaD-(*R,R*)-EP-CO₂Et (see Table 3.5, page 71). When there is steric bulk in that position, as seen with Cbz-DEVaD-(*R,R*)-EP-CON(Bzl)₂, potency greatly reduced compared to the (*S,S*) inhibitor (see Table 3.7, page 78). The (*R,R*) epoxide stereochemistry obviously changes the trajectory of the prime side substituent, which creates steric interactions that decrease potency.

X-ray crystal structure. As mentioned, the x-ray crystal structure of Cbz-DEVaD-(*S,S*)-EP-CON(Bzl)₂ **III-14a** bound to caspase-3 (1.70 Å) was obtained by Ganesan Rajkumar of Dr. Markus Grütter's lab at the University of Zurich (Figure 3.16). The crystal structure shows that the epoxide oxygen forms a hydrogen bond with the sidechain nitrogen of the His residue (2.94 Å). Also, the CO1 carbonyl clearly hydrogen bonds with the oxyanion hole.

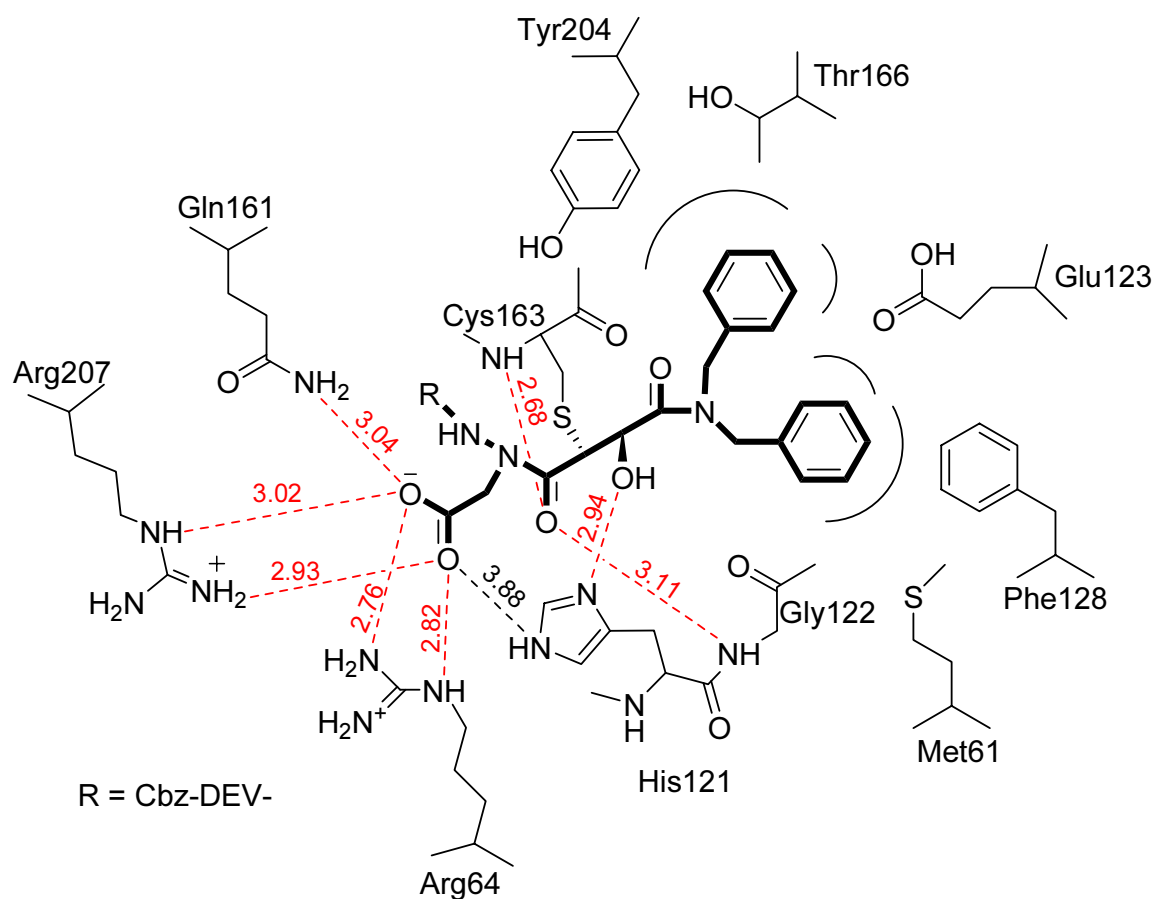


Figure 3.16 Schematic of caspase-3 – Cbz-DEVaD-(*S,S*)-EP-CON(Bzl)₂ complex

In comparing this crystal structure with 1PAU, the crystal structure used in the models discussed above, there are a few conformational changes of the enzyme sidechains. Rotation of the guanidino group in Arg207 allows for an additional hydrogen bond. Also, the unoccupied S1' subsite in 1PAU is bowl-shaped. Because the enzyme sidechains were fixed, the dibenzyl groups present in both the (*S,S*) and (*R,R*) models showed little to no interactions with this subsite. In the crystal structure, this subsite binds each benzyl group in two pockets. One pocket is formed by the sidechains of Tyr204, Thr166, and Glu123, and the other pocket is formed by the sidechains of Glu123, Phe128, and Met61. Compared to the models, the Glu123 sidechain is rotated to

accommodate the binding of the dibenzyl group. Also, the methyl of Met61 is rotated to accommodate the binding of the benzyl group in that pocket.

Compared to the models, the His121 sidechain is also rotated. This rotation allows for a possible hydrogen bond between the N3 of the imidazole ring and an oxygen atom from the AAsp carboxylate group, although the distance is slightly above normal heavy-atom distance for a hydrogen bond (3.88 Å). However, even if this hydrogen bond does not exist, this rotation likely allows room for the CO1 carbonyl to easily interact with the oxyanion hole. The N1 of the His imidazole forms a hydrogen bond with the oxygen of the opened epoxide and serves as a proton source for this atom.

Mechanism of inhibition. Based on the models, the (*S,S*) and (*R,R*) inhibitors will initially form a hydrogen bond between the N1 of the catalytic His121 and the CO1 carbonyl. However, this is not believed to be the correct mechanism. The models were based on an enzyme – inhibitor complex with an aldehyde inhibitor. This carbonyl in the aldehyde inhibitor does not interact with the oxyanion hole. However, in the crystal structures of the caspase-3 – aza-peptide epoxide complex, this carbonyl does rotate towards the oxyanion hole. Also, there is evidence that the catalytic His does not have to rotate to prevent this residue from interfering with the CO1 carbonyl's interaction with the oxyanion hole. This hypothesis is supported by a high-resolution (1.9 Å) unliganded caspase-3 crystal structure (1QX3).¹²⁴ Unlike the crystal structure used for the model, 1PAU, the unliganded crystal structure shows that the His121 is rotated in a similar manner as the aza-peptide epoxide crystal structure. Thus the His121 residue likely rotates in the enzyme – aldehyde inhibitor complexes, but not in the aza-peptide epoxide inhibitor complexes.

In addition to the interaction of the CO1 carbonyl with the oxyanion hole, several hydrogen bonds are made between the S1 subsite sidechains and the P1 AAsp. Upon reaction with the catalytic thiol, the epoxide ring is opened, the oxygen of the open epoxide is protonated by the catalytic His, and a hydrogen bond is formed (Figure 3.17).

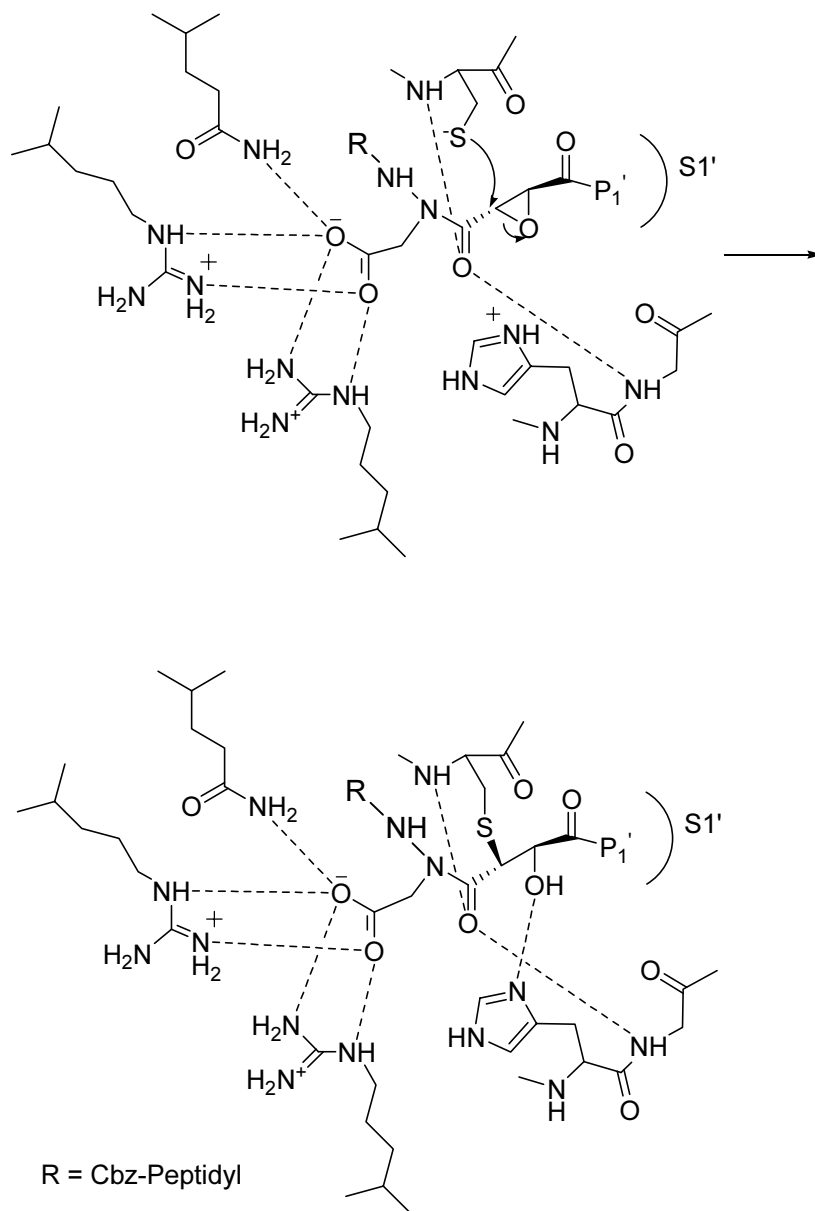


Figure 3.17 Proposed mechanism of inhibition

The mechanism of inhibition for the (*R,R*) inhibitor should proceed as shown for the (*S,S*) inhibitor. As mentioned, the (*R,R*) inhibitor model suggests that for the CO1 carbonyl to make the critical interaction with the oxyanion hole, the AAsp must be reoriented. This reorientation introduces strain in the system and slows down the reaction of the catalytic thiolate with the epoxide. Also, adding a large prime side substituent combined with the (*R,R*) stereochemistry greatly decreases potency with respect to its cognate (*S,S*) inhibitor. Thus, the positioning of the (*R,R*) inhibitor prime side substituent is not as ideal as in the (*S,S*) inhibitor, and potency is decreased. However, while less potent, the (*R,R*) stereochemistry could be useful towards designing more selective caspase inhibitors. Some caspases, such as caspase-8, have a decreased tolerance of the (*R,R*) stereochemistry compared to other caspases.

The conclusions discussed, including the proposed mechanism, are assumed to be true for all apoptotic caspases. Some questions remain, such as why caspase-8 is significantly less tolerant of the (*R,R*) stereochemistry than other caspases. However, an caspase – aza-peptide epoxide complex should always have these three elements: strong hydrogen bonding of the P1 Asp in the S1 subsite, interaction of the AAsp carbonyl (CO1) with the oxyanion hole via hydrogen bonds, and hydrogen bonding of the opened epoxide hydroxyl group with the catalytic His sidechain. In general, an inhibitor with the (*S,S*) stereochemistry can make these interactions quite easily, while these interactions in an inhibitor with the (*R,R*) stereochemistry results in a highly strained system. Other modeling results (not shown) suggest that the (*cis*) stereochemistry also results in a highly strained system.

Aza-peptide epoxides versus aza-peptide Michael acceptors

Aza-peptide Michael acceptors are another recently designed class of clan CD protease inhibitors.^{142,170} The design was based in part on the aza-peptide epoxide inhibitor design, replacing the epoxide moiety with the double bond, or Michael acceptor moiety. Like aza-peptide epoxides, given the appropriate sequence, aza-peptide Michael acceptors potently and specifically inhibit a variety of clan CD proteases, including legumain, caspases, and gingipains. However, the aza-peptide Michael acceptor inhibitors seem to show more selectivity between caspases and are sometimes more potent than aza-peptide epoxides. This section briefly discusses these differences. This work also presents a newly synthesized aza-peptide Michael acceptor.

The synthesis of the Michael acceptor moiety is shown below (Figure 3.18). Mono-ethyl fumarate was coupled to an amine via the mixed anhydride coupling method, and the ethyl ester was hydrolyzed with sodium hydroxide in ethanol. In the synthesis shown here, *N,N*-di(1-naphthylmethyl)amine was used, resulting in the new compound **III-19**.

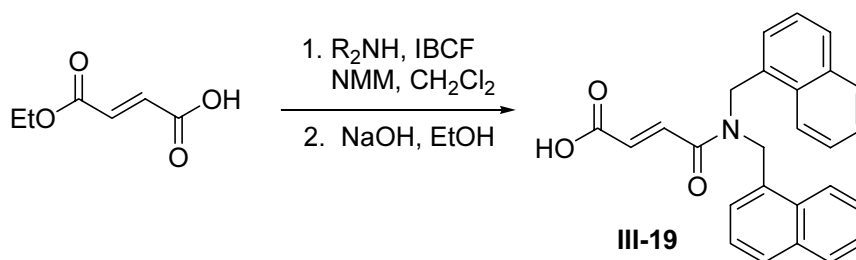


Figure 3.18 Michael acceptor moiety synthesis

This Michael acceptor precursor, **III-19**, was then coupled to the Cbz-DEV-NH-NH-CH₂CO₂-*t*-Bu sequence using the EDC/HOBt method. The Glu, Asp, and AAsp

sidechains were then deprotected with TFA, giving the new inhibitor Cbz-DEVaD-CH=CH-CON(1-CH₂-Naph)₂, **III-20a** (Figure 3.19).

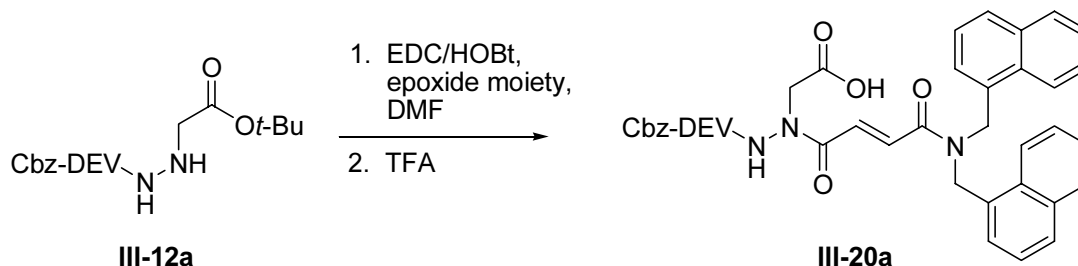


Figure 3.19 Aza-peptide Michael acceptor synthesis

The new inhibitor, Cbz-DEVaD-CH=CH-CO-N(1-CH₂-Naph)₂ **III-20a**, is the most potent caspase-3 and -7 aza-peptide Michael acceptor inhibitor to date, inhibiting caspase-3 at 5,620,000 M⁻¹s⁻¹ and inhibiting caspase-7 at 875,000 M⁻¹s⁻¹ (Table 3.8). Also, this inhibitor is highly selective for caspases-3 and -7. The cognate aza-peptide epoxide, Cbz-DEVaD-(*S,S*)-EP-CO-N(1-CH₂-Naph)₂, does not show such high reactivity and selectivity, inhibiting caspase-3 at only 457,000 M⁻¹s⁻¹.

Previously, Dr. Özlem D. Ekici synthesized the aza-peptide Michael acceptor Cbz-DEVaD-CH=CH-CON(Bzl)₂ **Oz-1** and found this inhibitor to be highly potent and selective for caspase-3 (3,000,000 M⁻¹s⁻¹, Table 3.8) against caspase-6 (588-fold) and caspase-8 (349-fold). While this inhibitor's aza-peptide epoxide analogue, Cbz-DEVaD-(*S,S*)EP-CON(Bzl)₂ **III-14a** is equipotent with caspase-3 (3,120,000 M⁻¹s⁻¹), it is much less specific for caspase-3 against caspase-6 (186-fold) and caspase-8 (13.3-fold).

Table 3.8 Aza-peptide epoxides vs. aza-peptide Michael acceptors

	R	k_2 ($M^{-1}s^{-1}$)			
		Casp-3	Casp-6	Casp-7	Casp-8
Oz-1^a		3,000,000 ± 80,000	5,100 ± 0	359,000 ± 8,400	8,600 ± 1,600
III-14a		3,120,000 ± 240,000	16,800 ± 7,650	292,000 ± 28,300	235,000 ± 37,000
III-16a		5,620,000 ± 1,120,000	29,700 ± 540	875,000 ± 106,000	9,460 ± 880
III-20a		457,000 ± 32,000	5,210 ± 80	63,400 ± 25,400	13,300

^aThis inhibitor was synthesized and tested with caspases-3, -6, and -8 by Dr. Özlem D. Ekici. All inhibitors shown were also tested with caspase-2 (110 – 786 $M^{-1}s^{-1}$), caspase-9 (66 – 542 $M^{-1}s^{-1}$), and caspase-10 (1,370 – 32,500 $M^{-1}s^{-1}$).

Crystal structures have been obtained of aza-peptide Michael acceptors complexes with caspases-3 and -8.¹⁴² None of these structures included either of the two aza-peptide Michael acceptors discussed in Table 3.8. However, these structures still provide valuable insight into explaining the kinetic results for these inhibitors.

interactions in the S1' subsite, since its reactivity is increased relative to Cbz-DEVaD-CH=CH-CON(Bzl)₂ **Oz-1**.

The absence of this critical hydrogen bond also explains the increased selectivity of the aza-peptide Michael acceptors for caspase-3 versus caspase-8. For caspase-8, Cbz-DEVaD-(*S,S*)-EP-CON(Bzl)₂ **III-14a** is relatively potent (235,000 M⁻¹s⁻¹), and thus is only 13.3-fold more selective for caspase-3 versus caspase-8. In contrast, the cognate aza-peptide Michael acceptors discussed are selective for caspase-3 over caspase-8 by >349-fold. For Cbz-DEVaD-(*S,S*)-EP-CON(Bzl)₂ **III-14a**, the critical hydrogen bond orients the dibenzyl group so that it binds favorably in the S1' subsite of caspase-8. As with caspase-3, the potency for Cbz-DEVaD-(*S,S*)-EP-CON(1-CH₂-Naph)₂ **III-16a** (13,300 M⁻¹s⁻¹) is decreased for caspase-8 because of the repulsive steric interactions of the more bulky prime side substituent.

The aza-peptide Michael acceptors, however, have decreased potency with caspase-8, relative to the aza-peptide epoxides, because they lack this critical hydrogen bond. The orienting effect of the hydrogen bond is lost, and while this is an advantage for caspase-3, it is a clear disadvantage for caspase-8. The S1' subsite of caspase-8 is less hydrophobic than the subsite of caspase-3, thus without any orientation, the bulky prime side substituent groups will likely make unfavorable steric interactions in the S1' subsite of caspase-8.

Thus, aza-peptide Michael acceptors have the advantage of being more selective, and sometimes more potent, inhibitors than their respective aza-peptide epoxides. However, this increase in selectivity is only seen with caspase-3 versus caspase-8. No increase of selectivity for any other caspase was observed in a series of compounds that

included the caspase-8 sequence Cbz-LETaD and the caspase-6 and -8 sequence Cbz-IETaD.¹⁴²

Also, aza-peptide Michael acceptors have the disadvantage of being reactive with simple thiols, as shown by Drs. Marion Götz and Özlem D. Ekici. However, this instability seems to not create any problems in cell death assays. Aza-peptide Michael acceptors were equipotent to aza-peptide epoxide in cell death assays performed in Dr. Jonathon Glass's laboratory at Emory University (*unpublished data*). Thus, it is uncertain as to whether one inhibitor design, aza-peptide epoxide or aza-peptide Michael acceptors, is advantageous over the other. Both designs are major advances in the design and synthesis of clan CD inhibitors.

CONCLUSIONS

Epoxide stereochemistry and prime side interactions have a significant influence on the reactivity and selectivity of aza-peptide epoxides with caspases. In general, the an aza-peptide epoxide with the (*S,S*) stereochemistry is the most potent, although increased selectivity between certain caspases can be obtained using the (*R,R*) stereochemistry. Reactivity increases with P1' substituent size up to a certain point. Very large, bulky groups decreased potency, but increased selectivity between certain caspases, such as caspase-3 over caspase-8.

This research also highlighted the importance of the S4 subsite. Occupancy of the S4 subsite for most caspases is needed for high potency, although inhibition of caspases-7, -8 and -9 is sometimes equipotent with a tri-peptide sequence. Also, the binding properties of the P4 residue in the S4 subsite greatly influences reactivity with respect to

epoxide stereochemistry. Various implications towards more selective aza-peptide epoxide inhibitors for the apoptotic caspases were also discussed.

Modeling studies and crystal structures have provided insight into the binding interactions of the various stereoisomers. Also, specific reasons as to why the (*S,S*) stereochemistry results in the most potent inhibitor were determined, and a detailed mechanism of inhibition was proposed.

Finally, aza-peptide epoxides were compared to another important class of clan CD inhibitors, aza-peptide Michael acceptors. Both designs have distinct advantages and are major advances in the work towards more potent and selective clan CD cysteine protease inhibitors.

PERSPECTIVES ON AZA-PEPTIDE EPOXIDES

Aza-peptide epoxides have the potential to be developed into useful biological tools and therapeutic agents. As irreversible inhibitors, the therapeutic potential of aza-peptide epoxides may be limited to short-term treatment of acute conditions, such as traumatic brain and spinal cord injury. Long-term use of irreversible inhibitors, specifically irreversible inhibitors of caspases, could lead to severe disruptions in the normal cell death cycle, and thus create toxic side effects. To develop a drug-like aza-peptide epoxide, the appropriate peptidomimetic chain is needed. However, since crystal structures are now available with aza-peptide epoxides, modeling studies would provide an efficient route towards designing the appropriate peptidomimetic chain.

As biological tools, the aza-peptide epoxides can be synthesized with the appropriate peptidyl sequences, epoxide stereochemistry, and P1' substituent. While

interesting inhibitors were synthesized in this work, some improvements could be made to develop more selective and potent inhibitors. Again, modeling studies would be essential towards developing highly potent and selective caspase inhibitors. Most interestingly, aza-peptide epoxides have shown promise toward developing small-molecule inhibitors highly selective and potent for caspase-6 and caspase-7. Obtaining selectivity for these caspases is difficult, and to our knowledge there has not yet been an inhibitor selective for caspase-7 over caspase-3 reported previously in the literature.

Details about the roles of these caspases are still not completely understood, and inhibitors highly selective and potent for these caspases would provide important information about their roles in the apoptotic cascade. For example, recently caspase-6 was implicated as being the primary executioner caspase activated in the AD brain. A highly potent and selective caspase-6 inhibitor could confirm this implication.^{171,172} Also, caspase-7 was recently shown to be expressed on a higher scale than previously realized after traumatic brain injury.¹⁷³ Caspase-7 has been thought to a redundant member of the apoptotic cascade, since it seems to be a somewhat weaker version of caspase-3. However, caspase-7 likely plays a more important role than previously realized. Selective inhibitors for caspase-6 and -7 would be useful towards determining the importance of these caspases.

For caspase-7, an analysis of the interactions of various Cbz-EVaD aza-peptide epoxide inhibitors with caspases-3, -7, and -8 would be a good starting point, with a focus on obtaining >10-fold selectivity for caspase-7 versus caspases-3 and -8. For caspase-6, and analysis of Cbz-IETaD aza-peptide epoxide inhibitors with the (*R,R*) stereochemistry

would provide essential information towards obtaining a highly selective and potent caspase-6 inhibitor.

For these studies, a combination of modeling studies and combinatorial library synthesis could be used. In the modeling studies, care must be taken to generate accurate models. Accurate model generation would require the flexibility of both the enzyme and inhibitor. Preferably both the enzyme backbone and sidechains should be flexible, but if the computational cost is too high, then at least the sidechains should have flexibility.

In conclusion, aza-peptide epoxides represent an important advance towards highly potent and selective caspase inhibitors, and there is much more work to be done to develop this class of inhibitors.

EXPERIMENTAL

Chemical Synthesis

Mono peptidyl methyl esters and benzyloxycarbonyl (Cbz) N^α-amino protected amino acids were purchased from Biochem Bioscience, Inc., King of Prussia, PA. Other reagents and reactants for synthesis were purchased from Fischer Scientific, Acros Organics and Sigma Aldrich. The ¹H NMR spectra were obtained using a Varian Mercury 400 MHz spectrometer. Electrospray ionization (ESI), fast-atom-bombardment (FAB), and high-resolution mass spectrometry were done using Micro-mass Quattro LC and VG Analytical 70-SE instruments. Elemental analysis was performed by Atlantic Microlab Inc., Norcross, GA.

Methyl ester peptidyl sequences, III-10a – III-10b. Methyl ester peptidyl sequences were synthesized using the appropriate mono peptidyl methyl esters and the

benzyloxycarbonyl (Cbz) N^α-amino protected amino acids. Sequences were synthesized using the mixed anhydride peptide coupling method. Each intermediate was characterized using ¹H NMR spectroscopy.

Cbz-Peptidyl-NHNH₂, III-11a – III-11c. To a solution of the methyl ester peptidyl sequence in MeOH was added hydrazine (10 eq) dropwise while stirring under argon at rt. The reaction was stirred overnight. The MeOH was removed and the product was washed with EtOH and Et₂O, resulting in a white solid.

Cbz-Peptidyl-(AA)_n-NHNHCH₂COO-*t*-Bu. A solution of the peptidyl hydrazide (1 eq) and NMM (1 eq) in DMF was cooled to -10 °C. To this solution *tert*-butyl bromoacetate (1.5 eq) was added. The reaction was stirred at -10 °C for 30 min and then stirred at rt overnight. The DMF was removed, and the product was purified using column chromatography. Sequence-specific purification conditions and ¹H NMR characterization are listed below.

Cbz-Glu(O-*t*-Bu)-Val-NHNH-CH₂CO₂-*t*-Bu, III-12b. Product was purified using 2:18:5 MeOH:CH₂Cl₂:EtOAc as the solvent system, then re-chromatographed using the same solvent system two times and recrystallized one time from the solvent system with excess hexanes, white solid, yield 43%. ¹H NMR (Acetone-d₆): 0.85-0.97 (m, 6H, Val), 1.42-1.48 (m, 18H, *t*-Bu), 1.87-1.94 (m, 2H, Glu), 2.09-2.12 (m, 1H, Val), 2.32-2.36 (t, 2H, Glu), 3.48-3.79 (m, 2H, AAsp), 4.21-4.29 (m, 2H, α-Hs), 5.00 (d, 1H, NH), 5.10 (s, 2H, Glu), 3.48-3.79 (m, 2H, AAsp), 4.21-4.29 (m, 2H, α-Hs), 5.00 (d, 1H, NH), 5.10 (s, 2H, Glu), 6.62 (d, 1H, NH), 7.29 -7.40 (m, 5H, Cbz-Ph), 8.32 (d, 1H, NH-N).

Cbz-Asp(O-*t*-Bu)-Glu(O-*t*-Bu)-Val-NHNH-CH₂CO₂-*t*-Bu, III-12a. Product was purified using 2:18:5 MeOH:CH₂Cl₂:EtOAc as the solvent system, then was recrystallized two times with 3:17 MeOH:CH₂Cl₂ and excess hexanes, white solid, yield 15%. ¹H

NMR (DMSO- d_6): 0.80-0.86 (m, 6H, Val), 1.36-1.47 (m, 27H, *t*-Bu), 1.72 (m, 1H, Val), 1.85-1.92 (m, 2H, Glu), 2.19-2.20 (m, 2H, Glu), 2.39-2.45, 2.61-2.66 (m, 2H, Asp), 3.37-3.45 (m, 2H, AAsp), 4.04 (t, 1H, α -H), 4.28-4.36 (m, 2H, α -Hs), 4.99-5.07 (m, 2H, Cbz), 7.31 -7.35 (m, 5H, Cbz-Ph), 7.62 (d, 1H, NH), 7.84 (d, 1H, NH), 7.95 (d, 1H, NH), 9.48 (d, 1H, NH-N).

Cbz-Ala-Glu(O-*t*-Bu)-Val-NHNH-CH₂CO₂-*t*-Bu, III-12c. Product was purified using 2:18:5 MeOH:CH₂Cl₂:EtOAc as the solvent system, white solid, yield 26%. ¹H NMR (CDCl₃): 0.90-0.98 (m, 6H, Val), 1.28-1.52 (m, 21H, *t*-Bu, Ala), 1.99-2.43 (m, 5H, Glu, Val), 3.49-3.73 (m, 2H, AAsp), 4.35-4.47 (m, 3H, α -Hs), 5.06-5.16 (m, 2H, Cbz), 5.60 (d, 1H, NH), 7.30-7.35 (m, 5H, Cbz-Ph), 7.80 (d, 1H, NH), 8.02 (s, 1H, NH), 8.57 (d, 1H, NH-N). MS (ESI): *m/z* 636.5 (M + H⁺).

(2*S*,3*S*) and (2*R*,3*R*)-Oxirane-2,3-dicarboxylic Acid Monoethyl Esters (Monoethyl Epoxysuccinates, HOOC-EP-COOEt). The diethyl *trans* epoxysuccinates were synthesized stereoselectively by a procedure adapted from one described previously by Mori and Iwasawa.⁸⁰ This procedure is the same used by James, *et al.*⁷³ The stereochemical control was the result of an anchimeric assistance mechanism. One ethyl ester was hydrolyzed using 1M KOH (1 eq) in EtOH at 0 °C. This hydrolysis was based on a procedure described previously by Rich and Schaschke.^{84,174}

(2*S*,3*S*)-Oxirane-2,3-dicarboxylic Acid Ethyl Ester (HOOC-EP-CO₂CH₂CH₃, III-2). ¹H NMR (DMSO- d_6): 1.20 (t, 3H, OCH₂CH₃), 3.58 (d, 1H, epoxy CH), 3.68 (d, 1H, epoxy CH), 4.16 (q, 2H, OCH₂CH₃).

(2*R*,3*R*)-Oxirane-2,3-dicarboxylic Acid Ethyl Ester (HOOC-EP-CO₂CH₂CH₃, III-2'). ¹H NMR (DMSO-d₆): 1.20 (t, 3H, OCH₂CH₃), 3.58 (d, 1H, epoxy CH), 3.67 (d, 1H, epoxy CH), 4.15 (q, 2H, OCH₂CH₃).

***cis*-Oxirane-2,3-dicarboxylic Acid Monoethyl Ester (Monoethyl Epoxysuccinate, HOOC-EP-COOEt, III-8).** The diethyl ester *cis* epoxysuccinate was synthesized using the same procedure previously described by James, *et al.*⁷³ The procedure described by James was adapted from a method previously described by Meth-Cohn.¹⁶⁸ One ethyl ester was selectively hydrolyzed as described by Rich and Schaschke.^{84,174} ¹H NMR (CDCl₃): 1.27-1.36 (m, 3H, OCH₂CH₃), 3.75-3.81 (dd, 2H, epoxy CH), 4.25-4.37 (m, 2H, OCH₂CH₃).

General Procedure for Coupling of the Mono Ethyl Ester Epoxysuccinates to

Amines. The method used was the mixed anhydride coupling method. The mono ethyl ester epoxysuccinate (1 eq) was dissolved in CH₂Cl₂ (~50 mL) and cooled to -20 °C. To the reaction mixture was added NMM (3 eq) and then IBCF (3 eq). The reaction mixture was stirred at -20 °C for 15-20 minutes and then the amine (3 eq) was added. The reaction mixture was then stirred at -20 °C for one hour and then at rt overnight. The solvent (CH₂Cl₂) was removed, and the crude product was dissolved in EtOAc (~75 mL). The organic layer was then washed with of H₂O, 2% citric acid, saturated NaHCO₃ and brine (~20 mL each). The product was purified with column chromatography as needed. Hydrolysis of the ethyl ester with 1 M NaOH (1.5 eq) in EtOH gave the desired amides, yields 59-96%.

(2*S*,3*S*)-Oxirane-2,3-dicarboxylic Acid Dibenzyl Amide (HOOC-EP-CON(CH₂Ph)₂, III-3). ¹H NMR (DMSO-d₆): 3.51 (d, 1H, epoxy CH), 4.03 (d, 1H, epoxy CH), 4.50 (dd, 2H, NCH₂Ph), 4.70 (dd, 2H, NCH₂Ph), 7.18-7.36 (m, 10H, N(CH₂Ph)₂).

(2*R*,3*R*)-Oxirane-2,3-dicarboxylic Acid Dibenzyl Amide (HOOC-EP-CON(CH₂Ph)₂). ¹H NMR (Acetone-d₆): 3.66 (d, 1H, epoxy CH), 4.05 (d, 1H, epoxy CH), 4.62 (dd, 2H, NCH₂Ph), 4.78 (dd, 2H, NCH₂Ph), 7.27-7.41 (m, 10H, N(CH₂Ph)₂).

(*cis*)-Oxirane-2,3-dicarboxylic Acid Dibenzyl Amide (HOOC-EP-CON(CH₂Ph)₂, III-9). ¹H NMR (DMSO-d₆): 3.79 (d, 1H, epoxy CH), 4.13 (d, 1H, epoxy CH), 4.23-4.63 (dd, 4H, NCH₂Ph), 7.16 (d, 2H, N(CH₂Ph)₂), 7.24-7.37 (m, 8H, N(CH₂Ph)₂).

(2*S*,3*S*)-Oxirane-2,3-dicarboxylic Acid di-1-CH₂-Naphthyl Amide (HOOC-EP-CON(1-CH₂-Naph)₂, III-5). ¹H NMR (Acetone-d₆): 3.59 (d, 1H, epoxy CH), 3.82 (d, 1H, epoxy CH), 5.21-5.36 (m, 4H, N(1-CH₂-Naph)₂), 7.37-7.56 (m, 8H, N(1-CH₂-Naph)₂), 7.84-7.96 (m, 5H, N(1-CH₂-Naph)₂), 8.15-8.18 (m, 1H, N(1-CH₂-Naph)₂).

(2*S*,3*S*)-Oxirane-2,3-dicarboxylic Acid Benzyl(1-CH₂-Naphth) Amide (HOOC-EP-CON(CH₂Ph)(1-CH₂-Naph), III-4). ¹H NMR (DMSO-d₆): 3.58 (dd, 1H, epoxy CH), 4.10 (dd, 1H, epoxy CH), 4.52-4.95 (m, 4H, N(CH₂Ph)(1-CH₂-Naph)), 7.22-7.41 (m, 6H, N(CH₂Ph)(1-CH₂-Naph)), 7.48-7.53 (m, 2H, N(1-CH₂-Naph)), 7.69-7.75 (m, 1H, N(1-CH₂-Naph)), 7.87-7.91 (m, 3H, N(1-CH₂-Naph)).

(2*S*,3*S*)-Oxirane-2,3-dicarboxylic Acid bis-2-CH₂-Furyl Amide (HOOC-EP-CON(2-CH₂-Furyl)₂, III-7). ¹H NMR (DMSO-d₆): 3.46 (d, 1H, epoxy CH), 4.21 (d, 1H, epoxy CH), 4.40-4.57 (dd, 2H, N(2-CH₂-furyl)), 4.60-4.83 (dd, 2H, N(2-CH₂-furyl)), 6.29-6.33 (dd, 2H, N(2-CH₂-furyl)), 6.38-6.40 (dd, 2H, N(2-CH₂-furyl)), 7.57 (d, 2H, N(2-CH₂-furyl)).

(2S,3S)-Oxirane-2,3-dicarboxylic Acid Benzyl(CH₂-Phenyl-4-Hydroxy) Amide

(HOOC-EP-CON(CH₂Ph)(CH₂-Ph-4-OH), III-6). ¹H NMR (DMSO-d₆): 3.33-3.53 (dd, 1H, epoxy CH), 4.02-4.15 (dd, 1H, epoxy CH), 4.29-4.98 (m, 4H, N(CH₂Ph)(CH₂-Ph-4-OH)), 6.74-6.83 (m, 2H, N(CH₂-Ph-4-OH)), 6.97-7.13 (m, 2H, N(CH₂-Ph-4-OH)), 7.19-7.36 (m, 1H, N(CH₂-Ph)), 9.59 (s, 1H, N(CH₂-Ph-4-OH)), 9.84 (s, 1H, CO₂H).

***trans*-3-di-1-CH₂-Naphthylcarbamoylacrylic Acid (HOOC-CH=CH-CON(1-CH₂-Naph)₂, III-II-19a).**

trans-3-di-1-CH₂-Naphthylcarbamoylacrylic acid ethyl ester was obtained by mixed anhydride coupling of equimolar amounts of monoethyl fumarate and *N,N*-di(1-naphthylmethyl)amine to give a clear, yellow syrup (71% yield). EtOOC-CH=CH-CON(1-CH₂-Naph)₂ was hydrolyzed in EtOH using NaOH (1M aqueous, 1.5 eq) under standard deblocking conditions to give a light tan solid. (52% yield). ¹H-NMR (DMSO-d₆): 5.21 (s, 4H, N-1-CH₂-Naph), 6.61-6.62 (d, 1H, *J* = 1.2 Hz, CH=CHCON), 6.69-6.72 (d, 1H, *J* = 14 Hz, CH=CHCON), 7.17-8.11 (m, 14H, N(1-CH₂-Naph)₂).

Cbz-Glu(O-*t*-Bu)-Val-AAsp(O-*t*-Bu)-(2R,3R)EP-CO₂CH₂CH₃. General Procedure

for Aza-peptide Epoxide Synthesis using the EDC/HOBt Coupling Method. To a solution of (2R,3R)-oxirane-2,3-dicarboxylic acid monoester (0.54 mmol, ~3 eq), HOBt (0.47 mmol, ~3 eq), and Cbz-Glu(O-*t*-Bu)-Val-NHNHCH₂COO-*t*-Bu (0.17 mmol, ~1 eq) in DMF (5 mL) at -10 °C was added EDC (0.51 mmol, ~3 eq) while stirring. The reaction mixture was stirred for ~1 hour at -10 °C and then was stirred overnight at rt. The DMF was removed. The product was purified by column chromatography on silica gel with 1:19:5 MeOH:CH₂Cl₂:EtOAc as the eluent; yield 42%. ¹H NMR (Acetone-d₆): 0.95 (d, 6H, Val), 1.26 (t, 3H, OCH₂CH₃), 1.37-1.45(m, 18 *t*-Bu), 1.87-1.95 (m, 2H, Glu), 2.04-2.21 (m, 3H, Glu, Val), 2.32-2.88 (dd, 2H, AAsp), 3.47 (d, 1H, epoxy CH), 4.10 (d,

1H, epoxy CH), 4.17-4.26 (m, 4H, α -H and OCH_2CH_3), 5.10 (s, 2H, Cbz), 6.56 (s, 1H, NH), 7.31 -7.39 (m, 5H, Cbz-Ph), 7.55 (d, 1H, NH), 9.93 (s, 1H, NH-N).

Cbz-Asp(O-*t*-Bu)-Glu(O-*t*-Bu)-Val-AAsp(O-*t*-Bu)-(cis)EP-CO₂CH₂CH₃ was obtained by the EDC/HOBt coupling method and purified by column chromatography on silica gel with 1:19:5 MeOH:CH₂Cl₂:EtOAc as the eluent, then re-chromatographed with 2:1

EtOAc:hexane as the eluent; yield 14%. ¹H NMR (Acetone-d₆): 0.98 (d, 6H, Val), 1.22 (t, 3H, OCH_2CH_3), 1.37-1.48 (m, 27H, *t*-Bu), 1.87-1.92 (m, 2H, Glu), 2.17-2.38 (m, 5H, Glu, Val, Asp), 2.69-3.11 (dd, 2H, AAsp), 3.13-3.96 (m, 2H, epoxy CH), 4.05-4.32 (m, 3H, α -H and OCH_2CH_3), 4.39-4.53 (m, 2H, α -H), 5.11 (dd, 2H, Cbz), 6.85 (d, 1H, NH), 7.35 -7.38 (m, 5H, Cbz-Ph), 7.55 (d, 1H, NH), 7.77 (t, 1H, NH), 9.58 (s, 1H, NH-N).

Cbz-Glu(O-*t*-Bu)-Val-AAsp(O-*t*-Bu)-(cis)EP-CO₂CH₂CH₃ was obtained by the EDC/HOBt coupling method and purified by column chromatography on silica gel with 1:19:5 MeOH:CH₂Cl₂:EtOAc as the eluent; yield 22%. ¹H NMR (Acetone-d₆): 0.98 (d, 6H, Val), 1.18-1.26 (m, 3H, OCH_2CH_3), 1.40-1.45 (m, 18 *t*-Bu), 1.87-1.97 (m, 2H, Glu), 2.11-2.17 (m, 3H, Glu, Val), 2.35 (t, 2H, AAsp), 3.70-3.76 (dd, 1H, epoxy CH), 3.90-3.94 (d, 1H, epoxy CH), 4.08-4.38 (m, 4H, α -H and OCH_2CH_3), 5.09 (s, 2H, Cbz), 6.63 (d, 1H, NH), 7.30 -7.39 (m, 5H, Cbz-Ph), 7.49-7.55 (m, 1H, NH), 9.70-9.76 (m, 1H, NH-N).

Cbz-Asp(O-*t*-Bu)-Glu(O-*t*-Bu)-Val-AAsp(O-*t*-Bu)-(2*S*,3*S*)EP-CON(CH₂Ph)₂ was obtained by the EDC/HOBt coupling method and purified two times by column chromatography on silica gel with 2:1 EtOAc:hexane as the eluent; yield 13%. ¹H NMR (Acetone-d₆): 0.86-0.98 (m, 6H, Val), 1.40-1.44 (m, 27H, *t*-Bu), 1.89-1.97 (m, 2H, Glu), 2.25-2.36 (m, 5H, Glu, Val, Asp), 2.69-2.88 (dd, 2H, AAsp), 3.87 (d, 1H, epoxy CH),

4.02-4.83 (m, 8H, epoxy CH, N(CH₂Ph)₂, α-Hs), 5.04-5.16 (m, 2H, Cbz), 6.85 (d, 1H, NH), 7.29-7.41 (m, 15H, Cbz-Ph, N(CH₂Ph)₂), 7.60 (d, 1H, NH), 7.82 (d, 1H, NH), 9.80 (s, 1H, NH-N).

Cbz-Asp(O-*t*-Bu)-Glu(O-*t*-Bu)-Val-AAsp(O-*t*-Bu)-(2*R*,3*R*)EP-CON(CH₂Ph)₂ was obtained by the EDC/HOBt coupling method and purified by column chromatography on silica gel with 2:1 EtOAc:hexane as the eluent; yield 20%. ¹H NMR (Acetone-d₆): 0.88-1.07 (m, 6H, Val), 1.29-1.47 (m, 27H, *t*-Bu), 1.84-2.00 (m, 2H, Glu), 2.15-2.32 (m, 5H, Glu, Val, Asp), 2.69-2.90 (dd, 2H, AAsp), 3.60-3.69 (dd, 1H, epoxy CH), 4.03-4.07 (dd, 1H, epoxy CH), 4.18-4.23 (m, 2H, α-Hs), 4.34-4.79 (m, 5H, α-H, N(CH₂Ph)₂), 4.92-5.26 (m, 2H, Cbz), 6.81-6.85 (m, 1H, NH), 7.21-7.43 (m, 15H, Cbz-Ph, N(CH₂Ph)₂), 7.51-7.95 (m, 2H, NH), 9.59-9.81 (m, 1H, NH-N).

Cbz-Asp(O-*t*-Bu)-Glu(O-*t*-Bu)-Val-AAsp(O-*t*-Bu)-(cis)EP-CON(CH₂Ph)₂ was obtained by the EDC/HOBt coupling method and purified two times by column chromatography on silica gel with 2:1 EtOAc:hexane as the eluent; yield 11%. ¹H NMR (Acetone-d₆): 0.93 (d, 6H, Val), 1.40-1.47 (m, 27H, *t*-Bu), 1.82-1.92 (m, 2H, Glu), 2.15-2.21 (m, 3H, Glu, Val), 2.28-2.34 (m, 2H, Asp), 2.67-2.73 (dd, 2H, AAsp), 3.77 (s, 1H, epoxy CH), 3.98-4.70 (m, 8H, epoxy CH, α-Hs, N(CH₂Ph)₂), 5.05-5.15 (m, 2H, Cbz), 6.81 (d, 1H, NH), 7.24-7.44 (m, 15H, Cbz-Ph, N(CH₂Ph)₂), 7.51 (d, 1H, NH), 7.68 (d, 1H, NH), 9.77 (s, 1H, NH-N).

Cbz-Glu(O-*t*-Bu)-Val-AAsp(O-*t*-Bu)-(2*S*,3*S*)EP-CON(CH₂Ph)₂ was obtained by the EDC/HOBt coupling method and purified by column chromatography on silica gel with 2:1 EtOAc:hexane as the eluent; yield 38%. ¹H NMR (Acetone-d₆): 0.90-1.01 (m, 6H, Val), 1.35-1.41 (m, 18H, *t*-Bu), 1.87-1.97 (m, 2H, Glu), 2.10-2.14 (m, 1H, Val), 2.21-

2.26 (m, 2H, Glu), 2.32-2.35 (dd, 2H, AAsp), 3.89 (s, 1H, epoxy CH), 4.34-4.28 (m, 2H, epoxy CH, α -H), 4.38-4.39 (m, 1H, α -H), 4.50-4.83 (m, 4H, N(CH₂Ph)₂), 5.04-5.13 (m, 2H, Cbz), 6.66 (d, 1H, NH), 7.28-7.41 (m, 15H, Cbz-Ph, N(CH₂Ph)₂), 7.62 (d, 1H, NH), 9.87 (s, 1H, NH-N).

Cbz-Glu(O-*t*-Bu)-Val-AAsp(O-*t*-Bu)-(2*R*,3*R*)EP-CON(CH₂Ph)₂ was obtained by the EDC/HOBt coupling method and purified by column chromatography on silica gel with 2:1 EtOAc:hexane as the eluent; yield 19%. ¹H NMR (Acetone-d₆): 0.86-0.95 (m, 6H, Val), 1.40-1.47 (m, 18H, *t*-Bu), 1.87-1.92 (m, 2H, Glu), 2.09-2.16 (m, 3H, Val, Glu), 2.31-2.35 (dd, 2H, AAsp), 4.03 (s, 1H, epoxy CH), 4.09 (s, 1H, epoxy CH), 4.22-4.27 (m, 1H, α -H), 4.34-4.91 (m, 5H, N(CH₂Ph)₂, α -H), 5.05-5.10 (m, 2H, Cbz), 5.14 (s, 1H, NH), 6.54 (d, 1H, NH), 7.29-7.40 (15H, Cbz-Ph, N(CH₂Ph)₂), 10.81 (s, 1H, NH-N).

Cbz-Glu(O-*t*-Bu)-Val-AAsp(O-*t*-Bu)-(cis)EP-CON(CH₂Ph)₂ was obtained by the EDC/HOBt coupling method and purified by column chromatography on silica gel with 1:19:5 MeOH:CH₂Cl₂:EtOAc as the eluent; yield 18%. ¹H NMR (Acetone-d₆): 0.91 (m, 6H, Val), 1.38-1.47 (m, 18H, *t*-Bu), 1.82-1.97 (m, 2H, Glu), 2.11-2.21 (m, 3H, Val, Glu), 2.28-2.37 (dd, 2H, AAsp), 3.71 (s, 1H, epoxy CH), 3.88-4.12 (dd, 1H, epoxy CH), 4.25-4.77 (m, 6H, α -Hs, N(CH₂Ph)₂), 5.10 (s, 2H, Cbz), 6.58 (d, 1H, NH), 7.24-7.40 (15H, Cbz-Ph, N(CH₂Ph)₂), 9.85 (s, 1H, NH-N).

Cbz-Ala-Glu(O-*t*-Bu)-Val-AAsp(O-*t*-Bu)-(2*S*,3*S*)EP-CO₂CH₂CH₃ was obtained by the EDC/HOBt coupling method and purified by column chromatography on silica gel with 2:18:5 MeOH:CH₂Cl₂:EtOAc as the eluent and then re-chromatographed with 2:1 EtOAc:hexanes as the eluent. Re-chromatographed a third time with 1:19:5 MeOH:CH₂Cl₂:EtOAc as the eluent. Product was precipitated with Et₂O and excess hexanes;

white solid, yield 38%. ^1H NMR (Acetone- d_6): 0.96-1.03 (m, 6H, Val), 1.23-1.27 (m, 3H, OCH_2CH_3), 1.38-1.46 (m, 21H, *t*-Bu, Ala), 1.89-2.00 (m, 2H, Glu), 2.11-2.29 (m, 3H, Val, Glu), 2.34-2.40 (dd, 2H, AAsp), 3.50 (s, 1H, epoxy CH), 4.13-4.30 (m, 3H, epoxy CH, OCH_2CH_3), 4.41 (m, 1H, α -H), 4.48-4.60 (m, 1H, α -H), 4.79 (d, 1H, α -H), 5.05-5.17 (m, 2H, Cbz), 6.83 (s, 1H, NH), 7.32-7.48 (5H, Cbz-Ph), 7.63 (s, 1H, NH), 7.80-7.87 (m, 1H, NH), 9.73 (s, 1H, NH-N).

Cbz-Ala-Glu(O-*t*-Bu)-Val-AAsp(O-*t*-Bu)-(2*R*,3*R*)EP-CO₂CH₂CH₃ was obtained by the EDC/HOBt coupling method and purified by column chromatography on silica gel with 2:18:5 MeOH:CH₂Cl₂:EtOAc as the eluent. Product was precipitated with Et₂O and excess hexanes; yield 55%. ^1H NMR (Acetone- d_6): 0.96-1.02 (m, 6H, Val), 1.21-1.28 (m, 3H, OCH_2CH_3), 1.38-1.49 (m, 21H, *t*-Bu, Ala), 1.87-1.97 (m, 2H, Glu), 2.09-2.25 (m, 3H, Val, Glu), 2.34-2.39 (dd, 2H, AAsp), 3.46 (s, 1H, epoxy CH), 4.13 (s, 1H, epoxy CH), 4.16-4.54 (m, 5H, OCH_2CH_3 , α -Hs), 5.05-5.17 (m, 2H, Cbz), 6.83 (s, 1H, NH), 7.31-7.38 (m, 5H, Cbz-Ph), 7.49 (d, 1H, NH), 7.80 (s, 1H, NH).

Cbz-Ala-Glu(O-*t*-Bu)-Val-AAsp(O-*t*-Bu)-(cis)EP-CO₂CH₂CH₃ was obtained by the EDC/HOBt coupling method and purified by column chromatography on silica gel with 2:18:5 MeOH:CH₂Cl₂:EtOAc as the eluent and then re-chromatographed with 1:19:5 MeOH:CH₂Cl₂:EtOAc as the eluent. Product was precipitated with Et₂O and excess hexanes; yield 15%. ^1H NMR (Acetone- d_6): 0.98-1.01 (m, 6H, Val), 1.23-1.28 (m, 3H, OCH_2CH_3), 1.40-1.49 (m, 21H, *t*-Bu, Ala), 1.89-1.97 (m, 2H, Glu), 2.21-2.28 (m, 2H, Glu), 2.34-2.40 (m, 2H, AAsp), 3.45-3.70 (dd, 1H, epoxy CH), 4.13-4.33 (m, 5H, epoxy CH, OCH_2CH_3 , α -Hs), 4.73-4.79 (m, 1H, α -H), 4.93-5.17 (m, 2H, Cbz), 6.81-6.95 (s, 1H,

NH), 7.33-7.38 (m, 5H, Cbz-Ph), 7.52-7.58 (m, 1H, NH), 7.82-7.98 (m, 1H, NH), 9.59-9.75 (m, 1H, NH-N).

Cbz-Asp(O-*t*-Bu)-Glu(O-*t*-Bu)-Val-AAsp(O-*t*-Bu)-(2*S*,3*S*)EP-CON(CH₂Ph-4-OH)(CH₂Ph) was obtained by the EDC/HOBt coupling method and purified by column chromatography on silica gel with 3:1 EtOAc:hexane as the eluent and then re-chromatographed with 2:1 EtOAc:hexane as the eluent. Product was precipitated with Et₂O and excess hexane. Re-chromatographed with 2:1 EtOAc:hexane as the eluent; yield 21%. ¹H NMR (Acetone-d₆): 0.88-1.03 (m, 6H, Val), 1.29-1.53 (m, 27H, *t*-Bu), 1.90-1.99 (m, 2H, Glu), 2.18-2.38 (m, 5H, Glu, Val), 2.70-2.94 (m, 2H, AAsp), 3.82 (d, 1H, epoxy CH), 4.10-4.96 (m, 8H, epoxy CH, N(CH₂Ph)(CH₂Ph-4-OH), α-Hs), 5.08-5.16 (m, 2H, Cbz), 6.77-7.86 (m, 16H, NHs, Cbz-Ph, N(CH₂Ph)(CH₂Ph-4-OH)), 9.27 (s, 1H, NH), 10.80 (s, 1H, NH-N).

Cbz-Asp(O-*t*-Bu)-Glu(O-*t*-Bu)-Val-AAsp(O-*t*-Bu)-(2*S*,3*S*)EP-CON(2-CH₂-furyl)₂ was obtained by the EDC/HOBt coupling method and purified by column chromatography on silica gel with 2:18:5 MeOH:CH₂Cl₂:EtOAc; yield 44%. MS (ESI): 1009.4 *m/z*.

Cbz-Asp(O-*t*-Bu)-Glu(O-*t*-Bu)-Val-AAsp(O-*t*-Bu)-(2*S*,3*S*)EP-CON(1-CH₂-Naph)(CH₂Ph) was obtained by the EDC/HOBt coupling method and purified two times by column chromatography on silica gel with 1:19:5 MeOH:CH₂Cl₂:EtOAc as the eluent and then re-chromatographed with 2:98:25 MeOH:CH₂Cl₂:EtOAc as the eluent; precipitated with Et₂O and excess hexane; yield 12%. ¹H NMR (Acetone-d₆): 0.84-0.99 (m, 6H, Val), 1.34-1.52 (m, 27H, *t*-Bu), 2.08 (m, 2H, Glu), 2.36-3.49 (m, 7H, Glu, Val, Asp, AAsp), 3.76 (s, 1H, epoxy CH), 3.88 (s, 1H, epoxy CH), 4.29-5.13 (m, 9H,

N(CH₂Ph)(1-CH₂-Naph), α -Hs, Cbz), 5.90 (s, 1H, NH), 7.00-7.81 (m, 19H, NHs, Cbz-Ph, N(CH₂Ph)(1-CH₂-Naph)), 9.43 (s, 1H, NH-N).

Cbz-Asp(O-*t*-Bu)-Glu(O-*t*-Bu)-Val-AAsp(O-*t*-Bu)-(2*S*,3*S*)EP-CON(1-CH₂-Naph)₂

was obtained by the EDC/HOBt coupling method and purified two times by column chromatography on silica gel with 2:1 EtOAc:hexane as the eluent and then precipitated with Et₂O and excess hexane; yield 25%. ¹H NMR (CDCl₃): 0.90-1.07 (m, 6H, Val), 1.33-1.54 (m, 27H, *t*-Bu), 1.84-1.97 (m, 2H, Glu), 2.22-2.34 (m, Asp, Glu), 2.64-2.75 (m, 2H, AAsp), 3.69 (s, 1H, epoxy CH), 4.12-4.54 (s, 1H, epoxy CH, α -Hs), 4.91-5.38 (m, 6H, N(1-CH₂-Naph)₂, Cbz), 6.76 (s, 1H, NH), 7.28-7.53 (m, 13H, Cbz-Ph, N(1-CH₂-Naph)₂), 7.67 (d, 1H, NH), 7.75-7.96 (m, 6H, 9.43, N(1-CH₂-Naph)₂), 8.08 (d, 1H, NH), 9.63 (s, 1H, NH-N).

Cbz-Asp(O-*t*-Bu)-Glu(O-*t*-Bu)-Val-AAsp(O-*t*-Bu)-CH=CH-CON(1-CH₂-Naph)₂

was obtained by the EDC/HOBt coupling method, and purified by column chromatography on silica gel with 2:1 EtOAc:hexane as the eluent; yield 17%. ¹H NMR (Acetone-d₆): 1.04 (d, 6H, Val), 1.35-1.43 (m, 27H, *t*-Bu), 1.97 (m, 2H, Glu), 2.17-2.38 (m, Glu, Val, Asp), 2.71 (dd, 1H, Asp), 4.30 (t, 1H, α -H), 4.51 (m, 2H, α -H), 5.10 (dd, 2H, N(1-CH₂-Naph)₂), 5.24 (s, 2H, N(1-CH₂-Naph)₂), 5.33 (s, 2H, Cbz), 6.85 (d, 1H, db), 7.29-7.95 (m, 16H, db, Cbz-Ph, and N(1-CH₂-Naph)₂), 8.18 (d, 1H, NH), 9.81 (s, 1H, NH-N).

Aza-peptide Epoxides. Deblocking of the *tert*-Butyl Protecting Groups. Aza-peptide epoxides were reacted with TFA at 0 °C for 1-3 h. The TFA was removed, and the final products were recrystallized from ether/hexane to give the final compounds, aza-peptide epoxide inhibitors.

(*cis*)-*N*²-(*N*-Benzyloxycarbonylaspartylglutamylvalyl)-*N*¹-carboxymethylhydrazino-carbonyl)oxirane-2-carboxylic Acid Ethyl Ester (Cbz-Asp-Glu-Val-AAsp-(*cis*)EP-CO₂CH₂CH₃, III-13a). Yield: 62%. ¹H NMR (Acetone-d₆): 0.99 (d, 6H, Val), 1.22 (t, 3H, OCH₂CH₃), 1.97-2.00 (m, 3H, Glu, Val), 2.21-2.25 (m, 2H, Glu), 2.45 (s, 2H, Asp), 2.88 (dd, 1H, AAsp), 2.94 (dd, 1H, AAsp), 3.73 (dd, 1H, epoxy CH), 3.94 (dd, 1H, epoxy CH), 4.04-4.55 (m, 5H, α-Hs, OCH₂CH₃), 4.57 (m, 2H, α-H), 5.06 (dd, 2H, Cbz), 6.92 (s, 1H, NH), 7.34 (m, 5H, Cbz-Ph), 7.58 (s, 1H, NH), 7.92 (s, 1H, NH), 9.68-9.80 (m, 1H, NH-N). HRMS (ESI) Calcd. for C₃₀H₄₀N₅O₁₅: 710.2530; Observed *m/z*: 710.2506. Anal. Calcd. for C₃₀H₃₉N₅O₁₅·0.4TFA·0.1H₂O·0.005C₄H₉: C, 48.86; H, 5.51; N, 9.25. Found: C, 48.77; H, 5.62; N, 9.59.

(2*R*,3*R*)-*N*²-(*N*-Benzyloxycarbonylglutamylvalyl)-*N*¹-carboxymethylhydrazino-carbonyl)oxirane-2-carboxylic Acid Ethyl Ester (Cbz-Glu-Val-AAsp-(2*R*,3*R*)EP-CO₂CH₂CH₃, III-13b). Yield: 31%. ¹H NMR (Acetone-d₆): 0.96 (d, 6H, Val), 1.23 (t, 3H, OCH₂CH₃), 1.89-2.00 (m, 2H, Glu), 2.07-2.22 (m, 3H, Val, Glu), 2.45 (t, 2H, AAsp), 3.47 (s, 1H, epoxy CH), 4.11 (s, 1H, epoxy CH), 4.15-4.31 (m, 4H, α-Hs, OCH₂CH₃), 5.09 (s, 2H, Cbz), 6.63 (s, 1H, NH), 7.29-7.39 (m, 5H, Cbz-Ph), 7.62 (d, 1H, NH), 10.05 (m, 1H, NH-N). HRMS (ESI) Calcd. for C₂₆H₃₅N₄O₁₂: 595.2246; Observed *m/z*: 595.2244. Anal. Calcd. for C₂₆H₃₄N₄O₁₂·0.1TFA·0.05H₂O·0.01C₄H₉: C, 51.87; H, 5.84; N, 9.22. Found: C, 51.77; H, 5.79; N, 9.12.

(*cis*)-*N*²-(*N*-Benzyloxycarbonylglutamylvalyl)-*N*¹-carboxymethylhydrazino-carbonyl)oxirane-2-carboxylic Acid Ethyl Ester (Cbz-Glu-Val-AAsp-(*cis*)EP-CO₂CH₂CH₃, III-13b). Yield: 70%. ¹H NMR (Acetone-d₆): 0.98 (d, 6H, Val), 1.18-1.23 (m, 3H, OCH₂CH₃), 1.96-2.00 (m, 2H, Glu), 2.11-2.21 (m, 3H, Val, Glu), 2.44-2.48 (m,

2H, AAsp), 3.73-3.77 (dd, 1H, epoxy CH), 3.94-3.96 (dd, 1H, epoxy CH), 4.13-4.35 (m, 4H, α -Hs, OCH_2CH_3), 5.09 (s, 2H, Cbz), 6.71 (s, 1H, NH), 7.31-7.37 (m, 5H, Cbz-Ph), 7.63 (d, 1H, NH), 9.93 (m, 1H, NH-N). HRMS (ESI) Calcd. for $\text{C}_{26}\text{H}_{35}\text{N}_4\text{O}_{12}$: 595.2246; Observed m/z : 595.2278. Anal. Calcd. for $\text{C}_{26}\text{H}_{34}\text{N}_4\text{O}_{12} \cdot 0.3\text{TFA} \cdot 0.1\text{H}_2\text{O}$: C, 50.64; H, 5.80; N, 8.88. Found: C, 50.34; H, 5.83; N, 9.18.

(2*S*,3*S*)-2-(di-Benzylcarbamoyl)-3-(*N*²-(*N*-benzyloxycarbonylaspartylglutamyl-valyl)-*N*¹-carboxymethylhydrazinocarbonyl)oxirane (Cbz-Asp-Glu-Val-AAsp-(2*S*,3*S*)EP-CON(CH_2Ph)₂, III-14a). Yield: 65%. ¹H NMR (Acetone- d_6): 0.90-0.96 (m, 6H, Val), 1.96-2.01 (m, 2H, Glu), 2.27-2.46 (m, 3H, Glu, Val), 2.85-3.04 (dd, 2H, AAsp), 4.00 (s, 1H, epoxy CH), 4.36-4.77 (m, 8H, α -Hs, $\text{N}(\text{CH}_2\text{Ph})_2$, epoxy CH), 5.09 (s, 2H, Cbz), 6.86 (d, 1H, NH), 7.28-7.43 (m, 15H, Cbz-Ph, $\text{N}(\text{CH}_2\text{Ph})_2$), 7.69 (d, 1H, NH), 7.97 (d, 1H, NH), 9.93 (s, 1H, NH-N). HRMS (ESI) Calcd. for $\text{C}_{42}\text{H}_{49}\text{N}_6\text{O}_{14}$: 861.3301; Observed m/z : 861.3342. Anal. Calcd. for $\text{C}_{42}\text{H}_{48}\text{N}_6\text{O}_{14} \cdot 0.4\text{TFA} \cdot 0.1\text{C}_4\text{H}_9$: C, 56.72; H, 5.39; N, 9.27. Found: C, 56.64; H, 5.59; N, 9.38.

(2*R*,3*R*)-2-(di-Benzylcarbamoyl)-3-(*N*²-(*N*-benzyloxycarbonylaspartylglutamyl-valyl)-*N*¹-carboxymethylhydrazinocarbonyl)oxirane (Cbz-Asp-Glu-Val-AAsp-(2*R*,3*R*)EP-CON(CH_2Ph)₂, III-14a). Yield: 53%. ¹H NMR (Acetone- d_6): 0.88-1.02 (m, 6H, Val), 1.89-1.97 (m, 2H, Glu), 2.09-2.29 (m, 3H, Glu, Val), 2.38-2.44 (m, 2H, Asp), 2.83-2.94 (m, 2H, AAsp), 3.68 (d, 1H, epoxy CH), 4.17-4.92 (m, 8H, α -Hs, $\text{N}(\text{CH}_2\text{Ph})_2$, epoxy CH), 5.04-5.13 (dd, 2H, Cbz), 6.85-6.90 (m, 1H, NH), 7.30-7.69 (m, 15H, Cbz-Ph, $\text{N}(\text{CH}_2\text{Ph})_2$), 7.80-7.96 (m, 2H, NH), 9.95 (s, 1H, NH-N). HRMS (ESI) Calcd. for $\text{C}_{42}\text{H}_{49}\text{N}_6\text{O}_{14}$: 861.3301; Observed m/z : 861.3401. Anal. Calcd. for

C₄₂H₄₈N₆O₁₄·0.65TFA·0.2H₂O·0.1C₄H₉: C, 55.40; H, 5.66; N, 8.95. Found: C, 55.38; H, 5.66; N, 8.97.

(*cis*)-2-(di-Benzylcarbamoyl)-3-(*N*²-(*N*-benzyloxycarbonylaspartylglutamylvalyl)-*N*¹-carboxymethylhydrazinocarbonyl)oxirane (Cbz-Asp-Glu-Val-AAsp-(*cis*)EP-

CON(CH₂Ph)₂, III-14a). Yield: 67%. ¹H NMR (Acetone-d₆): 0.91 (d, 6H, Val), 1.89-2.00 (m, 2H, Glu), 2.10-2.21 (m, 3H, Glu, Val), 2.41 (m, 2H, Asp), 2.78-2.94 (m, 2H, AAsp), 4.10-4.14 (dd, 1H, epoxy CH), 4.33-4.71 (m, 8H, α-Hs, N(CH₂Ph)₂, epoxy CH), 5.06-5.10 (m, 2H, Cbz), 6.86 (s, 1H, NH), 7.24-7.37 (m, 15H, Cbz-Ph, N(CH₂Ph)₂), 7.48 (d, 1H, NH), 7.82 (s, 1H, NH), 9.93 (s, 1H, NH-N). HRMS (ESI) Calcd. for C₄₂H₄₉N₆O₁₄: 861.3301; Observed *m/z*: 861.3302. Anal. Calcd. for

C₄₂H₄₈N₆O₁₄·0.4TFA·0.1H₂O·0.01C₄H₉: C, 56.60; H, 5.60; N, 9.25. Found: C, 56.21; H, 5.61; N, 9.64.

(2*S*,3*S*)-2-(di-Benzylcarbamoyl)-3-(*N*²-(*N*-benzyloxycarbonylglutamylvalyl)-*N*¹-carboxymethylhydrazinocarbonyl)oxirane (Cbz-Glu-Val-AAsp-(2*S*,3*S*)EP-

CON(CH₂Ph)₂, III-14b). Yield: 91%. ¹H NMR (Acetone-d₆): 0.94-1.03 (m, 6H, Val), 1.94-2.02 (m, 2H, Glu), 2.12-2.27 (m, 3H, Glu, Val), 2.42-2.46 (m, 2H, AAsp), 3.93 (s, 1H, epoxy CH), 4.26-4.30 (m, 2H, α-H, epoxy CH), 4.43-4.83 (α-H, N(CH₂Ph)₂), 5.04-5.12 (m, 2H, Cbz), 6.74 (d, 1H, NH), 7.28-7.41 (m, Cbz-Ph, N(CH₂Ph)₂), 7.74 (d, 1H, NH), 10.05 (s, 1H, NH-N). HRMS (ESI) Calcd. for C₃₈H₄₄N₅O₁₁: 746.3032; Observed *m/z*: 746.3051. Anal. Calcd. for C₃₈H₄₃N₅O₁₁·0.25TFA·0.1H₂O·0.01C₄H₉: C, 59.58; H, 5.88; N, 9.02. Found: C, 59.48; H, 5.79; N, 9.01.

(2*R*,3*R*)-2-(di-Benzylcarbamoyl)-3-(*N*²-(*N*-benzyloxycarbonylglutamylvalyl)-*N*¹-carboxymethylhydrazinocarbonyl)oxirane (Cbz-Glu-Val-AAsp-(2*R*,3*R*)EP-

CON(CH₂Ph)₂, III-14b). Yield: 84%. ¹H NMR (Acetone-d₆): 0.84-0.95 (m, 6H, Val), 1.92-1.99 (m, 2H, Glu), 2.09-2.21 (m, 3H, Glu, Val), 2.42-2.46 (m, 2H, AAsp), 4.19-4.71 (m, 8H, α-Hs, N(CH₂Ph)₂), epoxy CHs), 5.03-5.15 (m, 3H, Cbz, NH), 6.61 (d, 1H, NH), 7.26-7.41 (m, Cbz-Ph, N(CH₂Ph)₂), 7.46 (d, 1H, NH-N). HRMS (ESI) Calcd. for C₃₈H₄₄N₅O₁₁: 746.3104; Observed *m/z*: 746.3067. Anal. Calcd. for C₃₈H₄₃N₅O₁₁·0.2TFA·0.1H₂O·0.1C₄H₉: C, 60.03; H, 5.99; N, 9.02. Found: C, 60.06; H, 5.95; N, 8.63.

(*cis*)-2-(di-Benzylcarbamoyl)-3-(*N*²-(*N*-benzyloxycarbonylglutamylvalyl)-*N*¹-carboxymethylhydrazinocarbonyl)oxirane (Cbz-Glu-Val-AAsp-(*cis*)-EP-

CON(CH₂Ph)₂, III-14b). Yield: 61%. ¹H NMR (Acetone-d₆): 0.88-0.93 (m, 6H, Val), 1.89-1.99 (m, 2H, Glu), 2.11 (m, 3H, Glu, Val), 2.40-2.46 (m, 2H, AAsp), 3.83 (s, 1H, epoxy CH), 4.08-4.66 (m, 8H, α-Hs, N(CH₂Ph)₂, epoxy CH), 5.09 (m, 2H, Cbz), 6.66 (d, 1H, NH), 7.24-7.46 (m, Cbz-Ph, N(CH₂Ph)₂, NH), 10.02 (s, 1H, NH-N). HRMS (ESI) Calcd. for C₃₈H₄₄N₅O₁₁: 746.3032; Observed *m/z*: 746.3079. Anal. Calcd. for C₃₈H₄₃N₅O₁₁·0.2TFA·0.05H₂O·0.01C₄H₉: C, 59.94; H, 5.80; N, 9.10. Found: C, 59.84; H, 5.80; N, 9.37.

(2*S*,3*S*)-*N*²-(*N*-Benzyloxycarbonylalanylglutamylvalyl)-*N*¹-carboxymethylhydrazinocarbonyl)oxirane-2-carboxylic Acid Ethyl Ester (Cbz-Ala-Glu-Val-AAsp-(2*S*,3*S*)EP-CO₂CH₂CH₃, III-13c). Yield: 83%. ¹H NMR (Acetone-d₆): 0.98-1.03 (d, 6H, Val), 1.24-1.27 (m, 3H, OCH₂CH₃), 1.38 (d, 3H, Ala), 1.89-2.01 (m, 2H, Glu), 2.13-2.27 (m, 3H, Glu, Val), 2.43-2.46 (m, 2H, AAsp), 3.51 (s, 1H, epoxy CH), 4.13-4.58 (m, 6H, epoxy CH, α-Hs, OCH₂CH₃), 5.05-5.15 (m, 2H, Cbz), 6.83 (s, 1H, NH), 7.31-7.38 (m, 5H, Cbz-Ph), 7.56 (d, 1H, NH), 7.67-7.9 (m, 1H, NH), 9.92 (m, 1H, NH-N). HRMS

(ESI) Calcd. for $C_{29}H_{40}N_5O_{13}$: 666.2617; Observed m/z : 666.2588. Anal. Calcd. for $C_{29}H_{39}N_5O_{13} \cdot 0.25TFA \cdot 0.05H_2O \cdot 0.5CH_2Cl_2$: C, 48.85; H, 5.64; N, 9.50. Found: C, 48.49; H, 5.88; N, 9.59.

(2*R*,3*R*)-*N*²-(*N*-Benzyloxycarbonylalanylglutamylvalyl)-*N*¹-carboxymethylhydrazinocarbonyl)oxirane-2-carboxylic Acid Ethyl Ester (Cbz-Ala-Glu-Val-AAsp-(2*R*,3*R*)EP-CO₂CH₂CH₃, III-13c). Yield: 95%. ¹H NMR (Acetone-*d*₆): 0.95-1.03 (m, 6H, Val), 1.23-1.28 (m, 3H, OCH₂CH₃), 1.37-1.44 (m, 3H, Ala), 1.89-2.01 (m, 2H, Glu), 2.12-2.27 (m, 3H, Glu, Val), 2.43-2.47 (m, 2H, AAsp), 3.47 (s, 1H, epoxy CH), 3.84-4.53 (m, 6H, epoxy CH, α-Hs, OCH₂CH₃), 5.04-5.16 (m, 2H, Cbz), 6.81 (s, 1H, NH), 7.31-7.38 (m, 5H, Cbz-Ph), 7.56-7.65 (m, 1H, NH), 7.80-7.84 (m, 1H, NH), 9.91 (s, 1H, NH-N). HRMS (ESI) Calcd. for $C_{29}H_{40}N_5O_{13}$: 666.2617; Observed m/z : 666.2617. Anal. Calcd. for $C_{29}H_{39}N_5O_{13} \cdot 0.85TFA \cdot 0.15H_2O$: C, 48.16; H, 5.64; N, 9.15. Found: C, 48.14; H, 5.61; N, 9.35.

(*cis*)-*N*²-(*N*-Benzyloxycarbonylalanylglutamylvalyl)-*N*¹-carboxymethylhydrazinocarbonyl)oxirane-2-carboxylic Acid Ethyl Ester (Cbz-Ala-Glu-Val-AAsp-(*cis*)EP-CO₂CH₂CH₃, III-13c). Yield: 42%. ¹H NMR (Acetone-*d*₆): 0.98-1.01 (m, 6H, Val), 1.23-1.28 (m, 3H, OCH₂CH₃), 1.37-1.42 (m, 3H, Ala), 1.89-2.02 (m, 2H, Glu), 2.09-2.30 (m, 3H, Glu, Val), 2.45-2.47 (m, 2H, AAsp), 3.47-3.80 (m, 1H, epoxy CH), 4.16-4.35 (m, 5H, epoxy CH, α-Hs, OCH₂CH₃), 4.69-4.82 (m, 1H, α-Hs), 4.93-5.17 (m, 2H, Cbz), 6.85-6.99 (m, 1H, NH), 7.33-7.38 (m, 5H, Cbz-Ph), 7.58-7.64 (m, 1H, NH), 7.89-8.04 (m, 1H, NH), 9.68-9.86 (m, 1H, NH-N). HRMS (ESI) Calcd. for $C_{29}H_{40}N_5O_{13}$: 666.2617; Observed m/z : 666.2693. Anal. Calcd. for $C_{29}H_{39}N_5O_{13} \cdot 1.1TFA \cdot 0.2H_2O$: C, 47.17; H, 5.59; N, 8.81. Found: C, 46.98; H, 5.63; N, 8.63.

(2S,3S)-2-(Benzyl-(4-hydroxybenzyl)carbamoyl)-3-(N²-(N-benzyloxycarbonyl-aspartylglutamylvalyl)-N¹-carboxymethylhydrazinocarbonyl)oxirane (Cbz-Asp-Glu-Val-AAsp-(2S,3S)EP-CON(CH₂Ph-4-OH)(CH₂Ph), III-17a). Yield, 16%. ¹H NMR (Acetone-d₆): 0.90-1.05 (m, 6H, Val), 1.97-1.99 (m, 2H, Glu), 2.21-2.59 (m, 5H, Glu, Val, Asp), 2.79-3.01 (m, 2H, AAsp), 3.89 (d, 1H, epoxy CH), 4.23-4.99 (m, 8H, α-Hs, N(CH₂Ph)(CH₂Ph-4-OH), epoxy CH), 5.08-5.27 (m, 2H, Cbz), 6.79-7.99 (m, 17H, NHs, Cbz-Ph, N(CH₂Ph)(CH₂Ph-4-OH)), 9.85 (s, 1H, NH-N). HRMS (ESI) Calcd. for C₄₂H₄₉N₆O₁₅: 877.3256; Observed *m/z*: 861.3401. Anal. Calcd. for C₄₂H₄₈N₆O₁₅·0.99CH₂Cl₂·0.23TFA·0.325H₂O: C, 52.51; H, 5.75; N, 8.46. Found: C, 55.22; H, 5.45; N, 8.84.

(2S,3S)-2-(bis-(2-furylmethyl)carbamoyl)-3-(N²-(N-benzyloxycarbonylaspartylglutamylvalyl)-N¹-carboxymethylhydrazinocarbonyl)oxirane (Cbz-Asp-Glu-Val-AAsp-(2S,3S)EP-CON(2-CH₂-furyl)₂, III-18a). Yield, 75%. ¹H NMR (Acetone-d₆): 0.88-1.02 (m, 6H, Val), 1.89-2.01 (m, 2H, Glu), 2.11-2.45 (m, 5H, Glu, Val, Asp), 2.84-3.01 (m, 2H, AAsp), 3.60-3.69 (dd, 1H, epoxy CH), 4.15-4.75 (m, 8H, α-Hs, N(2-CH₂-furyl)₂, epoxy CH), 5.10 (s, 2H, Cbz), 6.32-6.39 (m, 2H, N(2-CH₂-furyl)₂), 6.86 (d, 1H, NH), 7.30-7.63 (m, 8H, NH, Cbz-Ph, N(2-CH₂-furyl)₂), 7.94 (d, 1H, NH), 9.91 (s, 1H, NH-N). HRMS (ESI) Calcd. for C₃₈H₄₅N₆O₁₆: 841.2887; Observed *m/z*: 841.2915. Anal. Calcd. for C₃₈H₄₄N₆O₁₆·0.45TFA·0.20H₂O: C, 52.13; H, 5.45; N, 9.38. Found: C, 55.06; H, 5.66; N, 9.33.

(2S,3S)-2-(benzyl-1-naphthylmethylcarbamoyl)-3-(N²-(N-benzyloxycarbonyl-aspartylglutamylvalyl)-N¹-carboxymethylhydrazinocarbonyl)oxirane (Cbz-Asp-Glu-Val-AAsp-(2S,3S)EP-CON(1-CH₂-Naph)(CH₂Ph), III-15a). Yield, 78%. ¹H

NMR (Acetone- d_6): 0.90-0.98 (m, 6H, Val), 1.89-1.96 (m, 2H, Glu), 2.09-2.40 (m, 5H, Glu, Val, Asp), 2.78-2.94 (m, 2H, AAsp), 3.82 (s, 1H, epoxy CH), 4.25-4.79 (m, 5H, α -Hs, N(CH_2 -benzyl), epoxy CH), 4.99-5.29 (m, 4H, Cbz, N(1- CH_2 -Naph)), 6.84 (s, 1H, NH), 7.29-7.52 (m, 14H, NH, Cbz-Ph, N(1- CH_2 -Naph), N(CH_2 Benzyl)), 7.79-8.02 (m, 5H, NH, N(1- CH_2 -Naph)), 9.94 (s, 1H, NH-N). HRMS (FAB) Calcd. for $C_{46}H_{51}N_6O_{14}$: 911.3463; Observed m/z : 911.3483. Anal. Calcd. for $C_{46}H_{50}N_6O_{14} \cdot 0.61TFA \cdot 0.16H_2O$: C, 57.65; H, 5.51; N, 8.55. Found: C, 57.69; H, 5.59; N, 8.84.

(2*S*,3*S*)-2-(bis-1-naphthylmethylcarbamoyl)-3-(N^2 -(*N*-benzyloxycarbonyl-aspartylglutamylvalyl)- N^1 -carboxymethylhydrazinocarbonyl)oxirane (Cbz-Asp-Glu-Val-AAsp-(2*S*,3*S*)EP-CON(1- CH_2 -Naph) $_2$, III-16a). Yield, 56%. 1H NMR (Acetone- d_6): 0.91-1.11 (m, 6H, Val), 1.90-1.96 (m, 2H, Glu), 2.10-2.46 (m, 5H, Glu, Val, Asp), 2.79-3.02 (m, 2H, AAsp), 3.69 (s, 1H, epoxy CH), 3.83 (s, 1H, epoxy CH), 4.24-4.55 (m, 3H, α -Hs), 4.91-5.45 (m, 6H, Cbz, N(1- CH_2 -Naph) $_2$), 6.83 (s, 1H, NH), 7.29-7.52 (m, 13H, NH, Cbz-Ph, N(1- CH_2 -Naph) $_2$), 7.74-7.93 (m, 7H, NH, N(1- CH_2 -Naph)), 8.07 (d, 1H, NH), 9.89 (d, 1H, NH-N). HRMS (ESI) Calcd. for $C_{50}H_{53}N_6O_{14}$: 961.3614; Observed m/z : 961.3605. Anal. Calcd. for $C_{50}H_{52}N_6O_{14} \cdot 1.35TFA \cdot 0.2H_2O \cdot 0.01C_4H_9$: C, 56.58; H, 5.17; N, 7.51. Found: C, 56.48; H, 5.24; N, 7.56.

N^2 -(*N*-Benzyloxycarbonylaspartylglutamylvalyl)- N^1 -carboxymethyl- N^1 -*trans*-(3-di-1- CH_2 -naphthylcarbamoylacryloyl)hydrazine (Cbz-Asp-Glu-Val-AAsp-CH=CH-CON(1- CH_2 -Naph) $_2$, III-20a). 1H NMR (Acetone- d_6): 1.03 (d, 6H, Val), 2.04-2.48 (m, 5H, Glu, Val, Asp), 2.88 (dd, 1H, Asp), 2.99 (dd, 1H, Asp), 4.46 (m, 1H, α -H), 4.57 (m, 2H, α -H), 5.09 (d, 2H, N(1- CH_2 -Naph) $_2$), 5.29-5.38 (m, 4H, N(1- CH_2 -Naph) $_2$, Cbz), 6.89 (d, $J = 7.2$ Hz, 1H, db), 7.30-7.99 (m, 21H, db, NH, Cbz-Ph, and N(1- CH_2 -Naph) $_2$),

8.15 (d, 1H, NH), 9.87 (s, 1H, NH-N). HRMS (ESI) Calcd. for $C_{50}H_{53}N_6O_{13}$: 945.3572; Observed m/z : 945.3665. Anal. Calcd. for $C_{50}H_{52}N_6O_{13} \cdot 0.6CF_3CO_2H \cdot 0.15H_2O$: C, 60.50; H, 5.51; N, 8.27. Found: C, 60.65; H, 5.57; N, 8.28.

Enzymatic Assays

All inhibitors were tested using the progress curve method, first described by Tian and Tsou.³⁶ The rate of substrate hydrolysis, in the presence of the inhibitor, was measured for a length of time appropriate for each enzyme. The [I]/[E] ratio was kept greater than or equal to 10:1 to ensure pseudo-first order kinetics. Assay conditions used for caspases-3, -6, and -8 were described previously by James, *et al*⁷³ and are described again below. Assay conditions for caspases-2, -7, -9, and -10 were adapted from previously described methods.¹³⁵

Caspases-2, -3, -6, -7, -8, -9 and -10 were expressed in *E. coli* and purified in Guy Salvesen's laboratory at the Burnham Institute, La Jolla, CA, according to the methods previously described by Stennicke and Salvesen.¹⁷⁵ Inhibition rates were determined by the progress curve method described by Tian and Tsou.³⁶

Assays using the fluorogenic substrates Ac-DEVD-AMC ($\lambda_{ex} = 360$ nm, $\lambda_{em} = 465$ nm), Cbz-VDVAD-AFC ($\lambda_{ex} = 430$ nm, $\lambda_{em} = 535$ nm), and Ac-LEHD-AFC were carried out on a Tecan Spectra Fluor microplate reader at 37 °C. The K_M values for Ac-DEVD-AMC with caspase-3 ($K_M = 9.7$ μ M), caspase-6 ($K_M = 236.35$ μ M), caspase-7 ($K_M = 23.0$ μ M), caspase-8 ($K_M = 6.79$ μ M), and caspase-10 ($K_M = 20.2$ μ M) were determined in the laboratory of Guy Salvesen. The K_M value for Ac-LEHD-AFC with caspase-9 ($K_M = 114$ μ M) was also determined in the laboratory of Guy Salvesen. The

K_M value for Ac-VDVAD-AFC with caspase-2 was also found to be 112 μM in the laboratory of Guy Salvesen. The K_M value for Cbz-VDVAD-AFC with caspase-2 was found to be 80.5 μM .

The k_2 values are 2.24-fold higher than the apparent rate for caspase-2 with Cbz-VDVAD-AFC as the substrate because of the 100 mM [S] and $K_M = 80.5 \mu\text{M}$. The k_2 values are 1.89-fold higher than the apparent rate for caspase-2 with Ac-VDVAD-AFC as the substrate because of the 100 mM [S] and $K_M = 112 \mu\text{M}$. The k_2 values are 11.31-fold higher than the apparent rate for caspase-3 because of the 100 mM [S] and $K_M = 9.7 \mu\text{M}$. The k_2 values are 1.42-fold higher than the apparent rate for caspase-6 because of the 100 mM [S] and $K_M = 236.35 \mu\text{M}$. The k_2 values are 5.35-fold higher than the apparent rate for caspase-7 because of the 100 mM [S] and $K_M = 23.0 \mu\text{M}$. The k_2 values are 15.73-fold higher than the apparent rate for caspase-8 because of the 100 mM [S] and $K_M = 6.79 \mu\text{M}$. The k_2 values are 2.32-fold higher than the apparent rate for caspase-9 because of the 150 mM [S] and $K_M = 114 \mu\text{M}$. The k_2 values are 8.43-fold higher than the apparent rate for caspase-10 because of the 150 mM [S] and $K_M = 20.2 \mu\text{M}$.

The concentration of the *caspase-3* stock solution was 2 nM in the assay buffer. Assay buffer is a 1:1 mixture of caspase buffer (40 mM Pipes, 200 mM NaCl, 0.2% (w/v) CHAPS, sucrose 20% (w/v)) and 20 mM DTT solution in H_2O at pH 7.2. The concentration of the substrate stock solution was 2 mM in DMSO. The enzyme was pre-activated for 10 min at 37 °C in the assay buffer. The standard 100 μL reaction was started by adding 40 μL of assay buffer, 5 μL of various amounts of inhibitor (stock solution concentrations varied from $5 \times 10^{-3} \text{ M}$ to $4.84 \times 10^{-7} \text{ M}$ in DMSO), and 5 μL of substrate in DMSO (100 μM final concentration) at 37 °C. 50 μL of 2 nM enzyme stock

solution (final concentration: 1 nM) was added to the mixture after 1 min and reading started immediately for 20 min at 37 °C. Inhibition experiments were repeated in duplicate and standard deviations determined.

Caspase-6 kinetic assays were performed using the same conditions and the same substrate (Ac-DEVD-AMC, 2 mM stock solution in DMSO). The enzyme stock solution was 10 nM (final concentration in the well: 5 nM) in the assay buffer. The inhibitor stock solution concentrations varied from 5×10^{-3} M to 2.42×10^{-6} M in DMSO.

Caspase-7 kinetic assays were performed using the same conditions and the same substrate (Ac-DEVD-AMC, 2 mM stock solution in DMSO). The enzyme stock solution was 10 nM (final concentration in the well: 5 nM) in the assay buffer. The inhibitor stock solution concentrations varied from 5×10^{-3} M to 2.5×10^{-6} M in DMSO.

Caspase-8 kinetic assays were performed using the same conditions and the same substrate (Ac-DEVD-AMC, 2 mM stock solution in DMSO). The enzyme stock solution was 100 nM (final concentration in the well: 50 nM) in the assay buffer. The inhibitor stock solution concentrations varied from 5×10^{-3} M to 2.42×10^{-6} M in DMSO.

Caspase-2 kinetic assays were performed using Ac-VDVAD-AFC as the substrate with aza-peptide epoxides and Cbz-VDVAD-AFC with aza-peptide Michael acceptors (2 mM stock solution in DMSO). The same conditions as caspase-3 were used. With Ac-VDVAD-AFC, the concentration of the caspase-2 stock solution was 86.7 nM in the assay buffer (final concentration in the well: 43.3 nM). With Cbz-VDVAD-AFC, the concentration of the caspase-2 stock solution was 200 nM in the assay buffer (final concentration in the well: 100 nM). The inhibitor stock solution concentrations varied from 5×10^{-3} M to 1×10^{-4} M in DMSO.

Caspase-9 kinetic assays were performed using Ac-LEHD-AFC as the substrate (3 mM stock solution in DMSO) and with the following conditions. The concentration of the caspase-9 stock solution was 150 nM in the assay buffer (final concentration in the well: 75 nM). Assay buffer is a 1:1 mixture of buffer (200 mM Hepes, 100 mM NaCl, 0.02% (w/v) CHAPS, sucrose 20% (w/v)) and 20 mM DTT solution in H₂O at pH 7.0). The assay buffer was supplemented with 0.7 M sodium citrate. The enzyme was pre-activated for 10 min at 37 °C in the assay buffer. The inhibitor stock solution concentrations varied from 5×10^{-3} M to 2.5×10^{-5} M in DMSO.

Caspase-10 kinetic assays were performed using the same substrate as caspase-3 (Ac-DEVD-AMC, 3 mM stock solution in DMSO) and with the following conditions. The concentration of the caspase-10 stock solution was 50 nM in the assay buffer (final concentration in the well: 25 nM). Assay buffer is a 1:1 mixture of buffer (200 mM Hepes, 0.2% (w/v) CHAPS, PEG 20% (w/v)) and 20 mM DTT solution in H₂O at pH 7.0). The enzyme was pre-activated for 10 min at 25 °C in the assay buffer. The inhibitor stock solution concentrations varied from 5×10^{-3} M to 2.5×10^{-5} M in DMSO.

Molecular modeling

All calculations were done using the Molecular Operating Environment (MOE), © Chemical Computing Group, Inc. The coordinates caspase-3 – Ac-DEVD-CHO were obtained from the Protein Data Bank. The aldehyde inhibitor was modified to an aza-peptide epoxide inhibitors Cbz-DEVaD-(*S,S*)-EP-CON(Bzl)₂ and Cbz-DEVaD-(*R,R*)-EP-CON(Bzl)₂ using the MOE builder tool. The C – S distance, with C = site of attack and S = thiolate sulfur atom, was restrained to 1.81 Å. Hydrogen atoms were added to the

structures. The heavy atoms of the enzyme were fixed; the hydrogen atoms of the enzyme and all atoms of the inhibitor remained flexible. The enzyme atoms within 7.5 – 10 Å proximity of the inhibitor were included in the calculations. Energy minimization was performed, using the MMFF94 force field with solvation. Energy minimization methods were used were Steepest Descent (SD), Conjugate Gradients (CG), and Truncated Newton (TN). Following energy minimization, the inhibitor was docked in the active site using the simulated annealing, a global optimization docking technique, again including solvation. The lowest energy conformations of the docked inhibitors are discussed. Figures 3.12 and 3.13 were rendered using Pymol.¹⁷⁶

REFERENCES

- (1) Schechter, I.; Berger, A. On the size of the active site in proteases. I. Papain. *Biochem Biophys Res Commun* **1967**, *27*, 157-162.
- (2) Stroud, R. M. *Sci. Am.* **1974**, *231*, 86.
- (3) Rawlings, N. D.; Barrett, A. J. Evolutionary families of peptidases. *Biochem J* **1993**, *290* (Pt 1), 205-218.
- (4) Barrett, A. J.; Rawlings, N. D. Evolutionary lines of cysteine peptidases. *Biol Chem* **2001**, *382*, 727-733.
- (5) Kamphuis, I. G.; Kalk, K. H.; Swarte, M. B.; Drenth, J. Structure of papain refined at 1.65 Å resolution. *J Mol Biol* **1984**, *179*, 233-256.
- (6) Smith, E. L. Active site and structure of crystalline papain. *Federation Proceedings* **1957**, *16*, 801-809.
- (7) Lecaille, F.; Kaleta, J.; Bromme, D. Human and parasitic papain-like cysteine proteases: their role in physiology and pathology and recent developments in inhibitor design. *Chem Rev* **2002**, *102*, 4459-4488.
- (8) Guroff, G. A Neutral, Calcium-Activated Proteinase From The Soluble Fraction Of Rat Brain. *J Biol Chem* **1964**, *239*, 149-155.
- (9) Goll, D. E.; Thompson, V. F.; Li, H.; Wei, W.; Cong, J. The calpain system. *Physiol Rev* **2003**, *83*, 731-801.
- (10) Carragher, N. O.; Frame, M. C. Calpain: a role in cell transformation and migration. *Int J Biochem Cell Biol* **2002**, *34*, 1539-1543.
- (11) Honda, S.; Marumoto, T.; Hirota, T.; Nitta, M.; Arima, Y. et al. Activation of m-calpain is required for chromosome alignment on the metaphase plate during mitosis. *J Biol Chem* **2004**, *279*, 10615-10623.
- (12) Zimmerman, U. J.; Boring, L.; Pak, J. H.; Mukerjee, N.; Wang, K. K. The calpain small subunit gene is essential: its inactivation results in embryonic lethality. *IUBMB Life* **2000**, *50*, 63-68.
- (13) Black, R. A.; Kronheim, S. R.; Sleath, P. R. Activation of interleukin-1 beta by a co-induced protease. *FEBS Lett* **1989**, *247*, 386-390.
- (14) Kostura, M. J.; Tocci, M. J.; Limjuco, G.; Chin, J.; Cameron, P. et al. Identification of a monocyte specific pre-interleukin 1 beta convertase activity. *Proc Natl Acad Sci U S A* **1989**, *86*, 5227-5231.

- (15) Jedeszko, C.; Sloane, B. F. Cysteine cathepsins in human cancer. *Biol Chem* **2004**, *385*, 1017-1027.
- (16) Yan, S.; Sloane, B. F. Molecular regulation of human cathepsin B: implication in pathologies. *Biol Chem* **2003**, *384*, 845-854.
- (17) Berdowska, I. Cysteine proteases as disease markers. *Clin Chim Acta* **2004**, *342*, 41-69.
- (18) Blomgren, K.; McRae, A.; Bona, E.; Saido, T. C.; Karlsson, J. O. et al. Degradation of fodrin and MAP 2 after neonatal cerebral hypoxic-ischemia. *Brain Res* **1995**, *684*, 136-142.
- (19) Huang, Y.; Wang, K. K. The calpain family and human disease. *Trends Mol Med* **2001**, *7*, 355-362.
- (20) Ray, S. K.; Banik, N. L. Calpain and its involvement in the pathophysiology of CNS injuries and diseases: therapeutic potential of calpain inhibitors for prevention of neurodegeneration. *Curr Drug Targets CNS Neurol Disord* **2003**, *2*, 173-189.
- (21) Sedarous, M.; Keramaris, E.; O'Hare, M.; Melloni, E.; Slack, R. S. et al. Calpains mediate p53 activation and neuronal death evoked by DNA damage. *J Biol Chem* **2003**, *278*, 26031-26038.
- (22) Shields, D. C.; Banik, N. L. Pathophysiological role of calpain in experimental demyelination. *J Neurosci Res* **1999**, *55*, 533-541.
- (23) Suzuki, K.; Hata, S.; Kawabata, Y.; Sorimachi, H. Structure, activation, and biology of calpain. *Diabetes* **2004**, *53 Suppl 1*, S12-18.
- (24) Johansson, A.; Kalfas, S. Characterization of the proteinase-dependent cytotoxicity of *Porphyromonas gingivalis*. *Eur J Oral Sci* **1998**, *106*, 863-871.
- (25) Brindley, P. J.; Kalinna, B. H.; Dalton, J. P.; Day, S. R.; Wong, J. Y. et al. Proteolytic degradation of host hemoglobin by schistosomes. *Mol Biochem Parasitol* **1997**, *89*, 1-9.
- (26) Uhlmann, F. The mechanism of sister chromatid cohesion. *Exp Cell Res* **2004**, *296*, 80-85.
- (27) Supuran, C.; Scozzafava, A.; Mastrolorenzo, A. Bacterial proteases: current therapeutic use and future prospects for the development of new antibiotics. *Expert Opinion on Therapeutic Patents* **2001**, *11*, 221-259.
- (28) Supuran, C. T.; Scozzafava, A.; Clare, B. W. Bacterial protease inhibitors. *Med Res Rev* **2002**, *22*, 329-372.

- (29) Turk, B.; Stoka, V.; Rozman-Pungercar, J.; Cirman, T.; Droga-Mazovec, G. et al. Apoptotic pathways: involvement of lysosomal proteases. *Biol Chem* **2002**, *383*, 1035-1044.
- (30) Altnauer, F.; Conus, S.; Cavalli, A.; Folkers, G.; Simon, H. U. Calpain-1 regulates Bax and subsequent Smac-dependent caspase-3 activation in neutrophil apoptosis. *J Biol Chem* **2004**, *279*, 5947-5957.
- (31) Menard, R.; Carriere, J.; Laflamme, P.; Plouffe, C.; Khouri, H. E. et al. Contribution of the glutamine 19 side chain to transition-state stabilization in the oxyanion hole of papain. *Biochemistry* **1991**, *30*, 8924-8928.
- (32) Fuentes-Prior, P.; Salvesen, G. S. The protein structures that shape caspase activity, specificity, activation and inhibition. *Biochem J* **2004**, *384*, 201-232.
- (33) Keillor, J. W.; Brown, R. S. Reaction of a distorted amide with nucleophilic thiolate-containing zwitterions produced from thiolamines - A model for the acylation step in cysteine proteases and transglutaminases. *J Am Chem Soc* **1991**, *113*, 5114-5116.
- (34) Keillor, J. W.; Brown, R. S. Attack of Zwitterionic Ammonium Thiolates on a Distorted Anilide as a Model for the acylation of Papain by amides - A Simple Demonstration of a Bell-Shaped pH Rate Profile. *J Am Chem Soc* **1992**, *114*, 7983-7989.
- (35) Kitz, R.; Wilson, I. B. Esters of methanesulfonic acid as irreversible inhibitors of acetylcholinesterase. *J Biol Chem* **1962**, *237*, 3245-3249.
- (36) Tian, W. X.; Tsou, C. L. Determination of the rate constant of enzyme modification by measuring the substrate reaction in the presence of the modifier. *Biochemistry* **1982**, *21*, 1028-1032.
- (37) Shuja, S.; Sheahan, K.; Murnane, M. J. Cysteine endopeptidase activity levels in normal human tissues, colorectal adenomas and carcinomas. *Int J Cancer* **1991**, *49*, 341-346.
- (38) Jia, Z.; Hasnain, S.; Hirama, T.; Lee, X.; Mort, J. S. et al. Crystal structures of recombinant rat cathepsin B and a cathepsin B-inhibitor complex. Implications for structure-based inhibitor design. *J Biol Chem* **1995**, *270*, 5527-5533.
- (39) Musil, D.; Zucic, D.; Turk, D.; Engh, R. A.; Mayr, I. et al. The refined 2.15 Å X-ray crystal structure of human liver cathepsin B: the structural basis for its specificity. *Embo J* **1991**, *10*, 2321-2330.
- (40) Stern, I.; Schaschke, N.; Moroder, L.; Turk, D. Crystal structure of NS-134 in complex with bovine cathepsin B: a two-headed epoxysuccinyl inhibitor extends along the entire active-site cleft. *Biochem J* **2004**, *381*, 511-517.

- (41) Turk, D.; Podobnik, M.; Popovic, T.; Katunuma, N.; Bode, W. et al. Crystal structure of cathepsin B inhibited with CA030 at 2.0-Å resolution: A basis for the design of specific epoxysuccinyl inhibitors. *Biochemistry* **1995**, *34*, 4791-4797.
- (42) Katunuma, N.; Kominami, E. Abnormal expression of lysosomal cysteine proteinases in muscle wasting diseases. *Rev Physiol Biochem Pharmacol* **1987**, *108*, 1-20.
- (43) Michaud, S.; Gour, B. Cathepsin B inhibitors as potential anti-metastatic agents. *Expert Opinion on Therapeutic Patents* **1998**, *8*, 645-672.
- (44) Buck, M. R.; Karustis, D. G.; Day, N. A.; Honn, K. V.; Sloane, B. F. Degradation of extracellular-matrix proteins by human cathepsin B from normal and tumour tissues. *Biochem J* **1992**, *282* (Pt 1), 273-278.
- (45) Lim, I. T.; Meroueh, S. O.; Lee, M.; Heeg, M. J.; Mobashery, S. Strategy in inhibition of cathepsin B, a target in tumor invasion and metastasis. *J Am Chem Soc* **2004**, *126*, 10271-10277.
- (46) Gan, L.; Ye, S.; Chu, A.; Anton, K.; Yi, S. et al. Identification of cathepsin B as a mediator of neuronal death induced by Abeta-activated microglial cells using a functional genomics approach. *J Biol Chem* **2004**, *279*, 5565-5572.
- (47) Azam, M.; Andrabi, S. S.; Sahr, K. E.; Kamath, L.; Kuliopulos, A. et al. Disruption of the mouse mu-calpain gene reveals an essential role in platelet function. *Mol Cell Biol* **2001**, *21*, 2213-2220.
- (48) Zhao, X.; Posmantur, R.; Kampfl, A.; Liu, S. J.; Wang, K. K. et al. Subcellular localization and duration of mu-calpain and m-calpain activity after traumatic brain injury in the rat: a casein zymography study. *J Cereb Blood Flow Metab* **1998**, *18*, 161-167.
- (49) Blomgren, K.; Zhu, C.; Wang, X.; Karlsson, J. O.; Leverin, A. L. et al. Synergistic activation of caspase-3 by m-calpain after neonatal hypoxia-ischemia: a mechanism of "pathological apoptosis"? *J Biol Chem* **2001**, *276*, 10191-10198.
- (50) Wang, K. K. Calpain and caspase: can you tell the difference? *Trends Neurosci* **2000**, *23*, 20-26.
- (51) Mehendale, H. M.; Limaye, P. B. Calpain: a death protein that mediates progression of liver injury. *Trends Pharmacol Sci* **2005**, *26*, 232-236.
- (52) Limaye, P. B.; Apte, U. M.; Shankar, K.; Bucci, T. J.; Warbritton, A. et al. Calpain released from dying hepatocytes mediates progression of acute liver injury induced by model hepatotoxicants. *Toxicol Appl Pharmacol* **2003**, *191*, 211-226.
- (53) Zatz, M.; Starling, A. Calpains and disease. *N Engl J Med* **2005**, *352*, 2413-2423.

- (54) Donkor, I. O. A survey of calpain inhibitors. *Curr Med Chem* **2000**, 7, 1171-1188.
- (55) Otto, H. H.; Schirmeister, T. Cysteine Proteases and Their Inhibitors. *Chem Rev* **1997**, 97, 133-172.
- (56) Powers, J. C.; Asgian, J. L.; Ekici, O. D.; James, K. E. Irreversible inhibitors of serine, cysteine, and threonine proteases. *Chem Rev* **2002**, 102, 4639-4750.
- (57) Hanada, K.; Tamai, M.; Yamagishi, M.; Ohmura, S.; Sawada, J. et al. Isolation and characterization of E-64, a new thiol protease inhibitor. *Agricultural and Biological Chemistry* **1978**, 42, 523-528.
- (58) Hanada, K.; Tamai, M.; Morimoto, S.; Adachi, T.; Ohmura, S. et al. Inhibitory activities of E-64 derivatives on papain. *Agricultural and Biological Chemistry* **1978**, 42, 537-541.
- (59) Hanada, K.; Tamai, M.; Ohmura, S.; Sawada, J.; Seki, T. et al. Structure and synthesis of E-64, a new thiol protease inhibitor. *Agricultural and Biological Chemistry* **1978**, 42, 529-536.
- (60) Libby, P.; Goldberg, A. L. Leupeptin, a protease inhibitor, decreases protein degradation in normal and diseased muscles. *Science* **1978**, 199, 534-536.
- (61) Hashida, S.; Towatari, T.; Kominami, E.; Katunuma, N. Inhibitions by E-64 derivatives of rat liver cathepsin B and cathepsin L in vitro and in vivo. *J Biochem (Tokyo)* **1980**, 88, 1805-1811.
- (62) Parkes, C.; Kembhavi, A. A.; Barrett, A. J. Calpain inhibition by peptide epoxides. *Biochem J* **1985**, 230, 509-516.
- (63) Gour-Salin, B. J.; Lachance, P.; Magny, M. C.; Plouffe, C.; Menard, R. et al. E64 [trans-epoxysuccinyl-L-leucylamido-(4-guanidino)butane] analogues as inhibitors of cysteine proteinases: investigation of S2 subsite interactions. *Biochem J* **1994**, 299 (Pt 2), 389-392.
- (64) Barrett, A. J.; Kembhavi, A. A.; Brown, M. A.; Kirschke, H.; Knight, C. G. et al. L-trans-Epoxysuccinyl-leucylamido(4-guanidino)butane (E-64) and its analogues as inhibitors of cysteine proteinases including cathepsins B, H and L. *Biochem J* **1982**, 201, 189-198.
- (65) Matsumoto, K.; Mizoue, K.; Kitamura, K.; Tse, W. C.; Huber, C. P. et al. Structural basis of inhibition of cysteine proteases by E-64 and its derivatives. *Biopolymers* **1999**, 51, 99-107.
- (66) Varughese, K. I.; Ahmed, F. R.; Carey, P. R.; Hasnain, S.; Huber, C. P. et al. Crystal structure of a papain-E-64 complex. *Biochemistry* **1989**, 28, 1330-1332.

- (67) Kim, M. J.; Yamamoto, D.; Matsumoto, K.; Inoue, M.; Ishida, T. et al. Crystal structure of papain-E64-c complex. Binding diversity of E64-c to papain S2 and S3 subsites. *Biochem J* **1992**, 287 (Pt 3), 797-803.
- (68) Yamamoto, D.; Matsumoto, K.; Ohishi, H.; Ishida, T.; Inoue, M. et al. Refined x-ray structure of papain.E-64-c complex at 2.1-Å resolution. *J Biol Chem* **1991**, 266, 14771-14777.
- (69) Yamamoto, A.; Tomoo, K.; Matsugi, K.; Hara, T.; In, Y. et al. Structural basis for development of cathepsin B-specific noncovalent-type inhibitor: crystal structure of cathepsin B-E64c complex. *Biochim Biophys Acta* **2002**, 1597, 244-251.
- (70) Moldoveanu, T.; Campbell, R. L.; Cuerrrier, D.; Davies, P. L. Crystal structures of calpain-E64 and -leupeptin inhibitor complexes reveal mobile loops gating the active site. *J Mol Biol* **2004**, 343, 1313-1326.
- (71) Broker, L. E.; Kruyt, F. A.; Giaccone, G. Cell death independent of caspases: a review. *Clin Cancer Res* **2005**, 11, 3155-3162.
- (72) Asgian, J. L.; James, K. E.; Li, Z. Z.; Carter, W.; Barrett, A. J. et al. Aza-peptide epoxides: a new class of inhibitors selective for clan CD cysteine proteases. *J Med Chem* **2002**, 45, 4958-4960.
- (73) James, K. E.; Asgian, J. L.; Li, Z. Z.; Ekici, O. D.; Rubin, J. R. et al. Design, synthesis, and evaluation of aza-peptide epoxides as selective and potent inhibitors of caspases-1, -3, -6, and -8. *J Med Chem* **2004**, 47, 1553-1574.
- (74) James, K. E.; Gotz, M. G.; Caffrey, C. R.; Hansell, E.; Carter, W. et al. Aza-peptide epoxides: potent and selective inhibitors of *Schistosoma mansoni* and pig kidney legumains (asparaginyl endopeptidases). *Biol Chem* **2003**, 384, 1613-1618.
- (75) Powers, J. C.; Asgian, J. L.; James, K. E.; Li, Z.-Z. Aza-peptide epoxides: PCT Int. Appl., 2004; pp 179.
- (76) Roush, W.; Hernandez, A.; McKerrow, J.; Selzer, P.; Hansell, E. et al. Design, synthesis and evaluation of D-homophenylalanyl epoxysuccinate inhibitors of the trypanosomal cysteine protease cruzain. *Tetrahedron* **2000**, 56, 9747-9762.
- (77) Fassler, A.; Bold, G.; Capraro, H. G.; Cozens, R.; Mestan, J. et al. Aza-peptide analogs as potent human immunodeficiency virus type-1 protease inhibitors with oral bioavailability. *J Med Chem* **1996**, 39, 3203-3216.
- (78) Dragovich, P. S.; Barker, J. E.; French, J.; Imbacuan, M.; Kalish, V. J. et al. Structure-based design of novel, urea-containing FKBP12 inhibitors. *J Med Chem* **1996**, 39, 1872-1884.

- (79) Batey, R.; Santhakumar, V.; Yoshina-Ishii, C.; Taylor, S. An efficient new protocol for the formation of unsymmetrical tri- and tetrasubstituted ureas. *Tetrahedron Lett* **1998**, *39*, 6267-6270.
- (80) Mori, K.; Iwasawa, H. Pheromone Synthesis.35. Stereoselective Synthesis of Optically-Active Forms of Delta-Multistriatin, the Attractant for European Populations of the Smaller European Elm Bark Beetle. *Tetrahedron* **1980**, *36*, 87-90.
- (81) Korn, A.; Rudolphbohner, S.; Moroder, L. A Convenient Synthesis of Optically Pure (2R,3R)-2,3-Epoxy succinyl-Dipeptides. *Tetrahedron* **1994**, *50*, 8381-8392.
- (82) Tamai, M.; Omura, S.; Kimura, M.; Hanada, K.; Sugita, H. Prolongation of life span of dystrophic hamster by cysteine proteinase inhibitor, loxistation (EST). *J Pharmacobiodyn* **1987**, *10*, 678-681.
- (83) Tamai, M.; Matsumoto, K.; Omura, S.; Koyama, I.; Ozawa, Y. et al. In vitro and in vivo inhibition of cysteine proteinases by EST, a new analog of E-64. *J Pharmacobiodyn* **1986**, *9*, 672-677.
- (84) Meara, J. P.; Rich, D. H. Mechanistic studies on the inactivation of papain by epoxysuccinyl inhibitors. *J Med Chem* **1996**, *39*, 3357-3366.
- (85) Lee, H. J.; Song, J. W.; Choi, Y. S.; Park, H. M.; Lee, K. B. A theoretical study of conformational properties of N-methyl azapeptide derivatives. *J Am Chem Soc* **2002**, *124*, 11881-11893.
- (86) Concha, N. O.; Abdel-Meguid, S. S. Controlling apoptosis by inhibition of caspases. *Curr Med Chem* **2002**, *9*, 713-726.
- (87) O'Brien, T.; Lee, D. Prospects for caspase inhibitors. *Mini Rev Med Chem* **2004**, *4*, 153-165.
- (88) Onteniente, B. Natural and synthetic inhibitors of caspases: targets for novel drugs. *Curr Drug Targets CNS Neurol Disord* **2004**, *3*, 333-340.
- (89) Talanian, R. V.; Brady, K. D.; Cryns, V. L. Caspases as targets for anti-inflammatory and anti-apoptotic drug discovery. *J Med Chem* **2000**, *43*, 3351-3371.
- (90) Assuncao Guimaraes, C.; Linden, R. Programmed cell deaths. Apoptosis and alternative deathstyles. *Eur J Biochem* **2004**, *271*, 1638-1650.
- (91) Egger, L.; Schneider, J.; Rheme, C.; Tapernoux, M.; Hacki, J. et al. Serine proteases mediate apoptosis-like cell death and phagocytosis under caspase-inhibiting conditions. *Cell Death Differ* **2003**, *10*, 1188-1203.

- (92) Stenson-Cox, C.; FitzGerald, U.; Samali, A. In the cut and thrust of apoptosis, serine proteases come of age. *Biochem Pharmacol* **2003**, *66*, 1469-1474.
- (93) Denault, J. B.; Salvesen, G. S. Caspases: keys in the ignition of cell death. *Chem Rev* **2002**, *102*, 4489-4500.
- (94) Kohler, C.; Orrenius, S.; Zhivotovsky, B. Evaluation of caspase activity in apoptotic cells. *J Immunol Methods* **2002**, *265*, 97-110.
- (95) Philchenkov, A. A. Caspases as regulators of apoptosis and other cell functions. *Biochemistry (Mosc)* **2003**, *68*, 365-376.
- (96) Stennicke, H. R.; Salvesen, G. S. Properties of the caspases. *Biochim Biophys Acta* **1998**, *1387*, 17-31.
- (97) Thornberry, N. A. Caspases: a decade of death research. *Cell Death Differ* **1999**, *6*, 1023-1027.
- (98) Thornberry, N. A.; Lazebnik, Y. Caspases: enemies within. *Science* **1998**, *281*, 1312-1316.
- (99) Yuan, J.; Horvitz, H. R. A first insight into the molecular mechanisms of apoptosis. *Cell* **2004**, *116*, S53-56, 51 p following S59.
- (100) Thornberry, N. A. Caspases: key mediators of apoptosis. *Chem Biol* **1998**, *5*, R97-103.
- (101) Fischer, U.; Schulze-Osthoff, K. Apoptosis-based therapies and drug targets. *Cell Death Differ* **2005**, *12 Suppl 1*, 942-961.
- (102) Wilson, K. P.; Black, J. A.; Thomson, J. A.; Kim, E. E.; Griffith, J. P. et al. Structure and mechanism of interleukin-1 beta converting enzyme. *Nature* **1994**, *370*, 270-275.
- (103) Kumar, S. ICE-like proteases in apoptosis. *Trends Biochem Sci* **1995**, *20*, 198-202.
- (104) Nicholson, D. W. Caspase structure, proteolytic substrates, and function during apoptotic cell death. *Cell Death Differ* **1999**, *6*, 1028-1042.
- (105) Fischer, U.; Janicke, R. U.; Schulze-Osthoff, K. Many cuts to ruin: a comprehensive update of caspase substrates. *Cell Death Differ* **2003**, *10*, 76-100.
- (106) Li, H.; Zhu, H.; Xu, C. J.; Yuan, J. Cleavage of BID by caspase 8 mediates the mitochondrial damage in the Fas pathway of apoptosis. *Cell* **1998**, *94*, 491-501.

- (107) Luo, X.; Budihardjo, I.; Zou, H.; Slaughter, C.; Wang, X. Bid, a Bcl2 interacting protein, mediates cytochrome c release from mitochondria in response to activation of cell surface death receptors. *Cell* **1998**, *94*, 481-490.
- (108) Milhas, D.; Cuvillier, O.; Therville, N.; Clave, P.; Thomsen, M. et al. Caspase-10 triggers Bid cleavage and caspase cascade activation in FasL-induced apoptosis. *J Biol Chem* **2005**, *280*, 19836-19842.
- (109) Lassus, P.; Opitz-Araya, X.; Lazebnik, Y. Requirement for caspase-2 in stress-induced apoptosis before mitochondrial permeabilization. *Science* **2002**, *297*, 1352-1354.
- (110) Robertson, J. D.; Enoksson, M.; Suomela, M.; Zhivotovsky, B.; Orrenius, S. Caspase-2 acts upstream of mitochondria to promote cytochrome c release during etoposide-induced apoptosis. *J Biol Chem* **2002**, *277*, 29803-29809.
- (111) Guo, Y.; Srinivasula, S. M.; Druilhe, A.; Fernandes-Alnemri, T.; Alnemri, E. S. Caspase-2 induces apoptosis by releasing proapoptotic proteins from mitochondria. *J Biol Chem* **2002**, *277*, 13430-13437.
- (112) Slee, E. A.; Harte, M. T.; Kluck, R. M.; Wolf, B. B.; Casiano, C. A. et al. Ordering the cytochrome c-initiated caspase cascade: hierarchical activation of caspases-2, -3, -6, -7, -8, and -10 in a caspase-9-dependent manner. *J Cell Biol* **1999**, *144*, 281-292.
- (113) Boatright, K. M.; Renatus, M.; Scott, F. L.; Sperandio, S.; Shin, H. et al. A unified model for apical caspase activation. *Mol Cell* **2003**, *11*, 529-541.
- (114) Donepudi, M.; Mac Sweeney, A.; Briand, C.; Grutter, M. G. Insights into the regulatory mechanism for caspase-8 activation. *Mol Cell* **2003**, *11*, 543-549.
- (115) Muzio, M.; Stockwell, B. R.; Stennicke, H. R.; Salvesen, G. S.; Dixit, V. M. An induced proximity model for caspase-8 activation. *J Biol Chem* **1998**, *273*, 2926-2930.
- (116) Renatus, M.; Stennicke, H. R.; Scott, F. L.; Liddington, R. C.; Salvesen, G. S. Dimer formation drives the activation of the cell death protease caspase 9. *Proc Natl Acad Sci U S A* **2001**, *98*, 14250-14255.
- (117) Salvesen, G. S.; Dixit, V. M. Caspase activation: the induced-proximity model. *Proc Natl Acad Sci U S A* **1999**, *96*, 10964-10967.
- (118) Stennicke, H. R.; Salvesen, G. S. Catalytic properties of the caspases. *Cell Death Differ* **1999**, *6*, 1054-1059.
- (119) www.rcsb.org/pdb.

- (120) Schweizer, A.; Briand, C.; Grutter, M. G. Crystal structure of caspase-2, apical initiator of the intrinsic apoptotic pathway. *J Biol Chem* **2003**, *278*, 42441-42447.
- (121) Becker, J. W.; Rotonda, J.; Soisson, S. M.; Aspiotis, R.; Bayly, C. et al. Reducing the peptidyl features of caspase-3 inhibitors: a structural analysis. *J Med Chem* **2004**, *47*, 2466-2474.
- (122) Rotonda, J.; Nicholson, D. W.; Fazil, K. M.; Gallant, M.; Gareau, Y. et al. The three-dimensional structure of apopain/CPP32, a key mediator of apoptosis. *Nat Struct Biol* **1996**, *3*, 619-625.
- (123) Mittl, P. R.; Di Marco, S.; Krebs, J. F.; Bai, X.; Karanewsky, D. S. et al. Structure of recombinant human CPP32 in complex with the tetrapeptide acetyl-Asp-Val-Ala-Asp fluoromethyl ketone. *J Biol Chem* **1997**, *272*, 6539-6547.
- (124) Ni, C. Z.; Li, C.; Wu, J. C.; Spada, A. P.; Ely, K. R. Conformational restrictions in the active site of unliganded human caspase-3. *J Mol Recognit* **2003**, *16*, 121-124.
- (125) Riedl, S. J.; Renatus, M.; Schwarzenbacher, R.; Zhou, Q.; Sun, C. et al. Structural basis for the inhibition of caspase-3 by XIAP. *Cell* **2001**, *104*, 791-800.
- (126) Lee, D.; Long, S. A.; Adams, J. L.; Chan, G.; Vaidya, K. S. et al. Potent and selective nonpeptide inhibitors of caspases 3 and 7 inhibit apoptosis and maintain cell functionality. *J Biol Chem* **2000**, *275*, 16007-16014.
- (127) Wei, Y.; Fox, T.; Chambers, S. P.; Sintchak, J.; Coll, J. T. et al. The structures of caspases-1, -3, -7 and -8 reveal the basis for substrate and inhibitor selectivity. *Chem Biol* **2000**, *7*, 423-432.
- (128) Watt, W.; Koeplinger, K. A.; Mildner, A. M.; Heinrikson, R. L.; Tomasselli, A. G. et al. The atomic-resolution structure of human caspase-8, a key activator of apoptosis. *Structure Fold Des* **1999**, *7*, 1135-1143.
- (129) Blanchard, H.; Donepudi, M.; Tschopp, M.; Kodandapani, L.; Wu, J. C. et al. Caspase-8 specificity probed at subsite S(4): crystal structure of the caspase-8-Z-DEVD-cho complex. *J Mol Biol* **2000**, *302*, 9-16.
- (130) Blanchard, H.; Kodandapani, L.; Mittl, P. R.; Marco, S. D.; Krebs, J. F. et al. The three-dimensional structure of caspase-8: an initiator enzyme in apoptosis. *Structure Fold Des* **1999**, *7*, 1125-1133.
- (131) Xu, G.; Cirilli, M.; Huang, Y.; Rich, R. L.; Myszka, D. G. et al. Covalent inhibition revealed by the crystal structure of the caspase-8/p35 complex. *Nature* **2001**, *410*, 494-497.
- (132) Shiozaki, E. N.; Chai, J.; Rigotti, D. J.; Riedl, S. J.; Li, P. et al. Mechanism of XIAP-mediated inhibition of caspase-9. *Mol Cell* **2003**, *11*, 519-527.

- (133) Sattar, R.; Ali, S. A.; Abbasi, A. Molecular mechanism of apoptosis: prediction of three-dimensional structure of caspase-6 and its interactions by homology modeling. *Biochem Biophys Res Commun* **2003**, 308, 497-504.
- (134) Chereau, D.; Kodandapani, L.; Tomaselli, K. J.; Spada, A. P.; Wu, J. C. Structural and functional analysis of caspase active sites. *Biochemistry* **2003**, 42, 4151-4160.
- (135) Garcia-Calvo, M.; Peterson, E. P.; Rasper, D. M.; Vaillancourt, J. P.; Zamboni, R. et al. Purification and catalytic properties of human caspase family members. *Cell Death Differ* **1999**, 6, 362-369.
- (136) Margolin, N.; Raybuck, S. A.; Wilson, K. P.; Chen, W.; Fox, T. et al. Substrate and inhibitor specificity of interleukin-1 beta-converting enzyme and related caspases. *J Biol Chem* **1997**, 272, 7223-7228.
- (137) Rano, T. A.; Timkey, T.; Peterson, E. P.; Rotonda, J.; Nicholson, D. W. et al. A combinatorial approach for determining protease specificities: application to interleukin-1beta converting enzyme (ICE). *Chem Biol* **1997**, 4, 149-155.
- (138) Stennicke, H. R.; Renatus, M.; Meldal, M.; Salvesen, G. S. Internally quenched fluorescent peptide substrates disclose the subsite preferences of human caspases 1, 3, 6, 7 and 8. *Biochem J* **2000**, 350 Pt 2, 563-568.
- (139) Talanian, R. V.; Quinlan, C.; Trautz, S.; Hackett, M. C.; Mankovich, J. A. et al. Substrate specificities of caspase family proteases. *J Biol Chem* **1997**, 272, 9677-9682.
- (140) Thornberry, N. A.; Rano, T. A.; Peterson, E. P.; Rasper, D. M.; Timkey, T. et al. A combinatorial approach defines specificities of members of the caspase family and granzyme B. Functional relationships established for key mediators of apoptosis. *J Biol Chem* **1997**, 272, 17907-17911.
- (141) Garcia-Calvo, M.; Peterson, E. P.; Leiting, B.; Ruel, R.; Nicholson, D. W. et al. Inhibition of human caspases by peptide-based and macromolecular inhibitors. *J Biol Chem* **1998**, 273, 32608-32613.
- (142) Ekici, O. D. L., Z.; James, K.E.; Asgian, J.L.; Mikolajczyk, J.; Salvesen, G.S.; Powers, J. C. Design, Synthesis, and Evaluation of Aza-Peptide Michael Acceptors as Selective and Potent Inhibitors of Caspases. *Manuscript in preparation, to be submitted to J. Med. Chem.*
- (143) Brady, K. D.; Giegel, D. A.; Grinnell, C.; Lunney, E.; Talanian, R. V. et al. A catalytic mechanism for caspase-1 and for bimodal inhibition of caspase-1 by activated aspartic ketones. *Bioorg Med Chem* **1999**, 7, 621-631.
- (144) Grimm, E. L.; Roy, B.; Aspiotis, R.; Bayly, C. I.; Nicholson, D. W. et al. Solid phase synthesis of selective caspase-3 peptide inhibitors. *Bioorg Med Chem* **2004**, 12, 845-851.

- (145) Han, Y.; Giroux, A.; Grimm, E. L.; Aspiotis, R.; Francoeur, S. et al. Discovery of novel aspartyl ketone dipeptides as potent and selective caspase-3 inhibitors. *Bioorg Med Chem Lett* **2004**, *14*, 805-808.
- (146) Harter, W. G.; Albrect, H.; Brady, K.; Caprathe, B.; Dunbar, J. et al. The design and synthesis of sulfonamides as caspase-1 inhibitors. *Bioorg Med Chem Lett* **2004**, *14*, 809-812.
- (147) Linton, S. D.; Aja, T.; Allegrini, P. R.; Deckwerth, T. L.; Diaz, J. L. et al. Oxamyl dipeptide caspase inhibitors developed for the treatment of stroke. *Bioorg Med Chem Lett* **2004**, *14*, 2685-2691.
- (148) Shahripour, A. B.; Plummer, M. S.; Lunney, E. A.; Sawyer, T. K.; Stankovic, C. J. et al. Structure-based design of caspase-1 inhibitor containing a diphenyl ether sulfonamide. *Bioorg Med Chem Lett* **2001**, *11*, 2779-2782.
- (149) Ullman, B. R.; Aja, T.; Deckwerth, T. L.; Diaz, J. L.; Herrmann, J. et al. Structure-activity relationships within a series of caspase inhibitors: effect of leaving group modifications. *Bioorg Med Chem Lett* **2003**, *13*, 3623-3626.
- (150) Wang, Y.; Huang, J. C.; Zhou, Z. L.; Yang, W.; Guastella, J. et al. Dipeptidyl aspartyl fluoromethylketones as potent caspase-3 inhibitors: SAR of the P2 amino acid. *Bioorg Med Chem Lett* **2004**, *14*, 1269-1272.
- (151) Yang, W.; Guastella, J.; Huang, J. C.; Wang, Y.; Zhang, L. et al. MX1013, a dipeptide caspase inhibitor with potent in vivo antiapoptotic activity. *Br J Pharmacol* **2003**, *140*, 402-412.
- (152) Rozman-Pungercar, J.; Kopitar-Jerala, N.; Bogyo, M.; Turk, D.; Vasiljeva, O. et al. Inhibition of papain-like cysteine proteases and legumain by caspase-specific inhibitors: when reaction mechanism is more important than specificity. *Cell Death Differ* **2003**, *10*, 881-888.
- (153) Gray, J.; Haran, M. M.; Schneider, K.; Vesce, S.; Ray, A. M. et al. Evidence that inhibition of cathepsin-B contributes to the neuroprotective properties of caspase inhibitor Tyr-Val-Ala-Asp-chloromethyl ketone. *J Biol Chem* **2001**, *276*, 32750-32755.
- (154) Schotte, P.; Declercq, W.; Van Huffel, S.; Vandenabeele, P.; Beyaert, R. Non-specific effects of methyl ketone peptide inhibitors of caspases. *FEBS Lett* **1999**, *442*, 117-121.
- (155) Knoblach, S. M.; Alroy, D. A.; Nikolaeva, M.; Cernak, I.; Stoica, B. A. et al. Caspase inhibitor z-DEVD-fmk attenuates calpain and necrotic cell death in vitro and after traumatic brain injury. *J Cereb Blood Flow Metab* **2004**, *24*, 1119-1132.

- (156) Valentino, K. L.; Gutierrez, M.; Sanchez, R.; Winship, M. J.; Shapiro, D. A. First clinical trial of a novel caspase inhibitor: anti-apoptotic caspase inhibitor, IDN-6556, improves liver enzymes. *Int J Clin Pharmacol Ther* **2003**, *41*, 441-449.
- (157) Caserta, T. M.; Smith, A. N.; Gultice, A. D.; Reedy, M. A.; Brown, T. L. Q-VD-OPh, a broad spectrum caspase inhibitor with potent antiapoptotic properties. *Apoptosis* **2003**, *8*, 345-352.
- (158) Lauffer, D. J.; Mullican, M. D. A practical synthesis of (S) 3-tert-butoxycarbonylamino-2-oxo-2,3,4,5-tetrahydro-1,5-benzodiazepine-1-a cetic acid methyl ester as a conformationally restricted dipeptido-mimetic for caspase-1 (ICE) inhibitors. *Bioorg Med Chem Lett* **2002**, *12*, 1225-1227.
- (159) Linton, S. D.; Karanewsky, D. S.; Ternansky, R. J.; Chen, N.; Guo, X. et al. Acyl dipeptides as reversible caspase inhibitors. Part 2: further optimization. *Bioorg Med Chem Lett* **2002**, *12*, 2973-2975.
- (160) Linton, S. D.; Karanewsky, D. S.; Ternansky, R. J.; Wu, J. C.; Pham, B. et al. Acyl dipeptides as reversible caspase inhibitors. Part 1: initial lead optimization. *Bioorg Med Chem Lett* **2002**, *12*, 2969-2971.
- (161) Linton, S. D.; Aja, T.; Armstrong, R. A.; Bai, X.; Chen, L. S. et al. First-in-Class Pan Caspase Inhibitor Developed for the Treatment of Liver Disease. *J Med Chem* **2005**, *48*, 6779-6782.
- (162) Lee, D.; Long, S. A.; Murray, J. H.; Adams, J. L.; Nuttall, M. E. et al. Potent and selective nonpeptide inhibitors of caspases 3 and 7. *J Med Chem* **2001**, *44*, 2015-2026.
- (163) Micale, N.; Vairagoundar, R.; Yakovlev, A. G.; Kozikowski, A. P. Design and synthesis of a potent and selective peptidomimetic inhibitor of caspase-3. *J Med Chem* **2004**, *47*, 6455-6458.
- (164) Allen, D. A.; Pham, P.; Choong, I. C.; Fahr, B.; Burdett, M. T. et al. Identification of potent and novel small-molecule inhibitors of caspase-3. *Bioorg Med Chem Lett* **2003**, *13*, 3651-3655.
- (165) Choong, I. C.; Lew, W.; Lee, D.; Pham, P.; Burdett, M. T. et al. Identification of potent and selective small-molecule inhibitors of caspase-3 through the use of extended tethering and structure-based drug design. *J Med Chem* **2002**, *45*, 5005-5022.
- (166) Wu, J. C.; Fritz, L. C. Irreversible caspase inhibitors: tools for studying apoptosis. *Methods* **1999**, *17*, 320-328.
- (167) Park, S. J.; Wu, C. H.; Gordon, J. D.; Zhong, X.; Emami, A. et al. Taxol induces caspase-10-dependent apoptosis. *J Biol Chem* **2004**, *279*, 51057-51067.

- (168) Meth-Cohn, O. M., C.; Taljaard, H.C. A Stereocontrolled Approach to Electrophilic Epoxides. *J. Chem. Soc. Perkin Trans. I* **1988**, 2663-2674.
- (169) Germain, M.; Affar, E. B.; D'Amours, D.; Dixit, V. M.; Salvesen, G. S. et al. Cleavage of automodified poly(ADP-ribose) polymerase during apoptosis. Evidence for involvement of caspase-7. *J Biol Chem* **1999**, *274*, 28379-28384.
- (170) Ekici, O. D.; Gotz, M. G.; James, K. E.; Li, Z. Z.; Rukamp, B. J. et al. Aza-peptide Michael acceptors: a new class of inhibitors specific for caspases and other clan CD cysteine proteases. *J Med Chem* **2004**, *47*, 1889-1892.
- (171) Cribbs, D. H.; Poon, W. W.; Rissman, R. A.; Blurton-Jones, M. Caspase-mediated degeneration in Alzheimer's disease. *Am J Pathol* **2004**, *165*, 353-355.
- (172) Guo, H.; Albrecht, S.; Bourdeau, M.; Petzke, T.; Bergeron, C. et al. Active caspase-6 and caspase-6-cleaved tau in neuropil threads, neuritic plaques, and neurofibrillary tangles of Alzheimer's disease. *Am J Pathol* **2004**, *165*, 523-531.
- (173) Larner, S. F.; McKinsey, D. M.; Hayes, R. L.; KK, W. W. Caspase 7: increased expression and activation after traumatic brain injury in rats. *J Neurochem* **2005**, *94*, 97-108.
- (174) Schaschke, N.; Assfalg-Machleidt, I.; Machleidt, W.; Turk, D.; Moroder, L. E-64 analogues as inhibitors of cathepsin B. On the role of the absolute configuration of the epoxysuccinyl group. *Bioorg Med Chem* **1997**, *5*, 1789-1797.
- (175) Stennicke, H. R.; Salvesen, G. S. Caspases: preparation and characterization. *Methods* **1999**, *17*, 313-319.
- (176) DeLano, W. L. "The PyMOL Molecular Graphics System." Delano Scientific LLC, San Carlos, CA USA. <http://www.pymol.org>.